关于乌鲁木齐市动物疾病控制与诊断中心申报2015年度自治区科技进步奖的说明

自治区科技奖励工作办公室:

根据自治区科技厅下发的《关于做好2015年度自治区科技进步奖推荐工作的补充通知》(新科成字〔2015〕72号)文件精神,乌鲁木齐市动物疾病控制与诊断中心作为第一完成单位主持实施的《乌鲁木齐市人畜间结核病流行病学调查与研究》,并在2013年进行了成果鉴定,成果登记号:(2013)新科鉴字第0057号。该项目2013年参加评奖未获奖后,一直持续至今开展相关的研究工作,并在创新内容上有实质、重大进展,获得发明专利2项,新发表论文7篇(具体说明见附件)。该项目具备申报资格,现申报2015年自治区科技进步奖。

特此说明。

联系人:李爱巧

联系电话:4616369,18999903925

乌鲁木齐市动物疾病控制与诊断中心

2015年7月13日

一种诊断牛结核病的重组蛋白及其制备方法（专利号为：ZL 200510005002.0）。

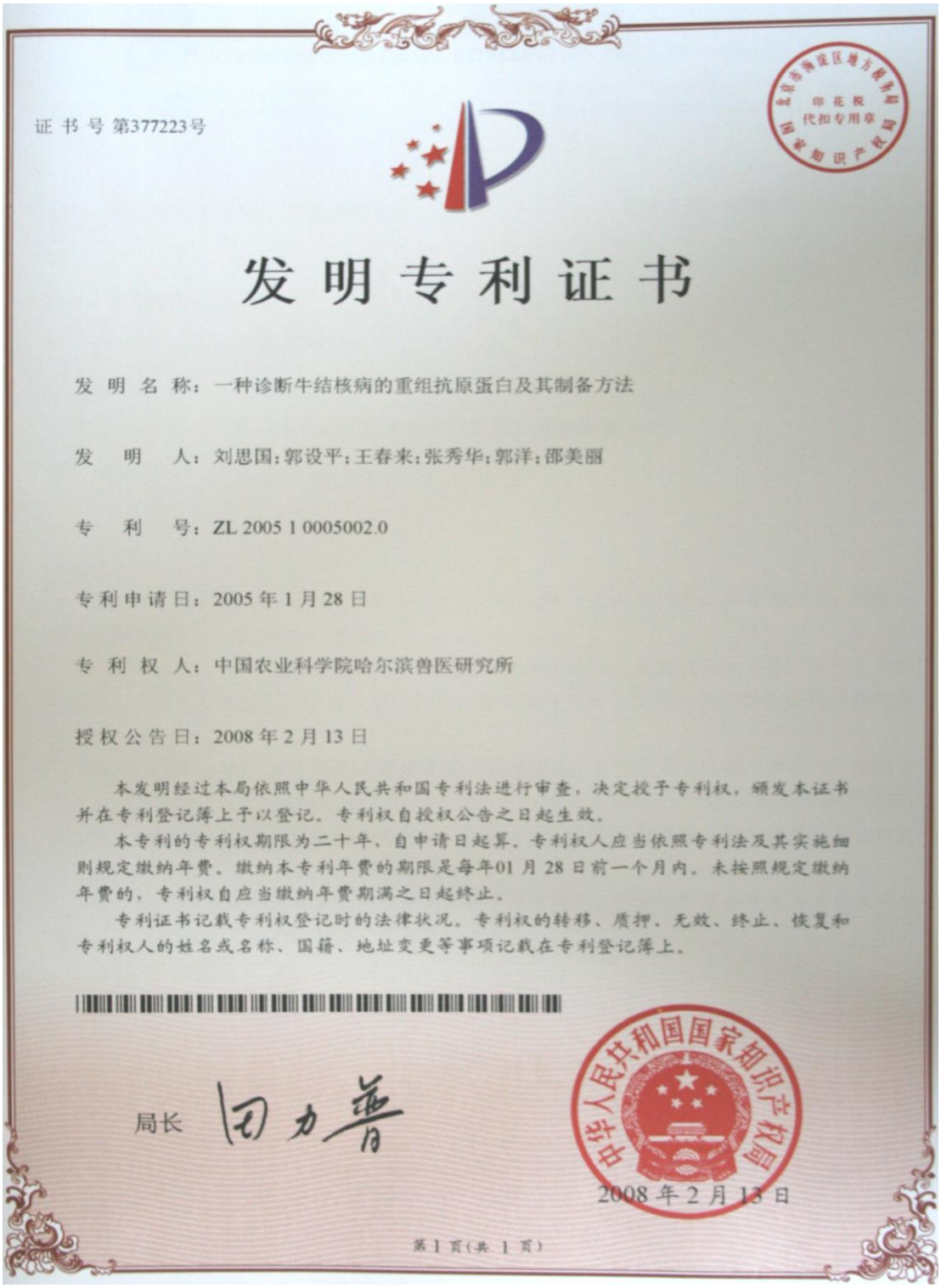

证书号第377223号

印花税代扣专用章

发明专利证书

发明名称：一种诊断牛结核病的重组抗原蛋白及其制备方法

发明人：刘思国;郭设平;王春来;张秀华;郭洋;邵美丽

专利号：ZL 2005 1 0005002.0

专利申请日：2005年1月28日

专利权人：中国农业科学院哈尔滨兽医研究所

授权公告日：2008年2月13日

本发明经过本局依照中华人民共和国专利法进行审查，决定授予专利权，颁发本证书并在专利登记簿上予以登记。专利权自授权公告之日起生效。

本专利的专利权期限为二十年，自申请日起算。专利权人应当依照专利法及其实施细则规定缴纳年费。缴纳本专利年费的期限是每年01月28日前一个月内。未按照规定缴纳年费的，专利权自应当缴纳年费期满之日起终止。

专利证书记载专利权登记时的法律状况。专利权的转移、质押、无效、终止、恢复和专利权人的姓名或名称、国籍、地址变更等事项记载在专利登记簿上。

局长 田力普

中华人民共和国国家知识产权局

2008年2月13日

第1页(共1页)

附件：

重新推荐自治区科技进步奖的项目需提交以下说明材料：

材料名称	上次推荐	本次推荐
推荐年度	2013 年	2015 年
项目名称	乌鲁木齐地区人畜间结核病的流行病学调查研究	人畜间结核病流行病学的调查与研究
完成单位	乌鲁木齐市动物疾病控制与诊断中心;新疆畜牧科学院兽医研究所;	乌鲁木齐市动物疾病控制与诊断中心;新疆畜牧科学院兽医研究所;中国农业科学院哈尔滨兽医研究所;
完成人员	李爱巧;呼西旦•阿巴拜克力;杨启元;王文秀;王六合;施远翔;徐志光;李君莲;徐敏;陈彪;刘思国;范伟兴	李爱巧;呼西旦•阿巴拜克力;刘思国；杨启元;王文秀;王六合;施远翔;陈丽苹；徐志光; 陈彪;徐敏;李君莲;
创新内容（创新点）	1、国内首次将γ-干扰素试验作为国标 PPD 检疫方法的补充或辅助检验方法列入了《牛结核病防治技术规范》新疆地方标准，而且是目前国家兽医行业第一个、也是目前唯一一个牛结核病防治技术规范的地方标准。对我国使用了 120 年来的结核病 PPD 诊断方法有了新突破，还将促进国家牛结核病诊断方法的补充、修改和完善。 2、在国内首次获得了乌鲁木齐地区人和奶牛结核病的流行病学背景资料。掌握了结核病的发病规律和发病特点，调查了乌鲁木	1、国内首次将γ-干扰素试验作为国内单纯颈部变态反应检疫方法的补充或辅助检验方法列入了《牛结核病防治技术规范》新疆地方标准，是目前国家兽医行业第一个、也是目前唯一一个结核病防治技术规范的地方标准。 2、获得了新疆人和乌鲁木齐市奶牛结核病的流行病学背景资料。掌握结核病的发病规律和发病特点，掌握了人和奶牛间结核病的相关性，调查和研究了乌鲁木齐市奶牛和人结核病阳性者的主要流行菌型和菌株以及基因分析。

	齐地区奶牛和人结核病阳性者的主要流行菌型和菌株。 3、国内首次同时应用免疫学方法（结核菌素变态反应、国外比较变态反应、γ-干扰素反应试验）和分子生物学方法（分枝杆菌种属的多重 PCR 方法、结核分枝杆菌复合群的多重 PCR 方法、牛分枝杆菌 MIRU-VNTR 基因分型）等 6 种不同的免疫学检测方法和分子生物学检测方法与病理学方法（剖检病理变化观察）和细菌学方法（结核菌分离培养鉴定）进行比对，对牛结核病现有诊断检测方法的特异性和准确性进行比较分析、研究。并将这些先进的结核病诊断技术引进、吸收、集成，在乌鲁木齐地区首次应用，提高牛结核病检疫的特异性。	3、国内同时应用免疫学方法（结核菌素变态反应、国外比较变态反应、γ-干扰素试验）和分子生物学方法（分枝杆菌种属的多重 PCR 方法、结核分枝杆菌复合群的多重 PCR 方法、牛分枝杆菌 MIRU-VNTR 基因分型）等 6 种不同的方法与病理学方法（剖检观察病理变化）和细菌学方法（分离培养鉴定细菌）进行比对，对牛结核病现有诊断检测方法的特异性和敏感性进行比较、分析、研究。并将这些先进的结核病诊断技术引进、吸收、集成，在乌鲁木齐市首次应用，提高牛结核病检疫的特异性。 4、首次建立了牛分枝杆菌的检测技术和分子分型方法。首次将 mpb70 基因、mpb83 基因和 esat-6 基因抗原置于同一表达载体中进行串连表达，建立了以融合蛋白 M70-M83-E6 为检测抗原的间接 ELISA 方法。 5、首次发现牛群中结核杆菌分离株呈现独特的基因型。解析了分离株的流行和演化规律。 6、揭示了牛结核病感染率与不同地区、饲养管理水

		平之间存在联系。
经济效益（万元）	4587	7403
社会效益	1、结核病对动物和人类危害都很大，严重地影响到畜牧业的持续发展和食品安全问题。2、牛结核病还对人类健康构成巨大威胁。新疆2010年结核病流行病学调查结果，新疆活动性肺结核病患　病率、涂阳肺结核患病率、菌阳肺结核患病率分别为全国平均水平的3.3倍、3倍、3.6倍。结核病是导致众多家庭因病返贫、因病致贫的重要原因之一。3、奶牛患有结核病,造成环境中的二次污染。4、有效防治牛结核病将减少人结核病的发生，保障人的身体健康和社会公共卫生安全。	1、结核病对动物和人类危害都很大，牛结核病的存在和流行、人畜间结核病的交叉传播，不仅对人类的身体健康造成威胁；而且还严重地影响到畜牧业的持续发展和食品安全问题。2、牛结核病还对人类健康构成巨大威胁。新疆2010 年结核病流行病学调查结果，新疆活动性肺结核病患　病率、涂阳肺结核患病率、菌阳肺结核患病率分别为全国平均水平的3.3 倍、3 倍、3.6 倍。结核病是导致众多家庭因病返贫、因病致贫的重要原因之一。3、奶牛患有结核病,造成环境中的土壤、水源和用具等的二次污染。4、有效防治牛结核病将减少人结核病的发生，保障人的身体健康和社会公共卫生安全。
发表论文题目、作者、刊名、年卷期	2012年以前发表的11篇论文。 1、《乌鲁木齐市人畜间结核病流行病学调查研究》发表在《新疆畜牧业》2011年第10期上；作者：李爱巧[1] 庆永兴[2] 杨启元[1] 王文秀[1] 王六合[1] 胡西丹[3] 李君莲[4] 刘思国[5] 范伟	2012 年以后新发表的论文7篇。 1 Yanfen Du, Yingfang Qi, Jingkai Lin, Siguo Liu*, Hongbo Ni, Huifang Liu, Hailing Zhao, Minglei He, Dan Wang, Chunlai Wang, Wei Si. Molecular characterization of *Mycobacterium tuberculosis* complex (MTBC) isolated from

	兴[6] 何华[7] 2、《奶牛结核病皮内变态反应与病理剖检对比实验》发表在《草食家畜》2010 年第 2 期；作者：王文秀[1] 杨启元[1] 李爱巧[1*] 何克明[1] 徐敏[1] 王六合[1] 孙国林[1] 呼西旦[2] 徐志光[2] 刘思国[3] 张喜悦[4] 3、《乌鲁木齐市人畜间结核病的流行病学特点》发表在《草食家畜》2011 年第 2 期；作者：王文秀[1] 孙国林[1] 李爱巧[1*] 徐敏[1] 王六合[1] 马卫平[1] 李兆新 呼西旦[2] 徐志光[2] 许礼仪 李君莲 4、《几种牛结核病检疫方法在结核污染牛群中的应用研究》发表在《草食家畜》2011 年第 2 期；作者：徐敏 许礼仪 王六合[1] 王文秀[1] 马卫平[1] 呼西旦[2] 徐志光[2] 孙国林 5、《农村奶牛结核病检疫概括及防控对策》发表在《现代农业科技》2011 第 21 期；作者：庆永兴[1] 李爱巧 6、《新疆牛结核病防控策略的初步探讨》发表在《草食家畜》2010 年第 1 期；作者：施远翔 杨启元 李爱巧 张春生 7、《牛结核分枝杆菌 ESAT-6 蛋白的原核表达和纯化》发表在《草食家畜》2010 年第 1 期；作者：徐志光 许礼仪 呼西旦 宋振忠 徐敏 8、《一株牛分支杆菌的分离与鉴定》发表在《草食家畜》2010 年第 3 期；作者：许礼仪 呼西旦 徐志光 宋振忠 杨启元 黄炯 9、《牛分支杆菌 ESAT-6 蛋白抗体间接 ELISA 方法的建立》发表在《草食家畜》2010 年第 2 期；作者：许	cattle in northeast and northwest of China, Res Vet Sci, 2011;90(3):385-391 (IF:1.345). **2** Jiubiao Guo, Lipeng Xu, Xiangdong Zeng, shentao Li, Xianggang Kong, Siguo Liu* and Hai Pang*, Crystal structure of a novel esterase Rv0045c from *Mycobacterium tuberculosis* at 2.8 angstroms resolution, submitted to pLOS One, 2011,6(5)e20506 (IF: 4.411). **3** Xianglian Yuan*, Liping Chen*, Jun Cao, Qiulong Yan, Yinbin Liu, Guanghui Dang, Shenye Yu, Wei Si, Xiumei Wang, Hai Pang*, Siguo Liu*, Characterization of rv0394c gene encoding hyaluronidase and chondrosulphatase activity from Mycobacterium tuberculosis H37Rv. Tuberculosis. 2013, 93, 396-300. (IF: 3.503). **4** Huanan Wang, Ting Zhu, Wei Si, Shenye Yu, Huifang Liu, Chunlai Wang, Hai Pang*, Siguo Liu*, A novel B cell epitope in cold-shock DEAD-box protein A from Mycobacterium tuberculosis, Research in Veterinary Science, 2013, 94: 406-412 (IF: 1.511). **5** 朱 婷，王华南，刘慧芳，于申业，王秀梅，陈利苹，司 微，赵海玲，刘思国，牛分枝杆菌与鸟型分枝杆菌 2 型重组蛋白 Ag85b 的血清学交叉反应研究，中国预防兽医学报， 2012，34（3）:223-226. **6** 鄢秋龙，陈利苹，刘银冰，曹俊，倪洪波，刘思国，结核分枝杆菌 rv3668c 基因的原核表达及多抗

	礼仪　徐志光　宋振忠　徐敏　古努尔　李爱巧　黄炯　呼西旦 10、《乌鲁木齐市奶牛结核病流行病学调查和防治》在《中国动物检疫》2012 年第 10 期上发表。作者：李爱巧[1]，赵建国[2]，胡德江[3]，陈彪[1]，王六合 11、地方标准：新疆维吾尔自治区地方标准《牛结核病防治技术规范》（DB65/T3296-2011）在《新疆畜牧业》2011 年第 12 期上。	制备，中国兽医科学，2013,43（06）:594-599. **7** 曹俊，陈利苹，刘银冰，鄢秋龙，刘思国，结核分枝杆菌 rv3036c 基因的原核表达及其多克隆抗体的制备，中国预防兽医学报，2013，35（8）:684-686.
获得的自主知识产权	无	专利：1、一种诊断牛结核病的重组抗原蛋白及其制备方法（专利号：ZL 200510005002.0） 2、抗结核分枝杆菌单克隆抗体及其识别的抗原表位和用途（专利号：ZL201110269165.5）
应用推广单位名称	1、乌鲁木齐市头屯河区 畜牧兽医站；2、乌鲁木齐市达坂城区 畜牧兽医站；3、乌鲁木齐市天山区畜 牧兽医站；4、乌鲁木齐市沙依巴克 区畜牧兽医站；5、乌鲁木齐市乌鲁木齐 县畜牧兽医站；6、乌鲁木齐市新市区畜牧兽医站；7、新疆兵团畜牧兽医工作总站；8、喀什地区动物疫病预防控制中心；9、哈密地区动物疫病预防控制中心；10、伊犁州动物疾病控制与诊断中心；11、阿克苏地区动物疫病 预防	1、新疆兵团畜牧兽医工作总站；2、喀什地区动物疫病预防控制中心；3、哈密地区动物疫病预防控制中心；4、伊犁州动物疾病控制与诊断中心；5、阿克苏地区动物疫病 预防控制中心；6、新疆绿城农业开发有限责任公司；7、乌鲁木齐市米东区畜牧兽医站；8、乌鲁木齐市头屯河区畜牧兽医站；9、乌鲁木齐市达坂城区 畜牧兽医站；10、乌鲁木齐市天山区畜 牧兽医站；11、乌鲁木齐市沙依巴克 区畜牧兽医站；12、乌鲁木齐市

	控制中心；12、新疆绿城农业开发有限责任公司；13、乌鲁木齐市米东区畜牧兽医站	乌鲁木齐 县畜牧兽医站；13、乌鲁木齐市新市区畜牧兽医站；

以上材料重新推荐前后有改变的需提供相关证明材料。

2012 年以后发表的文章

1 Yanfen Du, Yingfang Qi, Jingkai Lin, **Siguo Liu***, Hongbo Ni, Huifang Liu, Hailing Zhao, Minglei He, Dan Wang, Chunlai Wang, Wei Si. Molecular characterization of *Mycobacterium tuberculosis* complex (MTBC) isolated from cattle in northeast and northwest of China, **Res Vet Sci**, **2011;90(3):385-391** (**IF:1.345).**

2 Jiubiao Guo, Lipeng Xu, Xiangdong Zeng, shentao Li, Xianggang Kong, **Siguo Liu*** and Hai Pang*, Crystal structure of a novel esterase Rv0045c from *Mycobacterium tuberculosis* at 2.8 angstroms resolution, submitted to **pLOS One, 2011,6(5)e20506 (IF: 4.411).**

3 Xianglian Yuan*, Liping Chen*, Jun Cao, Qiulong Yan, Yinbin Liu, Guanghui Dang, Shenye Yu, Wei Si, Xiumei Wang, Hai Pang*, **Siguo Liu***, Characterization of rv0394c gene encoding hyaluronidase and chondrosulphatase activity from Mycobacterium tuberculosis H37Rv. Tuberculosis. 2013, 93, 396-300. (IF: 3.503).

4 Huanan Wang, Ting Zhu, Wei Si, Shenye Yu, Huifang Liu, Chunlai Wang, Hai Pang*, **Siguo Liu***, A novel B cell epitope in cold-shock DEAD-box protein A from Mycobacterium tuberculosis, Research in Veterinary Science, 2013, 94: 406-412 (IF: 1.511).

5 朱 婷，王华南，刘慧芳，于申业，王秀梅，陈利苹，司 微，赵海玲，刘思国，牛分枝杆菌与鸟型分枝杆菌 2 型重组蛋白 Ag85b 的血清学交叉反应研究，中国预防兽医学报，2012，34（3）:223-226.

6 鄢秋龙，陈利苹，刘银冰，曹俊，倪洪波，刘思国，结核分枝杆菌 rv3668c 基因的原核表达及多抗制备，中国兽医科学，2013,43（06）:594-599.

7 曹俊，陈利苹，刘银冰，鄢秋龙，刘思国，结核分枝杆菌 rv3036c 基因的原核表达及其多克隆抗体的制备，中国预防兽医学报， 2013，35（8）:684-686.

Protein Expression and Purification 104 (2014) 50–56

Contents lists available at ScienceDirect

Protein Expression and Purification

journal homepage: www.elsevier.com/locate/yprep

Characterization of a novel exported esterase Rv3036c from *Mycobacterium tuberculosis*

Liping Chen [a,1], Guanghui Dang [a,b,c,1], Xiaoxia Deng [b], Jun Cao [a], Shenye Yu [a], Defeng Wu [c], Hai Pang [b,*], Siguo Liu [a,*]

[a] Division of Bacterial Diseases, State Key Laboratory of Veterinary Biotechnology, Harbin Veterinary Research Institute, Chinese Academy of Agricultural Sciences, Harbin 15000, PR China
[b] School of Medicine, Tsinghua University, Beijing 100084, PR China
[c] Fujian Agriculture and Forestry University, Fuzhou 350002, PR China

ARTICLE INFO

Article history:
Received 26 June 2014
and in revised form 5 September 2014
Available online 16 September 2014

Keywords:
Mycobacterium tuberculosis
Exported esterase
rv3036c

ABSTRACT

Mycobacterium tuberculosis possesses an unusually high number of genes involved in the metabolism of lipids. Driven by a newly described esterase motif SXXK in the amino acid sequence and a predicted signal peptide, the gene *rv3036c* from *M. tuberculosis* was cloned and characterized biochemically. Rv3036c efficiently hydrolyzes soluble *p*-nitrophenyl esters but not emulsified lipid. The highest activity of this enzyme was observed when *p*-nitrophenyl acetate (C_2) was used as the substrate. Based on the activities, Rv3036c was classified as a nonlipolytic hydrolase. The results of immunoreactivity studies on the subcellular mycobacterial fractions suggested that the enzyme was present in the cell wall and cell membrane in mycobacteria. In summary, Rv3036c was characterized as a novel cell wall-anchored esterase from *M. tuberculosis*.

Introduction

Tuberculosis (TB)[2], caused by *Mycobacterium tuberculosis*, is one of the major public health threats worldwide [1,2]. According to WHO data, TB was the second leading cause of death among infectious diseases. Coinfection with human immunodeficiency virus and the emergence of extensively drug-resistant *M. tuberculosis* strains make it difficult to treat. Thus, new drugs and the development of an effective vaccine are urgently needed to control this disease.

M. tuberculosis uses carbohydrates when growing in vitro, but prefers fatty acids as a carbon source when growing in vivo [3,4]. After entering its host, *M. tuberculosis* is able to remain dormant for decades while waiting for the host's immune system to weaken; it then reactivates and causes disease [5]. During the dormant state, *M. tuberculosis* accumulates lipids from host cells in the form of intracellular lipid inclusion bodies [6]. Fatty acids have been shown to be the energy source for *M. tuberculosis* during this dormant state [5,7,8]. Lipid storage not only provides the bacterium with energy [9,10] but also supplies the lipid components required for the synthesis of the bacterial cell wall or cell membrane, an important aspect of *M. tuberculosis* pathogenicity [11,12]. Therefore, the lipid metabolism of *M. tuberculosis* should be emphasized in studies focused on understanding the molecular basis of this bacterium's pathogenicity.

The availability of the *M. tuberculosis* genome sequence has facilitated the elucidation of this bacterium's pathogenicity at the level of molecular biology [13,14]. Although lipases/esterases are crucial for the basic metabolism and pathogenicity of *M. tuberculosis*, *M. tuberculosis* lipases/esterases have not been well characterized, and the possible involvement of these lipases/esterases in pathogenesis remains unclear. Furthermore, despite the presence of many proteins with functions that could not be predicted by bioinformatics, more than 250 enzymes were predicted to be involved in lipid metabolism in *M. tuberculosis* H37Rv [13]. Twenty-one genes in the *M. tuberculosis* genome were annotated as encoding putative lipases/esterases genes [14], and 94 gene products were predicted to contain the α/β-hydrolase fold that characterizes lipases/esterases [15]. Before this study, only seven lipase/esterase genes had been characterized in *M. tuberculosis*, including *lipA*

* Corresponding authors.
E-mail addresses: pangh@xtal.tsinghua.edu.cn (H. Pang), siguo_liu@hvri.ac.cn (S. Liu).

[1] Both authors contributed equally to this work.

[2] *Abbreviations used:* TB, tuberculosis; OADC, oleic acid–albumin–dextrose complex; IPTG, isopropyl b-D-1-thiogalactopyranoside; BCA, bicinchoninic acid; PMF, peptide mass fingerprint; *p*NP, *p*-nitrophenyl; TP, total protein; LH, lipolytic hydrolase; NLH, nonlipolytic hydrolases.

http://dx.doi.org/10.1016/j.pep.2014.09.003
1046-5928/

(*rv2224*), *lipC* (*rv0220*), *lipH* (*rv1399c*), *lipF* (*rv3487c*), *lipY* (*rv3097c*), *rv0183* and *rv0045c* [16–22], and the contribution of these genes to pathogenesis has only been investigated for *lipA*, *lipY* and *rv0183* [18–21].

As members of the α/β hydrolase fold family, the sequences of most lipases/esterases contain the classical motif GXSXG. Some lipases, however, contain the nonclassical motifs GGGX, RGD or HGGG [23–26]. Herein, we report the cloning and characterization of an esterase from *M. tuberculosis* H37Rv, which contains a novel, recently described esterase motif.

Materials and methods

Strains and growth conditions

Escherichia coli strains DH5α and BL21 (DE3) (Novagen, Germany) were used as host strains for plasmid propagation and protein expression. The *E. coli* strains were grown in Luria–Bertani broth or on LB agar. When required, antibiotics were added at the appropriate concentrations (kanamycin, 50 μg/ml; ampicillin, 100 μg/ml). The *Mycobacterium bovis* bacille Calmette–Guerin (BCG) strain Tokyo 172 was purchased from ATCC. Mycobacterial strains were grown in Middlebrook 7H9 broth (Difco, United States) supplemented with 10% oleic acid–albumin–dextrose complex (OADC) enrichment (BBL, United States), 0.05% Tween 80 and 0.2% glycerol.

Cloning of rv3036c from H37Rv

The amino acid sequence of Rv3036c was searched for a potential signal peptide sequence using the SignalP 4.0 server (http://www.cbs.dtu.dk/services/SignalP/), for conserved protein domains using the Pfam database and for transmembrane helix using the TMHMM Server v. 2.0 (http://www.cbs.dtu.dk/services/TMHMM-2.0/). The *rv3036c* coding sequence without the predicted signal peptide was amplified from *M. tuberculosis* H37Rv genomic DNA using *Pfu* DNA polymerase (Fermentas, United States) and the following primers: HYP-F (5-TTT GGA TCC CCG TCA TGC GCC GGC-3) and HYP-R (5-GTG GAA TTC TTA GAT TGC CAG CGG CGG A-3. The PCR program was performed on a thermal cycler (LabCycler, SensoQuest, Germany) with the following procedure: (1) predenaturing (95 °C, 3 min); (2) 30 cycles of denaturing (95 °C, 30 s), annealing (55 °C, 30 s) and extension (72 °C, 1.2 min), and (3) a final extension (72 °C, 10 min). The amplified product was purified and digested by the restriction endonucleases *BamH*I and *Eco*RI (Fermentas, United States). The product was cloned into the pET28a (+) expression vector (Novagen, Germany) that had been digested by the same enzymes, giving the plasmid designated p28-HYP.

Expression and purification of rRv3036c

After the recombinant plasmid p28-HYP was confirmed by sequencing, it was transformed into *E. coli* BL21 (DE3), and then, a single clone was grown overnight in LB media containing 50 μg/ml kanamycin at 37 °C. The overnight culture was subinoculated into fresh LB media. When the culture reached optical density of 0.6 (A_{600} = 0.6), the expression of the target protein was induced with 0.5 mM isopropyl b-D-1-thiogalactopyranoside (IPTG) for 20 h at 16 °C. The cells were harvested by centrifugation, resuspended in solution A (20 mM Tris buffer, 150 mM NaCl, 10 mM imidazole and 10% glycerol, pH 7.5) and sonicated in an ice bath. The soluble fraction was cleared by centrifugation at 12,000*g* for 20 min and was then filtered through 0.22-micron filters (Millipore, United States) at 4 °C.

The His6-tag fusion protein was loaded onto a Ni Sepharose 6 Fast Flow column (GE Healthcare, United States) that had been pre-equilibrated with solution A. After washing with solution B (20 mM Tris buffer, 150 mM NaCl, 20 mM imidazole and 3% glycerol, pH 7.5), the target protein was eluted with increasing concentrations of imidazole (100 mM, 200 mM and 500 mM). The purified protein was desalted and concentrated simultaneous by ultrafiltration three times in solution C (20 mM tris buffer, pH 7.5). The concentrated product was sequentially applied to Hitrap_DEAE FF and Hitrap_CM FF 1 ml columns (GE Healthcare, United States) and eluted with solution C at gradient NaCl concentrations ranging from 0 to 2 M respectively. Finally, the protein was applied to a Superdex 75 10/300 gel column (GE Healthcare, United States). The products were collected fractionally and analyzed by sodium dodecyl sulfate polyacrylamide gel electrophoresis (SDS–PAGE). The protein concentrations were determined using a bicinchoninic acid (BCA) protein assay kit (Beyotime, China).

MALDI-TOF peptide mass fingerprint (PMF) spectrometry of the Rv3036c protein

The target protein was removed from the SDS–PAGE gel stained with Coomassie brilliant blue and cut into 1 mm^3 pieces. The gel pieces were dipped in 100 μl of 25 mM ammonium bicarbonate, pH 8.0 (Fluka, United States), containing 50% acetonitrile (Fisher, United States) three times for 15 min each. After the color was removed, the gel pieces were dehydrated in acetonitrile for 5 min and completely dried in a speed-vac. The protein was digested in 0.1 mg/ml trypsin (Promega, United States) overnight at 37 °C. The digested sample (0.3 μl) was mixed with 0.3 μl of matrix solution [5 mg/mL α-cyano-4-hydroxycinnamic-acid (Fluka, United States) in 50% (v/v) acetonitrile (Fisher, United States) and 0.1% (w/v) trifluoroacetic acid (DIMA, United States)] and spotted onto the sample plate for MALDI-TOF MS analysis using the positive ion reflection mode. The protein was identified by searching the NCBI non-redundant and Swissprot databases with following parameters: (1) precursor tolerance of ±0.2 Da; (2) MS/MS tolerance of ±0.8 Da; (3) missed cleavages of 1.

Circular dichroism spectroscopy analysis

Circular dichroism spectroscopy analysis was performed using the purified rRv3036c protein (0.35 mg/mL) in 20 mM Tris (pH 7.5) on a JASCO 715 spectropolarimeter (JASCO). The protein was analyzed at different pH values (pH 2.0–12.0; with an interval of 1.0 except for at pH 5.0, which is too close to the pI of Rv3036c) at room temperature. The UV CD spectra between 190 and 250 nm were collected using 1 mm quartz cuvettes filled with 200 μl of the protein solutions at a scanning speed of 50 nm/min, a bandwidth of 2.0 nm and a data pitch of 0.1 nm. Experimental data were obtained in triplicate.

Esterase activity analysis

The esterase activity of Rv3036c was measured according to the method of Zhang et al. using the following *p*-nitrophenyl (*p*NP) esters with carbon chain lengths ranging from C_2 to C_{16} as substrates: acetate (C_2), butyrate (C_4), caprylate (C_6), caproate (C_8), laurate (C_{12}), myristate(C_{14}) and palmitate (C_{16}) [17]. Briefly, the reaction mixture (500 μl) containing 40 mM Britton–Robinson buffer, 1 mg/ml purified protein, 0.6% Triton X-100 and 10 mM substrate was incubated for 1 h, and the reactions were then terminated by freezing for 15 min at −20 °C. The negative controls were a mixture with no protein and a mixture with protein added at the end of the incubation period. The enzymatic activities were quantified in a 96-well plate by measuring the amount of *p*NP

released at 405 nm using a BioTek ELx808 Absorbance Microplate Reader (BioTek, Winooski, United States). The reactions were carried out in triplicate, and the results were expressed as specific activities in units/mg. One enzymatic activity unit is defined as the amount of enzyme required to release 1 μmol of *p*NP per min. The pH- and temperature-dependent activities were analyzed by adjusting the buffer to different pH values (6.0, 7.0, 8.0 and 9.0) and incubating at different mild temperatures (36 °C, 37 °C, 38 °C, 39 °C and 40 °C) using acetate (C_2) as the substrate.

Preparation of the antiserum against the rRv3036c protein

Purified rRv3036c protein was mixed with an equal amount of Freund's incomplete adjuvant for emulsification. New Zealand rabbits were immunized with the emulsification product, and booster inoculations were performed at two-week intervals. The double agar diffusion precipitation test was applied to check the titer of the antiserum. When the titer reached 1:16, blood was harvested from the carotid artery, and the antiserum was separated after the blood coagulated.

Preparation of subcellular fractions from mycobacteria

Preparation of subcellular fractions from the *M. bovis* BCG strain was performed as described previously [27]. Briefly, 5 g (wet weight) of mycobacteria were suspended in 10 ml of PBS containing the Benzonase nuclease and proteinase inhibitor (1 mM phenylmethylsulfonylfluoride [PMSF] and 1 mM EDTA). The suspension was sonicated for 20 min in an ice bath. The sonicated product was centrifuged at 650*g* for 20 min to remove the unbroken cells in the pellet. The supernatant was then centrifuged at 36,000*g* for 45 min at 4 °C. The final supernatant was used as the total protein (TP) in the immunodetection assays. The protein concentration was determined using the BCA kit.

A 25-ml culture of mycobacteria was centrifuged at 10,000*g* for 20 min at 4 °C, and the supernatant was filtered using a 0.2-μm pore membrane to generate the culture filtrate fraction. To obtain subcellular fractions, the bacterial pellet was resuspended in PBS containing proteinase inhibitor and was sonicated two times for 15 min in an ice bath, with a 15-min interval for cooling. The sonicated product was centrifuged at 3000*g* for 5 min at 4 °C, and the supernatant was then centrifuged at 27,000*g* for 1 h at 4 °C. The supernatant was collected for further handling. the pellet was resuspended in PBS containing lysozyme, incubated at 37 °C for 50 min and centrifuged at 27,000*g* for 1 h at 4 °C. The pellet was resuspended in 10 mM ammonium bicarbonate and was used as the cellular wall fraction in the immunodetection assays. The supernatant was mixed with the fraction that was collected from the previous centrifugation and was centrifuged at 100,000*g* for 4 h at 4 °C. The final supernatant was labeled as the cytosolic fraction, and the pellet served as the membrane protein fraction. The protein concentrations of the fractions were quantified using a BCA kit and stored at −70 °C until use.

Western-blotting analysis

The protein samples were separated by 12% SDS–PAGE and transferred to a nitrocellulose membrane by using a semi-dry transfer apparatus (Bio-Rad, United States). The nitrocellulose membrane was blocked overnight with 5% skim milk (DB, Becton, Dickinson and Company, United States) and then incubated with mouse anti-hexahistidine antiserum (Invitrogen, United States) for recombinant protein confirmation or using rabbit with antiserum against the recombinant protein for the detection of the natural Rv3036c protein. The secondary anti-mouse or anti-rabbit IgG peroxidase-conjugated antibody (Rockland, United States) was used at a dilution of 1:3000. Reactivity was assessed using the ECL Western blotting substrate (Pierce, Thermo Scientific, United States). For subcellular localization analysis of Rv3036c, 0.3 mg of each sample was loaded per gel and then transferred to nitrocellulose membrane. The secondary anti-rabbit IgG Dylight 800-labeled antibody (KPL, United States) was used at a dilution of 1:10000. Reactivity was assessed and recorded on a Li-Cor Odyssey imaging system (Li-Cor Biosciences, United States).

Results

Sequence analysis of Rv3036c

SignalP 4.0 predicted a signal peptide sequence at the N terminus of Rv3036c. The nucleotide sequence of *rv3036c* and the derived amino acid sequences are conserved among the species of *M. tuberculosis* complex, including *M. bovis*, *M. bovis* BCG strains, *Mycobacterium africanum* and *Mycobacterium canettii* with identities ranging from 99% to 100%. Blast searching revealed the conserved domain DUF3298 (GenBank Accession No. PF11738) from residues Q106 to A226. Several proteins containing this domain are annotated as endo-1,4-beta-xylanase-like protein, but their predicted functions have not been confirmed. Furthermore, BLAST searching revealed three proteins with 13–16.5% identities that were annotated as extracellular DNases (GenBank Accession Nos. YP_006712063.1 YP_003865589.1 and ZP_06873138.1) and two proteins with 16.5% identity that were annotated as carbohydrate esterases (GenBank Accession Nos. ZP_17655890.1 and YP_077882.2). These results provided clues for the investigation regarding the biochemical function of Rv3036c.

Expression and purification of the recombinant protein

Heterologous over-expression of Rv3036c with a C-terminal hexahistidine tag was induced at varying temperatures (37 °C, 30 °C, 23 °C and 16 °C). SDS–PAGE analysis of the products showed that the most abundant recombinant protein, with a molecular weight of approximately 25 kD, was obtained when the cells were induced with 0.5 mM IPTG at 16 °C for 20 h.

Through successive purification procedures, including Ni^{2+}-affinity chromatography (Fig. 1), anion exchange chromatography (Fig. 2A), cation exchange chromatography (Fig. 2B) and gel filtration chromatography (Fig. 2C), rRv3036c was obtained at a purity level greater than 99%. To confirm that our purified product was the expected rRv3036c, Western blotting to detect the 6His-tag and MALDI-TOF mass spectrometry was performed. The results showed that a protein band with the expected size (approximately 25 kD) reacted with the anti-His6 antibody, indicating that our

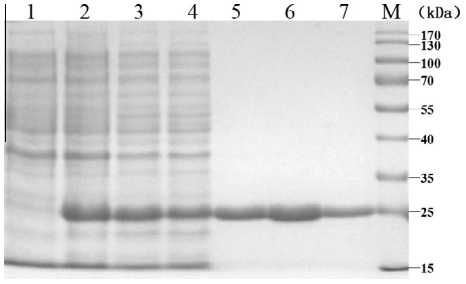

Fig. 1. SDS–PAGE analysis of rRv3036c expression and affinity chromatography. Lane 1, culture pellet (uninduced); lane 2, culture pellet (induced with 1 mM IPTG at 16 °C for 12 h); lane 3, the supernatant of the induced cells after sonication; lane 4, Ni^{2+}-affinity chromatography column flow-through; lanes 5–7, purified Rv3036c protein eluted with 100 mM Tris, 200 mM NaCl and 500 mM imidazole; and lane M, molecular mass markers.

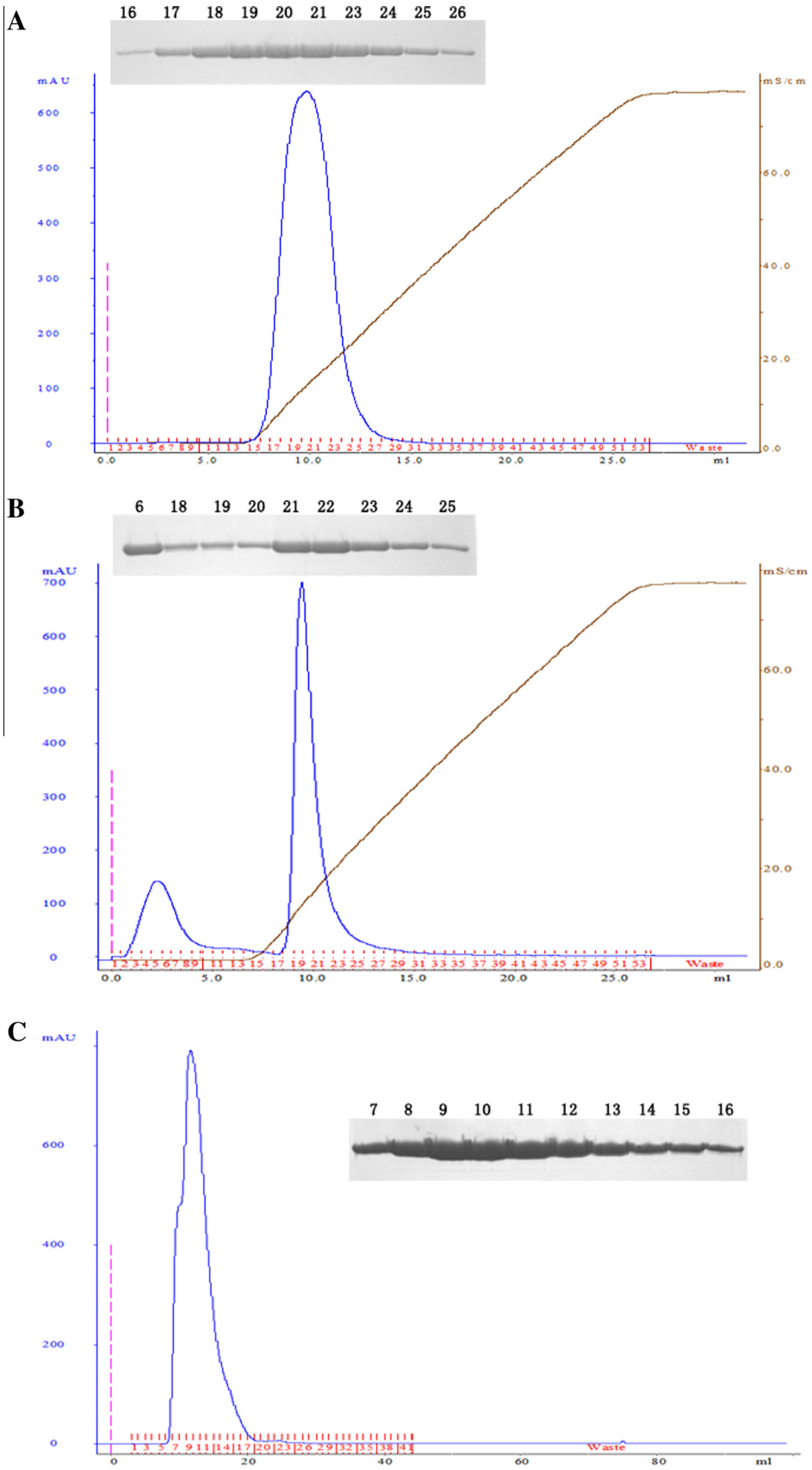

Fig. 2. Purification of rRv3036c by ion exchange chromatography and gel filtration chromatography. The rRv3036c protein was purified by (A) anion exchange chromatography, (B) cation exchange chromatography, (C) and gel filtration chromatography. The purity was analyzed by SDS–PAGE.

purified product was a His6-tag recombinant protein (Fig. 3A). The specificity of antiserum against rRv3036c was confirmed by Western blotting (Fig. 3B). In addition, the PMF of the purified recombinant protein showed that the hypothetical protein Rv3036c (NP_214908.1) from *M. tuberculosis* H37Rv was purified, with a hit score of 361, indicating that the recombinant protein purified was indeed Rv3036c (Fig. 4).

Circular dichroism of the Rv3036c protein

To investigate the secondary structural elements in Rv3036c, CD spectroscopy data were collected at wavelengths ranging from 260 to 190 nm. The curves converged at a pH range from 3.0 to 10.0, but were distorted and disordered at extreme pH values ($pH \leqslant 2$ or $pH \geqslant 11.0$). At pH values ranging from 2.0 to 11.0 or 12.0, the conformation of the protein was quite different from that at physiological conditions (pH 7.0 and pH 8.0), indicating the protein had been denatured (Fig. 5).

Esterase activity of Rv3036c

As shown in Table 1, rRv3036c hydrolyzes ester substrates carbon chain lengths ranging from C_2 to C_{14}; acetate (C_2), butyrate (C_4) and caprylate (C_6) were hydrolyzed with relatively high efficiencies. However, rRv3036c displayed relative low hydrolase activities against caproate (C_8), laurate (C_{12}) and myristate (C_{14}), with lowest activity being observed when palmitate (C_{16}) was used as the substrate. The highest activity, with a value of 1315.97 U/mg, occurred with the substrate acetate (C_2). Temperature- and pH-dependent analyses showed that the most efficient hydrolysis occurred at 38 °C (among five different temperatures ranging from 36 °C to 40 °C) and at pH 8.0 (among four different pH values tested from 6.0 to 9.0) (Fig. 6). In addition, the esterase activity of Rv3036c was almost absent at pH 6.0, regardless of the reaction temperature. At pH 7.0 and 9.0, the esterase activity was similar across the different temperatures (Fig. 6).

Subcellular localization of Rv3036c in mycobacteria

Rv3036c was predicted to be a secretory protein in genomic sequence annotations of the *M. tuberculosis* strain H37Rv in the NCBI database, and SignalP 4.0 predicted a signal peptide sequence at the N-terminus of the protein. Thus, Western blotting analysis was performed to investigate the subcellular localization of Rv3036c in mycobacteria, using the antiserum against rRv3036c prepared in rabbits. The reaction specificity of the antiserum was confirmed by Western blotting analysis before experimental use (Fig. 3B). Because a homologue (JTY_3055) with 100% identity to Rv3036c was present in the *M. bovis* BCG strain Tokyo 172, the BCG strain was cultured for preparation of the subcellular fractions. The Western blotting results showed that Rv3036c immunoreactivity was absent from the culture supernatant, indicating that the protein was not secreted to the extracellular milieu (Fig. 7). However, the antiserum reacted with the cell wall, membrane and cytosolic fractions (Fig. 7). In contrast, the pre-immune serum, set as the negative control, failed to react with any BCG proteins (Fig. 7). These results suggest that the natural Rv3036c is anchored in the cell wall and cell membrane of mycobacteria via an N-terminal transmembrane helix.

Discussion

Although Rv3036c was annotated as a putative protein of unknown function, an analysis of the predicted secreted proteins showed that it had low levels of sequence similarity with an extracellular deoxyriboendonuclease (GenBank Accession No. YP_006712063.1), a carbohydrate esterase (GenBank Accession No. YP_077882.2) and a xylanase/chitin deacetylase (GenBank Accession No. ZP_17655890.1) from *Bacillus licheniformis*. This suggested that Rv3036c might have an enzymatic activity with potential functions such as a xylanase, extracellular DNAse or carbohydrate esterase. Because the enzymes involved in saccharometabolism, DNA degradation and lipid metabolism are crucial for pathogenic bacteria [28–30]; any of these three potential functions could contribute to *M. tuberculosis* pathogenicity.

An analysis of the Rv3036c amino acid sequence did not identify the common esterase motifs GXSXG, GGGX, RGD or HGGG [23–26]. However, an SXXK motif, which was recently identified as indicative of esterase activity by metagenome sequencing technology, is present in the Rv3036c amino acid sequence [31,32]. We assessed the esterase activity in Rv3036c, and the results were positive. We also analyzed xylanase activity and DNase activity, and the results of these experiments were negative. Thus a novel *M. tuberculosis* esterase was identified in our study. This finding provides new information for the discovery of novel esterases in mycobacteria.

Esterases/lipases are crucial to the pathogenicity of mycobacteria, and approximately 250 genes in *M. tuberculosis* are predicted to be involved in lipid metabolism [29]. However, the esterases/lipases from mycobacteria have not been sufficiently characterized. This may be partially due to the difficulty of obtaining active esterase/lipases products in an *E. coli* expression system [17,20,33].

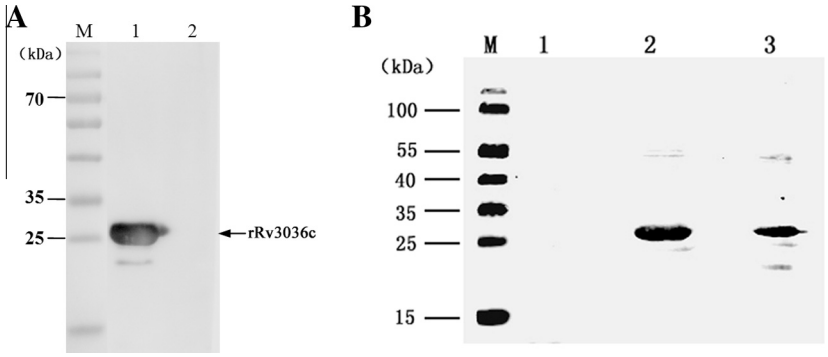

Fig. 3. Immunoblotting assessment of Rv3036c. (A) Recombinant Rv3036c was assessed using His6-tag antiserum. Line 1, purified rRv3036c and line 2, *E. coli* BL21 (DE3) lysate. The reaction of the His6-tag antiserum with the purified protein with a molecular size of approximately 25 kDa verified that the purified product was our expected recombinant protein. (B) The specificity of the anti-rRv3036c antibody was assessed. Line 1, *E. coli* BL21 (DE3) lysate; line 2, lysate of *E. coli* BL21 (DE3) containing recombinant plasmid p28-HYP; line 3, purified rRv3036c. The anti-rRv3036c antibody prepared in rabbits did not react with the lysate of the host strain *E. coli* BL21 (DE3), verifying the specificity of the antibody.

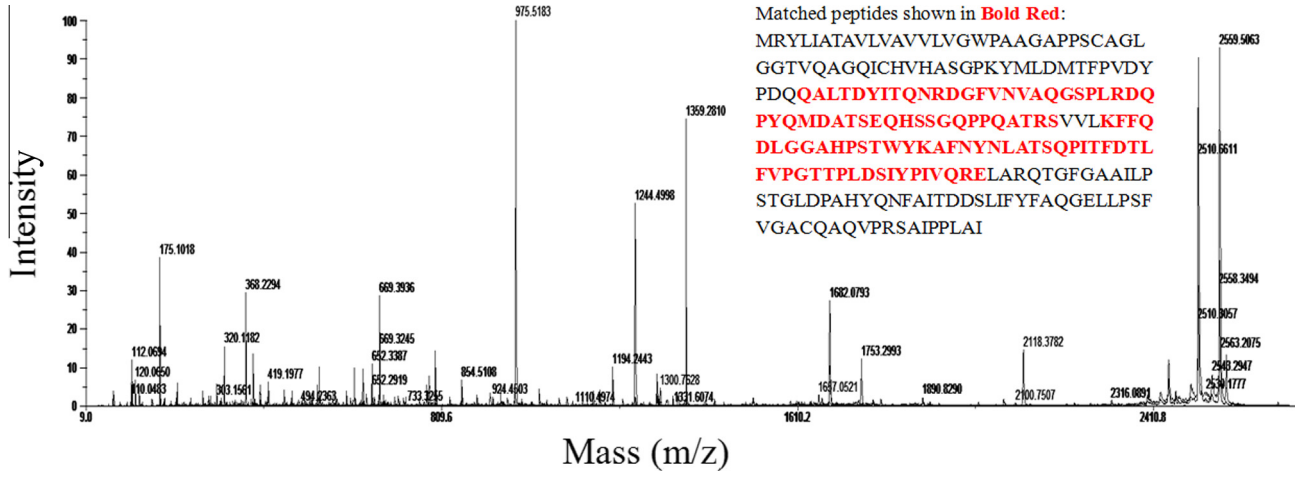

Fig. 4. MALDI-TOF peptide mass fingerprint (PMF) spectrometry of rRv3036c. PMF analysis was performed on fragments of purified rRv3036c digested with trypsin. The expected tryptic masses matched the calculated values (1 Da tolerance). The sequence coverage of these fragments in Rv3036c is shown in bold red. (For interpretation of the references to colour in this figure legend, the reader is referred to the web version of this article.)

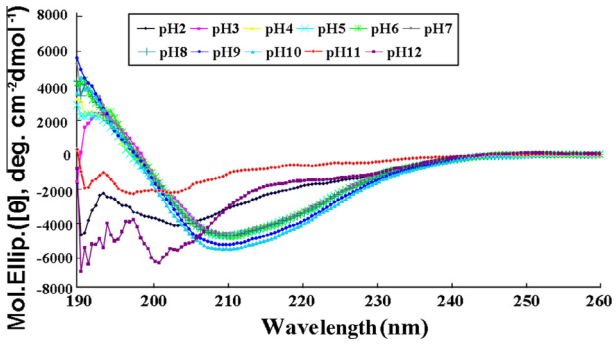

Fig. 5. Effects of pH on the structural stability of Rv3036c. The CD measurements were made in buffers with various pH values ranging from 2.0 to 12.0 at room temperature. The values shown represent the mean ± SD obtained from three experiments. The concentration of Rv3036c used in the study was 0.08 mg/ml in 10 mM sodium dihydrogen phosphate and potassium dihydrogen phosphate buffer.

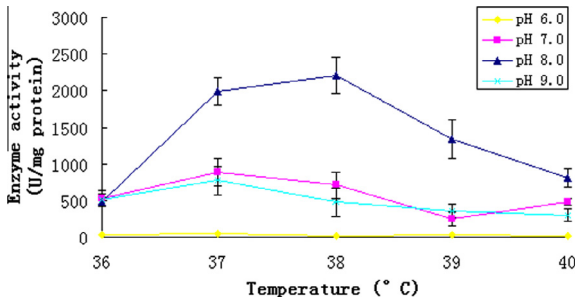

Fig. 6. Effects of temperature and pH on the enzyme activity of rRv3036c protein. The enzyme activities were measured using *p*-nitrophenyl acetate (C2) as the substrate at the mild temperatures (36 °C–40 °C) at pH 6.0 (yellow), pH 7.0 (purple), pH 8.0 (blue) and pH 9.0 (green). Values represent the mean ± SD of three independent trials. The concentration of the Rv3036c protein was fixed at 1 mg/ml in 20 mM Tris (pH 7.0). The enzyme activities were expressed as units/mg protein and one hydrolase unit is defined as the quantity of enzyme required to increase the absorbance by 0.01 units per min at 405 nm. (For interpretation of the references to colour in this figure legend, the reader is referred to the web version of this article.)

Table 1
Relative esterase activity of the rRv3036c protein toward *p*-nitrophenyl derivatives at pH 7.5 and 37 °C.

Substrate	Relative activity (%)[a]
p-Nitrophenyl acetate (C_2)	100
p-Nitrophenyl butyrate (C_4)	62.5
p-Nitrophenyl caproate (C_6)	25.9
p-Nitrophenyl caprylate (C_8)	9.8
p-Nitrophenyl laurate (C_{12})	17.4
p-Nitrophenyl myristate (C_{14})	12.7
p-Nitrophenyl palmitate (C_{16})	4.2

[a] The specific activity toward *p*-nitrophenyl acetate (C_2) corresponding to 1315.97 U/mg protein was defined as 100%. One esterase unit is the quantity of enzyme required to release 1 μmol *p*NP per min.

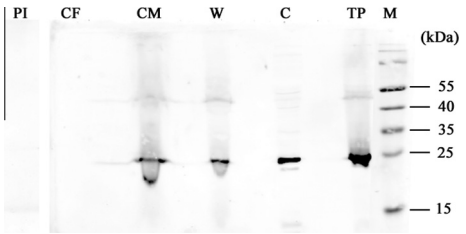

Fig. 7. Assessment of the subcellular localization of Rv3036c in *M. bovis* BCG. Specific antisera raised in rabbits were used to assess the presence of Rv3036c (also the protein JTY_3055 in the *M. bovis* BCG strain Tokyo 172) in the total protein (TP), cell wall (W), cell membrane (CM), cytosolic (C) and culture filtrate (CF) fractions of *M. bovis* BCG. The reactivity of the rabbit pre-immune serum to mycobacterial total proteins was assessed as the negative control (PI), and no recognition was detected. The results showed the detection of Rv3036c in the total protein, cell wall, membrane and cytosolic fractions of *M. bovis* BCG Tokyo 172.

The esterase/lipase proteins formed inclusion bodies in the ordinary expression systems, and recombinant proteins had to be successfully renatured to investigate their enzymatic activities [16,18,19,21,34]. Nevertheless, esterase Rv3036c was expressed in a soluble form in our study, facilitating the purification and enzymatic detection.

Ester hydrolase can be classified into the following two classes: esterases and lipases. Lipase refers to a lipolytic hydrolase (LH) that shows activity against water-insoluble lipids, and esterase refers to the remaining members of the lipase family that exhibit maximal activity against esters in solution; esterases are also nonlipolytic hydrolases (NLH) ([16,35]). Within the *M. tuberculosis* lipase family, the proteins encoded by the genes *rv0183*, *lipC* and *lipY* were characterized as having lipase activity [20,34,21], and the proteins encoded by the genes *lipH*, *lipF* and *rv2224c* were

described as carboxyl esterases [16,17,19]. Our enzymatic investigation results showed that Rv3036c preferentially hydrolyzes short chain esters, such as *p*-nitrophenyl acetate and butyrate. Because the preferred substrates of Rv3036c for hydrolysis are water-soluble, Rv3036c can be classified as an NLH rather than an LH.

Surface lipids are crucial for the virulence of mycobacteria [36,37]. Western-blotting data in this study indicated that Rv3036c is anchored to the surface of mycobacteria where it may gain access to the host's lipids and function as an esterase. Esterase activity against host esters could provide a source of fatty acids for mycobacteria to use nutritionally. Additionally, as a surface-anchored esterase, Rv3036c may play a role in structurally modifying the cell wall composition [38]. Further studies are needed to address the specific contribution of Rv3036c in disease progression. Due to the bacterial surface exposure and the possible accessibility of Rv3036c to the host immune system, it may provide a target candidate for drug development in the future.

Acknowledgments

This work was supported by the Major State Basic Research Development Program of China (973 program) (No. 2012CB518800), the National Natural Science Foundation of China (Nos. 31201920, 31272538), the State Key Laboratory of Veterinary Biotechnology Research Fund (No. SKLVBP201417) and the Shanghai tuberculosis Key Laboratory Open Research Fund (No. 2013K03).

References

[1] C.Y. Chiang, C. Van Weezenbeek, T. Mori, D.A. Enarson, Challenges to the global control of tuberculosis, Respirology (2013).
[2] C. Dye, S. Scheele, P. Dolin, V. Pathania, M.C. Raviglione, Consensus statement. Global burden of tuberculosis: estimated incidence, prevalence, and mortality by country. WHO Global Surveillance and Monitoring Project, JAMA 282 (1999) 677–686.
[3] H. Bloch, W. Segal, Biochemical differentiation of *Mycobacterium tuberculosis* grown in vivo and in vitro, J. Bacteriol. 72 (1956) 132–141.
[4] S.K. Jackson, J.M. Stark, S. Taylor, J.L. Harwood, Changes in phospholipid fatty acid composition and triacylglycerol content in mouse tissues after infection with bacille Calmette–Guerin, Br. J. Exp. Pathol. 70 (1989) 435–441.
[5] D.G. Russell, Phagosomes, fatty acids and tuberculosis, Nat. Cell Biol. 5 (2003) 776–778.
[6] N.J. Garton, H. Christensen, D.E. Minnikin, R.A. Adegbola, M.R. Barer, Intracellular lipophilic inclusions of mycobacteria in vitro and in sputum, Microbiology 148 (2002) 2951–2958.
[7] J. Daniel, C. Deb, V.S. Dubey, T.D. Sirakova, B. Abomoelak, H.R. Morbidoni, P.E. Kolattukudy, Induction of a novel class of diacylglycerol acyltransferases and triacylglycerol accumulation in *Mycobacterium tuberculosis* as it goes into a dormancy-like state in culture, J. Bacteriol. 186 (2004) 5017–5030.
[8] E.J. Munoz-Elias, J.D. McKinney, *Mycobacterium tuberculosis* isocitrate lyases 1 and 2 are jointly required for in vivo growth and virulence, Nat. Med. 11 (2005) 638–644.
[9] H.I. Boshoff, C.E. Barry, A low-carb diet for a high-octane pathogen, Nat. Med. 11 (2005) 599–600.
[10] K. Honer zu Bentrup, D.G. Russell, Mycobacterial persistence: adaptation to a changing environment, Trends Microbiol. 9 (2001) 597–605.
[11] P.J. Brennan, H. Nikaido, The envelope of mycobacteria, Annu. Rev. Biochem. 64 (1995) 29–63.
[12] L. Kremer, C. de Chastellier, G. Dobson, K.J. Gibson, P. Bifani, S. Balor, J.P. Gorvel, C. Locht, D.E. Minnikin, G.S. Besra, Identification and structural characterization of an unusual mycobacterial monomeromycolyl–diacylglycerol, Mol. Microbiol. 57 (2005) 1113–1126.
[13] J.C. Camus, M.J. Pryor, C. Medigue, S.T. Cole, Re-annotation of the genome sequence of *Mycobacterium tuberculosis* H37Rv, Microbiology 148 (2002) 2967–2973.
[14] S.T. Cole, R. Brosch, J. Parkhill, T. Garnier, C. Churcher, D. Harris, S.V. Gordon, K. Eiglmeier, S. Gas, C.E. Barry 3rd, F. Tekaia, K. Badcock, D. Basham, D. Brown, T. Chillingworth, R. Connor, R. Davies, K. Devlin, T. Feltwell, S. Gentles, N. Hamlin, S. Holroyd, T. Hornsby, K. Jagels, A. Krogh, J. McLean, S. Moule, L. Murphy, K. Oliver, J. Osborne, M.A. Quail, M.A. Rajandream, J. Rogers, S. Rutter, K. Seeger, J. Skelton, R. Squares, S. Squares, J.E. Sulston, K. Taylor, S. Whitehead, B.G. Barrell, Deciphering the biology of *Mycobacterium tuberculosis* from the complete genome sequence, Nature 393 (1998) 537–544.
[15] T. Hotelier, L. Renault, X. Cousin, V. Negre, P. Marchot, A. Chatonnet, ESTHER, the database of the alpha/beta-hydrolase fold superfamily of proteins, Nucleic Acids Res. 32 (2004) D145–147.
[16] S. Canaan, D. Maurin, H. Chahinian, B. Pouilly, C. Durousseau, F. Frassinetti, L. Scappuccini-Calvo, C. Cambillau, Y. Bourne, Expression and characterization of the protein Rv1399c from *Mycobacterium tuberculosis*. A novel carboxyl esterase structurally related to the HSL family, Eur. J. Biochem. 271 (2004) 3953–3961.
[17] M. Zhang, J.D. Wang, Z.F. Li, J. Xie, Y.P. Yang, Y. Zhong, H.H. Wang, Expression and characterization of the carboxyl esterase Rv3487c from *Mycobacterium tuberculosis*, Protein Expr. Purif. 42 (2005) 59–66.
[18] C. Deb, J. Daniel, T.D. Sirakova, B. Abomoelak, V.S. Dubey, P.E. Kolattukudy, A novel lipase belonging to the hormone-sensitive lipase family induced under starvation to utilize stored triacylglycerol in *Mycobacterium tuberculosis*, J. Biol. Chem. 281 (2006) 3866–3875.
[19] S. Lun, W.R. Bishai, Characterization of a novel cell wall-anchored protein with carboxylesterase activity required for virulence in *Mycobacterium tuberculosis*, J. Biol. Chem. 282 (2007) 18348–18356.
[20] K. Cotes, R. Dhouib, I. Douchet, H. Chahinian, A. de Caro, F. Carriere, S. Canaan, Characterization of an exported monoglyceride lipase from *Mycobacterium tuberculosis* possibly involved in the metabolism of host cell membrane lipids, Biochem. J. 408 (2007) 417–427.
[21] G. Shen, K. Singh, D. Chandra, C. Serveau-Avesque, D. Maurin, S. Canaan, R. Singla, D. Behera, S. Laal, LipC (Rv0220) is an immunogenic cell surface esterase of *Mycobacterium tuberculosis*, Infect. Immun. 80 (2012) 243–253.
[22] J. Guo, X. Zheng, L. Xu, Z. Liu, K. Xu, S. Li, T. Wen, S. Liu, H. Pang, Characterization of a novel esterase Rv0045c from *Mycobacterium tuberculosis*, PLoS One 5 (2010).
[23] C.C. Akoh, G.C. Lee, Y.C. Liaw, T.H. Huang, J.F. Shaw, GDSL family of serine esterases/lipases, Prog. Lipid Res. 43 (2004) 534–552.
[24] J.L. Arpigny, K.E. Jaeger, Bacterial lipolytic enzymes: classification and properties, Biochem. J. 343 (Pt. 1) (1999) 177–183.
[25] E. Henke, U.T. Bornscheuer, R.D. Schmid, J. Pleiss, A molecular mechanism of enantiorecognition of tertiary alcohols by carboxylesterases, Chembiochem: Eur. J. Chem. Biol. 4 (2003) 485–493.
[26] J. Wang, Y. Cao, G. Zheng, Mutation in the RGD motif decreases the esterase activity of Xcc_est, Biotechnol. Lett. 31 (2009) 1445–1449.
[27] C. Vizcaino, D. Restrepo-Montoya, D. Rodriguez, L.F. Nino, M. Ocampo, M. Vanegas, M.T. Reguero, N.L. Martinez, M.E. Patarroyo, M.A. Patarroyo, Computational prediction and experimental assessment of secreted/surface proteins from *Mycobacterium tuberculosis* H37Rv, PLoS Comput. Biol. 6 (2010) e1000824.
[28] K. Beiter, F. Wartha, B. Albiger, S. Normark, A. Zychlinsky, B. Henriques-Normark, An endonuclease allows *Streptococcus pneumoniae* to escape from neutrophil extracellular traps, Curr. Biol. 16 (2006) 401–407.
[29] G. Singh, D. Jadeja, J. Kaur, Lipid hydrolyzing enzymes in virulence: *Mycobacterium tuberculosis* as a model system, Crit. Rev. Microbiol. 36 (2010) 259–269.
[30] A. Sonawane, S. Mohanty, L. Jagannathan, A. Bekolay, S. Banerjee, Role of glycans and glycoproteins in disease development by *Mycobacterium tuberculosis*, Crit. Rev. Microbiol. 38 (2012) 250–266.
[31] J.H. Jeon, S.J. Kim, H.S. Lee, S.S. Cha, J.H. Lee, S.H. Yoon, B.S. Koo, C.M. Lee, S.H. Choi, S.H. Lee, S.G. Kang, Novel metagenome-derived carboxylesterase that hydrolyzes beta-lactam antibiotics, Appl. Environ. Microbiol. 77 (2011) 7830–7836.
[32] L.M. Ouyang, J.Y. Liu, M. Qiao, J.H. Xu, Isolation and biochemical characterization of two novel metagenome-derived esterases, Appl. Biochem. Biotechnol. 169 (2013) 15–28.
[33] R. Dhouib, F. Laval, F. Carriere, M. Daffe, S. Canaan, A monoacylglycerol lipase from *Mycobacterium smegmatis* Involved in bacterial cell interaction, J. Bacteriol. 192 (2010) 4776–4785.
[34] K.C. Mishra, C. de Chastellier, Y. Narayana, P. Bifani, A.K. Brown, G.S. Besra, V.M. Katoch, B. Joshi, K.N. Balaji, L. Kremer, Functional role of the PE domain and immunogenicity of the *Mycobacterium tuberculosis* triacylglycerol hydrolase LipY, Infect. Immun. 76 (2008) 127–140.
[35] H. Chahinian, Y.B. Ali, A. Abousalham, S. Petry, L. Mandrich, G. Manco, S. Canaan, L. Sarda, Substrate specificity and kinetic properties of enzymes belonging to the hormone-sensitive lipase family: comparison with non-lipolytic and lipolytic carboxylesterases, Biochim. Biophys. Acta. 1738 (2005) 29–36.
[36] G.K. Khuller, R. Taneja, S. Kaur, J.N. Verma, Lipid composition and virulence of *Mycobacterium tuberculosis* H37Rv, Aust. J. Exp. Biol. Med. Sci. 60 (Pt. 5) (1982) 541–547.
[37] M.B. Reed, P. Domenech, C. Manca, H. Su, A.K. Barczak, B.N. Kreiswirth, G. Kaplan, C.E. Barry 3rd, A glycolipid of hypervirulent tuberculosis strains that inhibits the innate immune response, Nature 431 (2004) 84–87.
[38] O.A. Trivedi, P. Arora, A. Vats, M.Z. Ansari, R. Tickoo, V. Sridharan, D. Mohanty, R.S. Gokhale, Dissecting the mechanism and assembly of a complex virulence mycobacterial lipid, Mol. Cell 17 (2005) 631–643.

OPEN ACCESS Freely available online

PLoS one

Crystal Structure of a Novel Esterase Rv0045c from *Mycobacterium tuberculosis*

Xiangdong Zheng[1,2☯], Jiubiao Guo[1,2☯], Lipeng Xu[1], Honglei Li[1], Dongwei Zhang[3], Kai Zhang[4], Fei Sun[4], Tingyi Wen[5], Siguo Liu[2]*, Hai Pang[1]*

1 School of Medicine, Tsinghua University, Beijing, China, **2** Harbin Veterinary Research Institute, Chinese Academy of Agriculture, Harbin, China, **3** Department of Oral Biological and Medical Sciences, University of British Columbia, Vancouver, Canada, **4** Institute of Biophysics, Chinese Academy of Sciences, Beijing, China, **5** Department of Industrial Microbiology and Biotechnology, Institute of Microbiology, Chinese Academy of Sciences, Beijing, China

Abstract

There are at least 250 enzymes in *Mycobacterium tuberculosis* (*M. tuberculosis*) involved in lipid metabolism. Some of the enzymes are required for bacterial survival and full virulence. The esterase Rv0045c shares little amino acid sequence similarity with other members of the esterase/lipase family. Here, we report the 3D structure of Rv0045c. Our studies demonstrated that Rv0045c is a novel member of α/β hydrolase fold family. The structure of esterase Rv0045c contains two distinct domains: the α/β fold domain and the cap domain. The active site of esterase Rv0045c is highly conserved and comprised of two residues: Ser154 and His309. We proposed that Rv0045c probably employs two kinds of enzymatic mechanisms when hydrolyzing C-O ester bonds within substrates. The structure provides insight into the hydrolysis mechanism of the C-O ester bond, and will be helpful in understanding the ester/lipid metabolism in *M. tuberculosis*.

Citation: Zheng X, Guo J, Xu L, Li H, Zhang D, et al. (2011) Crystal Structure of a Novel Esterase Rv0045c from *Mycobacterium tuberculosis*. PLoS ONE 6(5): e20506. doi:10.1371/journal.pone.0020506

Editor: Olivier Neyrolles, Institut de Pharmacologie et de Biologie Structurale, France

Received January 4, 2011; **Accepted** May 4, 2011; **Published** May 26, 2011

Funding: This work was financially supported by the Foundation of State Key Laboratory of Veterinary Biotechnology (SKLVBF2009), Harbin Veterinary Research Institute (HVRI), the National Drug Discovery Program (Grant 2008ZX09401-05), the National Natural Science Foundation of China (No. 30770439), the 973 Project of the Major State Basic Research Development Program of China (No. 2006CB504400) and the Tsinghua-Yue-Yuen Medical Sciences Fund (20240000551). The funders had no role in study design, data collection and analysis, decision to publish, or preparation of the manuscript.

Competing Interests: The authors have declared that no competing interests exist.

* E-mail: siguo_liu@yahoo.com.cn (SL); pangh@xtal.tsinghua.edu.cn (HP)

☯ These authors contributed equally to this work.

Introduction

M. tuberculosis is the most prevalent pathogen causing tuberculosis in humans and animals [1]. The bacteria is characterized by an unusual waxy coating on the cell surface (primarily mycolic acid) and it expresses more than 250 enzymes related to ester/lipid metabolism. In contrast, only about 50 enzymes are involved in the ester/lipid metabolism in *Escherichia coli* (*E. coli*) [2,3]. These enzymes in *M. tuberculosis* which catalyze ester/lipid and carbohydrate metabolism are more likely to be required and essential to bacterial existence and survival [4]. In 2007, a cell wall-associated carboxyl esterase, Rv2224c, of *M. tuberculosis* H37Rv was identified as a major virulence gene and was further found to be required for bacterial survival in mice [5]. Rv0045c, participating in ester/lipid metabolism in *M. tuberculosis*, was predicted to be a hydrolase belonging to α/β hydrolase fold family based on bioinformatics studies. However, little is known about its substrate specificity and mechanism of action.

The α/β hydrolase fold was identified in 1992, by comparing five hydrolytic enzymes with widely different catalytic function [6]. Since then, more than 50 members belonging to this family have been identified and characterized by structure determination [7]. The α/β hydrolase fold involves a variety of enzymes including esterases, lipases, epoxide hydrolases, dehalogenases, proteases, and peroxidases, making it one of the most versatile protein families known [8]. The conversed feature of the α/β hydrolase fold has been described as a mostly parallel, eight-stranded β sheet surrounded on both sides by α helices (only the second β strand is antiparallel) [9–11].

The Rv0045c gene encodes a polypeptide chain of 298 amino acids with a putative hydrolase activity. Sequence comparisons show that Rv0045c shares a low sequence identity (<30%) to other members of the α/β hydrolase fold family, however, the consensus sequence G-X-S-X-G of the nucleophile elbow and the catalytic residues are highly conserved. Similar to other α/β hydrolases, it has been previously shown that Rv0045c can hydrolyze ester bonds within a series of *p*-nitrophenyl derivatives (C_2–C_{14}) [12]. The purified enzyme can effectively hydrolyze *p*-nitrophenyl derivatives with short hydrocarbon chains, especially C_2–C_8. We identified *p*-nitrophenyl caproate (C_6) as the most suitable substrate of Rv0045c at the assay conditions of 39°C and pH 8.0 [12].

To understand the active site and enzymatic mechanism of esterase Rv0045c, we determined the crystal structure of the enzyme and performed docking experiments. Our studies clearly revealed that 1) Rv0045c contains two distinguished domains: the α/β fold domain and the cap domain, 2) Rv0045c, from *M. tuberculosis*, is a novel member of α/β hydrolase fold family, and 3) Rv0045c probably employs two kinds of enzymatic mechanisms (indirect and/or direct) where S154 attacks the carbonyl carbon within the C-O ester bond using or without using an activated water molecule.

Results

Structure determination and features of Rv0045c

The purified Rv0045c protein and selenomethionine (Se-Met) labeled Rv0045c protein were crystallized in the same condition (0.2 M $MgCl_2$, 100 mM imidazole, pH 7.0, 19% (*w*/*v*) PEG 4000). However, both crystals revealed different space groups (Table 1). The crystal structure of Rv0045c was determined by SAD and was refined to 2.8 Å resolution. The final model (Fig. 1) of Rv0045c consists of residues 38–193 and 205–329 with the missing residues being not visible in the density maps. The analysis of Ramachandran plot by COOT [13] showed that most of the modeled residues were in preferred and allowed regions (Table 1). The model clearly contains two distinct structural domains: an almost globular α/β fold domain (α1β1β2β3α2α3β4α4β5α5β6α6-α9β9α10β10α11α12) and an inserted cap domain (α7α8β7β8) which interacts with the α/β fold domain.

Table 1. Data collection and refinement statistics.

	Native Rv0045c	SeMet Rv0045c
Data Collection		
Synchrotron	SSRF	PF-BL17A
Wavelength (Å)	1.072	0.9790
Resolution (Å)	50-2.8	50-2.6
Space group	$P3_1$	$P3_121$
Cell-unit parameters (Å)	a = b = 73.465, c = 48.063	a = b = 130.330, c = 48.785
Matthew's coefficient	2.1	3.4
% solvent	41.7	64.0
No. of molecule per ASU	1	1
No. observations	47965	157440
No. unique reflections	7159	14797
Redundancy	6.7 (5.3)	10.6 (8.3)
R_{sym}[a]	0.079 (0.397)	0.144 (0.778)
Mean I/σ_I	26.5 (3.0)	17.7 (2.0)
Completeness (%)	100.0 (100.0)	100.0 (99.7)
Refinement		
Resolution (Å)	38.35-2.8	
No. reflections (total)	6810	
No. reflections (free)	336	
R factor (%)[b]	21.69	
R_{free} (%)[b]	28.57	
Figure of merit	0.8296	
No. of waters	36	
Overall B factor	53.10	
Wilson B factor	80.80	
rmsd bond lengths (Å)[c]	0.0129	
rmsd bond angles (°)[c]	1.570	
Ramachandran plot		
Preferred (%)	93.5	
Allowed (%)	6.1	
Outliers (%)	0.4	

[a]$R_{sym} = \Sigma_h\Sigma_i \mid I_{h,i} - I_h \mid / \Sigma_h\Sigma_i I_{h,i}$, where I_h is the mean intensity of the *i* observations of symmetry-related reflections of *h*.

[b]$R = \Sigma \mid F_{obs} - F_{calc} \mid / \Sigma F_{obs}$, where $F_{obs} = F_P$, and F_{calc} is the calculated protein structure factor from the atomic model (R_{free} was calculated with 5% of the observed reflections).

[c]rmsd (root-mean-square deviation) in bond lengths and angles are the deviations from ideal values.

doi:10.1371/journal.pone.0020506.t001

Structure of the α/β fold domain

Like other members of the α/β hydrolase fold family, the α/β fold domain represents the core of Rv0045c (Fig. 1A and 1B). The α/β fold domain of Rv0045c consists of a mostly parallel, 8-stranded β sheet surrounded by α-helices on both sides (only the second strand is antiparallel), which has been regarded as the "canonical" feature of the α/β hydrolase fold family [8]. The last strand is oriented with a twisting angle of approximately 120° to the first one (Fig. 1B). The topology of β-α-β motifs (β3-α2-α3-β4, β5-α5-β6 and β9-α10-β10) in the centre displays a right-handed super helical twist (Fig. 1C). The α/β hydrolase fold domain provides the stable scaffold for the active site of Rv0045c. Sequence alignments revealed that the "nucleophile elbow" of G-X-S-X-G sequence motif is located in the sharp turn connecting β5 and α5 (Fig. 1C and 2) and is highly conversed among these enzymes (Fig. 2), although Rv0045c shows no significant sequence homology to any other α/β hydrolase fold family member.

Structure of the cap domain

The polypeptide region, Arg205 - Ile252, in Rv0045c forms the cap domain. The cap domain comprises two sequential α-helices (α7, α8) and another two consecutive β-strands (β7, β8). Unlike the α/β fold domain, structural homologies of the cap domain cannot be absolutely identified among the superposed α/β hydrolase fold family members (Fig. 3A and 3B). The alignment and orientation of α-helices and β-strands within the cap domain show a little difference. The inserted cap domain is supposedly related to substrate binding both in E-2AMS hydrolase [14] and esterase ybfF [15] and may provide clues about these two enzymes' substrate specificity, however, no devotion contributed by the cap domain of Rv0045c was revealed when *p*-nitrophenyl caproate was docked into the active site (Fig. 4A and 4B). Residues 194–204 are missed in this domain, for the reason that this region is much more flexible and reveals very poor electron density.

Active site of Rv0045c

The putative active site of Rv0045c was identified via sequence alignment (Fig. 2) and structural homology (Fig. 3) with other α/β fold hydrolases. The active site formed by Ser154 and His309 is shielded by the cap domain. The putative nucleophilic residue Ser154 is located at the beginning of α5. Results of docking experiment indicated that Gly90, Gln92, Leu155, Ile252 and Phe255 help *p*-nitrophenyl caproate locate onto the active site, and that these residues comprise the binding site of Rv0045c (Fig. 4B). Three hydrophobic residues, including Leu155, Ile252 and Phe255, contribute to the stable conformation of the hydrocarbon chain of *p*-nitrophenyl caproate. The substrate is further stabilized by two hydrogen bond contributed by Gly90 and Gln92 (Fig. 4B, blue dotted line). Residues involved in forming active site and binding site devote themselves shaping the active groove (Fig. 4C), which can well accomodate *p*-nitrophenyl caproate (Fig. 4D).

Discussion

The α/β hydrolase fold family has been structurally well characterized and comprises a variety of enzymes including esterases, lipases, epoxide hydrolases, dehalogenases, proteases, and peroxidases, catalyzing myriad reactions. Analysis of the primary sequence for Rv0045c using BLAST suggested that this

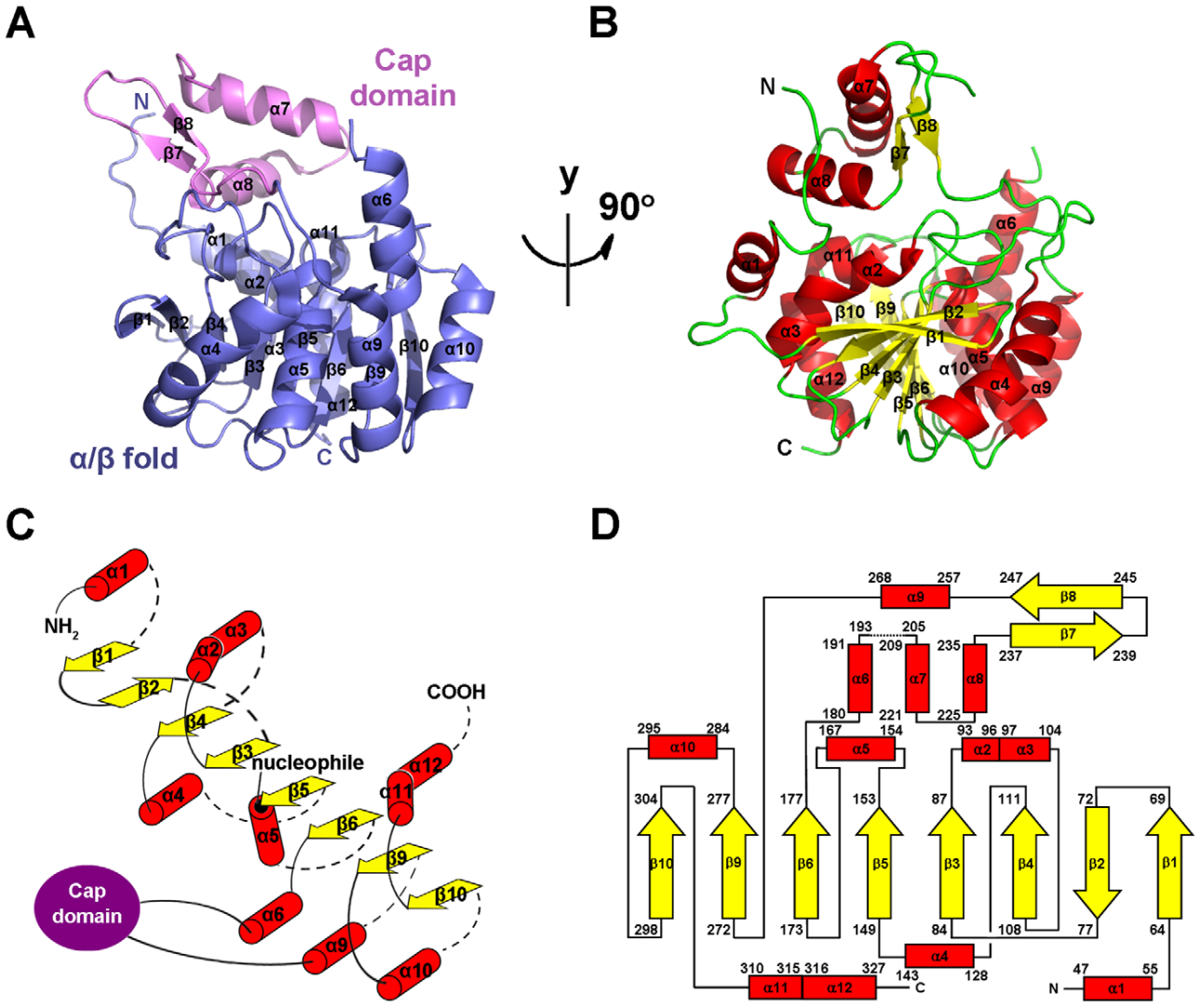

Figure 1. Overall structure of Rv0045c. (A–B) Cartoon representation of Rv0045c in two views related by a vertical rotation of 90 degrees. The secondary structural elements (α1–α12, β1–β10) were labeled. The core structural elements are colored slate and the cap domain in violet (A). α-helices (red) and β-strands (yellow) are differentiated by colors (B). (C) Secondary structure diagram of the α/β fold core of Rv0045c. α-helices, β-strands and the cap domain are represented by red cylinders, yellow arrows and a violet ellipse, respectively. The α/β fold core consists of a mostly parallel, 8-stranded β sheet surrounded on both sides by α-helices (only β2 is antiparallel). The nucleophilic residue, Ser154, positioned at the beginning of α5, is marked with a black dot. (D) Topology diagram of Rv0045c using the same color scheme as (B). The missing region between α6 and α7 (residues 194–204) is represented as dotted line.
doi:10.1371/journal.pone.0020506.g001

enzyme shares little sequence identity to other members of the α/β hydrolase fold family, though the enzyme was structurally characterized to be a novel member of the family. A DALI [16] search was performed using the structure of Rv0045c, and these results confirmed that Rv0045c shows little sequence identity but high structural similarity to other members of the α/β hydrolase fold family. Related members of this family are shown in Table 2, and their similarity to Rv0045c is presented by Z score, rmsd, identity and number of aligned residues [14,15,17–19]. Data of superposition of Rv0045c with E-2AMS hydrolase and esterase ybfF showed that the cores of the three enzymes, which are all comprised of eight stranded β-sheets with α-helices on both sides, overlap with each other (Fig. 3A and 3B). However, there is a little difference in the alignment and orientation of the cap domain. The cap domain of Rv0045c is an insertion between α6 and α9, including two stranded antiparallel β-sheets (β7 and β8) and two α-helices (α7 and α8). This feature is similar to that in E-2AMS hydrolase and esterase ybfF, but the cavity formed by the cap domain and the α/β fold domain in esterase ybfF is a little more expanding. The flexible region in the cap domain, from residue 194 to 204, is not visible in the density map of Rv0045c. The cap domain and the α/β fold domain within Rv0045c provide a wide and open cavity for larger substrates. It is probably that the missing region becomes to be stable and visible when a large substrate is bond to the protein. In that case, the interaction between the cap domain and substrate may transform the flexible region into a stable conformation.

The members of α/β hydrolase fold family utilize a highly conserved catalytic nucleophile which contains a serine, cysteine or aspartic acid residue [8]. The nucleophile of Rv0045c is Ser154,

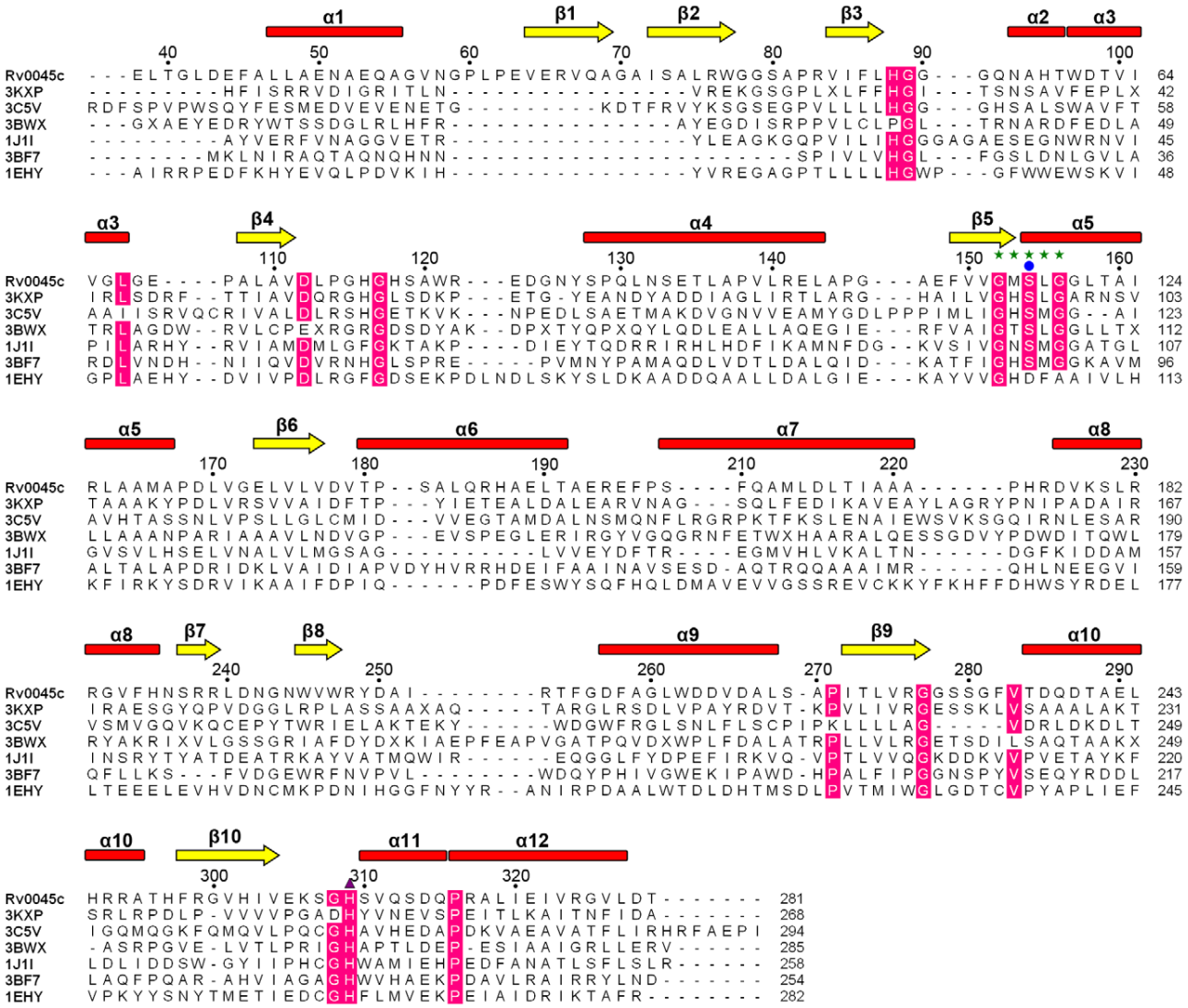

Figure 2. Sequence alignment of Rv0045c with other structurally homologous enzymes. Included enzymes are E-2AMS hydrolase (PDB ID: 3KXP), methylesterase PME-1 (PDB ID: 3C5V), hydrolase YP_496220.1 (PDB ID: 3BWX), CarC enzyme (PDB ID: 1J1I), esterase ybfF (PDB ID: 3BF7) and soluble epoxide hydrolase (PDB ID: 1EHY). Secondary structural elements and every the tenth residue of Rv0045c are indicated above the alignment. The "nucleophile elbow" of G-X-S-X-G sequence motif is marked with green stars and the nucleophilic serine residue Ser with a blue circle. The other catalytic residue is labeled using a purple triangle. Strictly conserved residues with the identity of >80% are highlighted by pink front.
doi:10.1371/journal.pone.0020506.g002

positioned as the first residue at the beginning of α5. The active site of Rv0045c (Ser154 and His309) identified by sequence alignment is highly conserved among the enzymes aligned. Both in E-2AMS hydrolase and esterase ybfF, the cap domain directly contributes to the substrate binding, which is not observed in Rv0045c when *p*-nitrophenyl caproate was docked into the active site. As shown in a docking experiment, when a small substrate, *p*-nitrophenyl caproate, was bound, the cap domain is not involved in the binding of the substrate to the protein. The binding site is located on the surface of the α/β fold domain. Three hydrophobic residues (Leu155 in α5, Ile252 and Phe255 after β8) help the hydrocarbon chain of *p*-nitrophenyl caproate to obtain an optimum conformation to reduce the binding energy. The orientation of the C-O ester bond of *p*-nitrophenyl caproate is stabilized via two hydrogen bonds contributed by Gly90 and Gln92 after β3. It has been already known that Ser is an executive residue in both E-2AMS hydrolase and esterase ybfF [14,15]. To confirm the activity of Ser154 within Rv0045c, we generated a mutant of this enzyme, but no any activity could be detected (data not shown).

A previous study about the biochemical activity of Rv0045c suggested that the enzyme can hydrolyze the ester bond of *p*-nitrophenyl derivatives and *p*-nitrophenyl caproate was identified as the most effective substrate [12]. As an esterase, Rv0045c can hydrolyze the C-O ester bond of *p*-nitrophenyl caproate to produce *p*-nitrophenol and caproic acid (Fig. 5A). In the model of Rv0045c binding *p*-nitrophenyl caproate, the hydroxyl oxygen of Ser154 is 3.2 Å (purple dotted line, Fig. 4B) from the carbonyl carbon of the C-O ester bond of the substrate. The indirect and direct enzymatic mechanisms of Rv0045c can be subsequently hypothesized (Fig. 5B). It is probable that Ser154 interacts with the C-O ester bond indirectly, using an activated water molecule

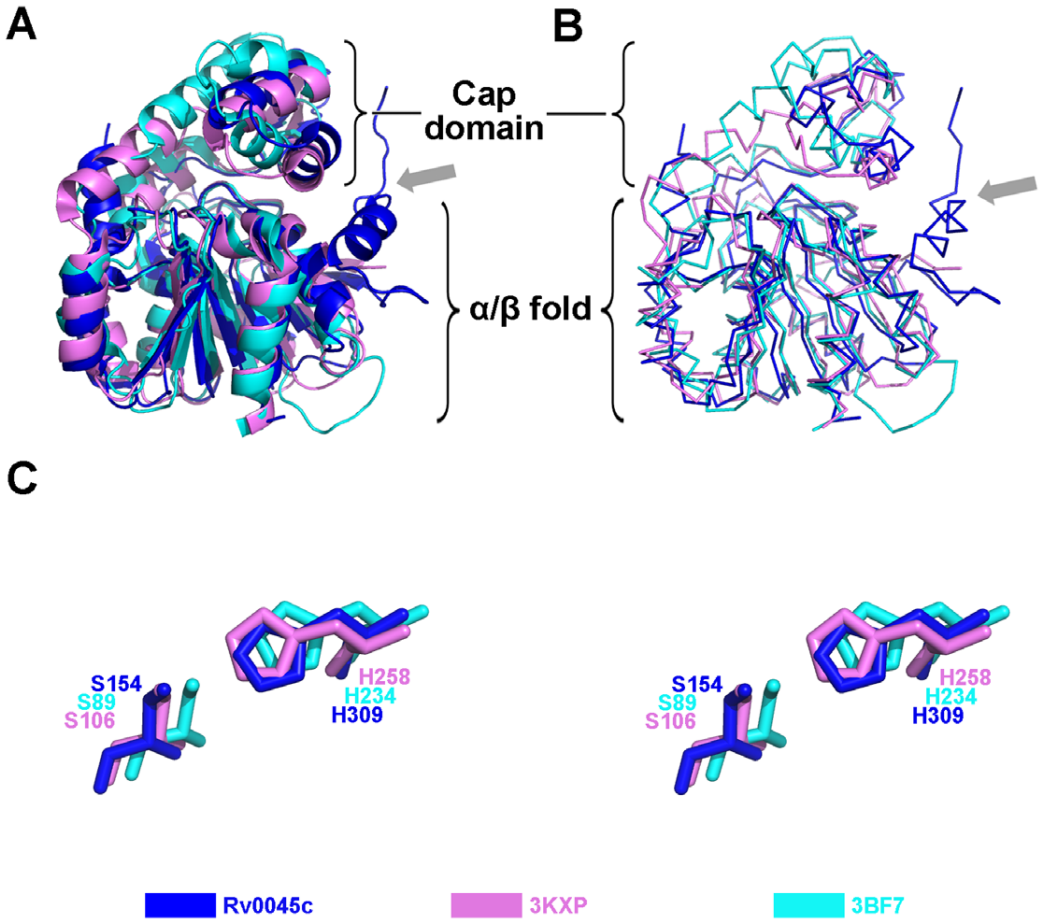

Figure 3. Superposition of Rv0045c with other members of the α/β hydrolase fold family. Cartoon (A) and ribbon (B) diagrams are presented. The α/β fold core of Rv0045c (blue) superposes well with those of E-2AMS hydrolase from *Mesorhizobium loti* (PDB ID: 3KXP) (violet) and esterase ybfF from *Escherichia coli* (PDB ID: 3BF7) (cyan) except for α1 which is marked with a gray arrow. (C) Close-up view of catalytic residues. The catalytic residues of three α/β fold cores are differentiated and labeled using the same color scheme as (A) and (B).
doi:10.1371/journal.pone.0020506.g003

(Mechanism 1, Fig. 5B), for the reason that it is too long (3.2 Å) for Ser154 to directly attack the carbonyl carbon within the C-O ester bond. Similar to the mechanism proposed in the model of E-2AMS hydrolase [14], there must be some small molecules, for instance the water molecules, mediating the hydrolysis reaction. In detail, the hydroxyl oxygen of Ser154 is firstly polarized by adjacent His309 before Ser154 attacks the hydrogen atom of a free water molecule, and then, the activated water molecule attacks the carbonyl carbon within the C-O ester bond.

However, it cannot be ignored that the binding of substrate to Rv0045c may cause conformational change of the enzyme. In that case, Ser154 might be close enough to directly attack the carbonyl carbon within the C-O ester bond and the enzyme employed a direct mechanism (Mechanism 2, Fig. 5B). Rv0045c can catalyze a mount of substrates with hydrocarbon chains of different length. We infer that Rv0045c may adopt different enzymatic mechanisms (direct and/or indirect) when binding different substrates. We have performed co-crystallization with ligands, however, no esterase Rv0045c-substrate complex has been successfully crystallized by now. We will continue to seek the way to get solvable crystals of Rv004c-substrate complex to clarify the catalytic mechanism of Rv0045c.

Tuberculosis is a contagious respiratory system disease, which is caused by *M. tuberculosis* via infecting the lungs of mammalian. *M. tuberculosis* can tolerate and withstand rigorous condition and weak disinfectants to survive in a dry state for weeks. It was reported that the unusual cell wall, rich in lipids, is likely responsible for this resistance [20]. Rv0045c is proposed to be an esterase or hydrolase involved in lipid metabolism. Our study determines for the first time the structure of Rv0045c and will give further insight into the mechanism of esters or lipids hydrolysis in *M. tuberculosis*. This work will help to design and screen inhibitors against Rv0045c to verify the function and role of this enzyme in *M. tuberculosis*.

Materials and Methods

Protein preparation

The expression construct was generated using a standard PCR procedure. Full-length Rv0045c was sub-cloned into pET28a vector (Invitrogen). The production induced with 0.3 mM IPTG was overexpressed at 16°C for 20 h in *E. coli* BL21 (DE3) strain (Novagen). The soluble fraction of Rv0045c from cell lysate was purified by Ni Sepharose™ 6 Fast Flow resin (GE Healthcare) to homogeneity and further polished by ion-exchange chromatography (Resource Q and S 1 mL, GE Healthcare) and gel filter chromatography (Superdex 75 10/300 GL, GE Healthcare). Se-Met labeled Rv0045c was produced by growing the *E. coli* cells in a minimum medium containing selenomethionine and purified in the same way as described above.

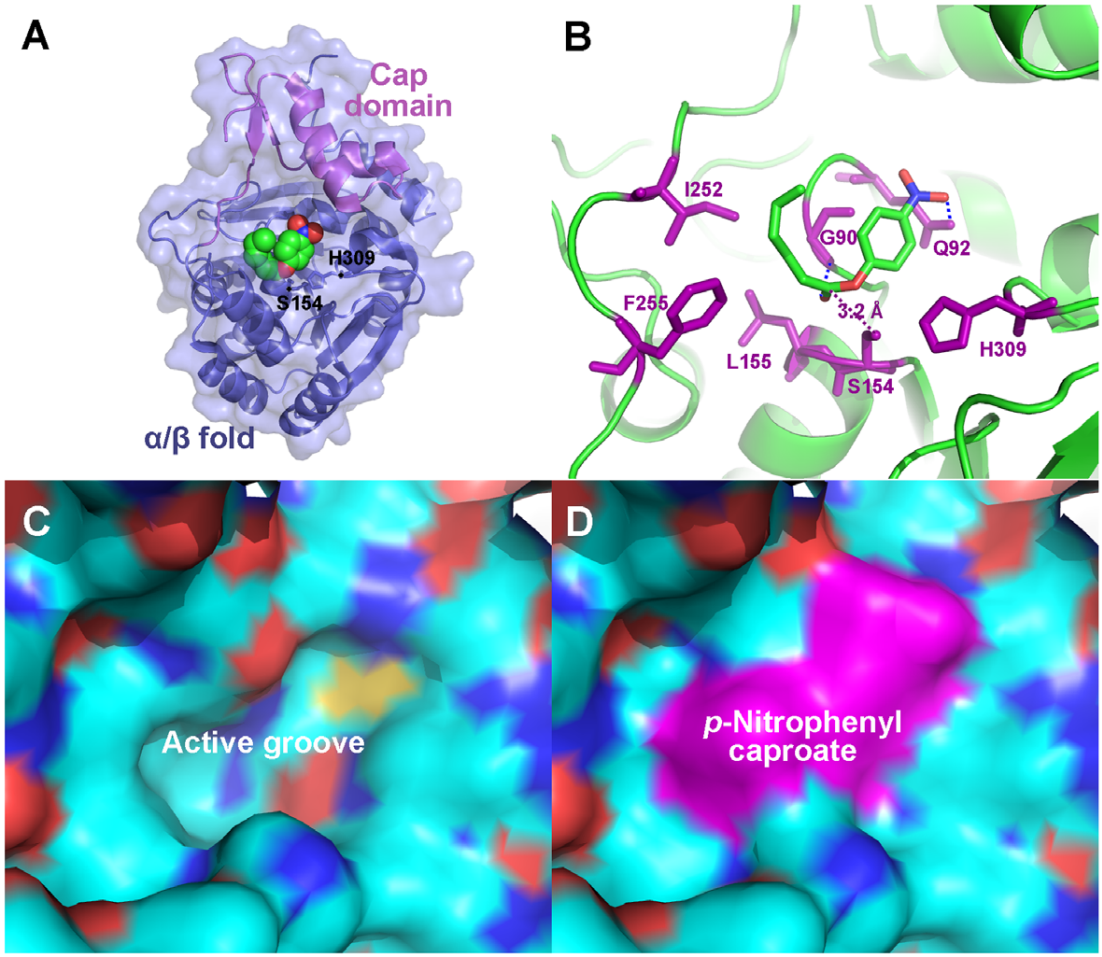

Figure 4. Modeling of *p*-nitrophenyl caproate in the active site of Rv0045c. (A) The modeled *p*-nitrophenyl caproate, which is displayed as space-filling pattern, was bound to the active site under the cap domain. The cap domain and α/β fold of Rv0045c are differentiated by colors. Ser154 and His309 within the active site are labeled. (B) Ribbon diagram of the binding site and active site of Rv0045c with *p*-nitrophenyl caproate manually modeled. The binding site is formed by Gly90, Gln92, Leu155, Ile252 and Phe255. The compound was stabilized by two hydrogen bound (shown as blue dotted line) contributed by Gly90 and Gln92. The binding site and active site constitute the active groove (C) on the surface of Rv0045c and the modeled *p*-nitrophenyl caproate fits it quite well (D).
doi:10.1371/journal.pone.0020506.g004

Table 2. Enzymes Identified as Structurally Homologous to Rv0045c through DALI.

	PDB ID	Z score	rmsd (Å)	Identity (%)	NRES[a]	RN[b]
E-2AMS hydrolase	3KXP	28.3	2.3	24	268	14
Methylesterase PME-1	3C5V	24.3	2.9	20	294	17
hydrolase YP_496220.1	3BWX	24.3	3.2	21	285	
CarC enzyme	1J1I	23.8	2.7	18	258	18
esterase ybfF	3BF7	23.1	3.0	20	254	15
soluble epoxide hydrolase	1EHY	23.0	3.0	17	282	19

[a]NRES = No. of aligned residues.
[b]RN = Reference Number.
doi:10.1371/journal.pone.0020506.t002

Crystallization and data collection

The diffracting crystals of native and Se-Met labeled Rv0045c were grown at 16°C using the hanging-drop vapor-diffusion method by mixing 1 µL protein (5 mg/mL) with an equal volume of reservoir solution. The Crystal Screen kit I and Crystal Screen kit II of Hampton Research (Aliso Viejo, CA, USA) were used for preliminary screen. Both the native and Se-Met labeled Rv0045c were crystallized in the same condition consisting of 0.2 M $MgCl_2$, 100 mM Tris-HCl pH 8.5, 30% (*w*/*v*) PEG4000 with, however, the different space groups. The native crystals are in the space group $P3_1$, with unit cell parameters a = b = 73.465 Å, c = 48.063 Å, and the Se-Met labeled crystals in $P3_121$ with a = b = 130.330 Å, c = 48.785 Å. For data collection, 20% (v/v) glycerol was added to the crystallizing precipitant as a cryoprotectant and the crystals were flash frozen in a −173°C nitrogen-gas stream. A complete 2.8 Å native dataset and a complete 2.6 Å Se-Met MAD dataset were respectively collected on beamline BL17U at Shanghai Synchrotron Radiation Facility (SSRF, Shanghai, China) and beamline BL17A at the Photon Factory (Tsukuba, Japan) and processed using the HKL-2000 program package [21].

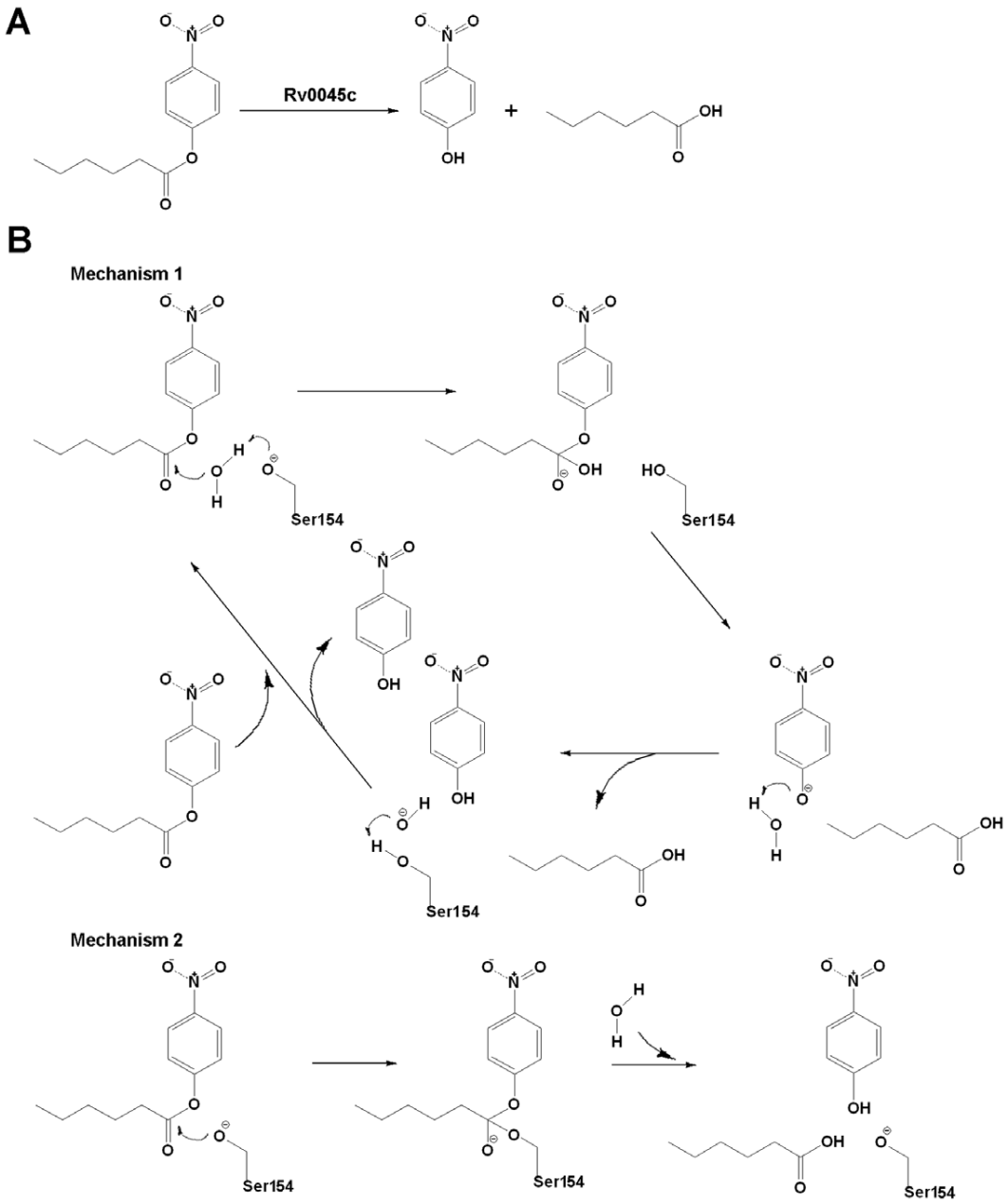

Figure 5. Proposed mechanisms for the hydrolysis of *p*-nitrophenyl caproate. (A) The reaction for the hydrolysis of *p*-nitrophenyl caproate by Rv0045c. Rv0045c hydrolyzes *p*-nitrophenyl caproate to produce *p*-nitrophenol and caproic acid. (B) Proposed mechanisms for the hydrolysis reaction. Mechanism 1 utilizes Ser154 to activate a water molecule for attacking the carbonyl carbon of the C-O ester bond. Mechanism 2 utilizes Ser154 to directly attack the carbonyl carbon of the C-O ester bond.
doi:10.1371/journal.pone.0020506.g005

Structure determination

The structure of Rv0045c was determined by single-wavelength anomalous dispersion (SAD). Selenium atom coordinates were determined using the HKL2MAP [22] program suite and initial SAD phases were calculated and improved with the program SOLVE/RESOLVE [23,24]. The residues of Rv0045c were built manually using the program COOT [13] and the refinement was performed with CCP4 refmac5 [25]. The Rv0045c crystal structure has been refined to 2.8 Å resolution and working and free R factors are 21.69% and 28.57%, respectively. The PyMOL (http://www.pymol.org) molecular graphics program of DeLano Scientifics was used to present the final structure and to produce figures. The data statistics are summarized in Table 1.

Docking experiment

For docking experiment, the AutoDockTool [26–28] software was used for macromolecule and ligand preparing, macromolecule-ligand docking and result analysis. The orientations of nitro-group and hydrocarbon chain of *p*-nitrophenyl caproate were allowed to rotate until the favorable docking position and conformation were found. The docking did not require reorientation of the macromolecule side chains.

Accession numbers

The atomic coordinates and structure factors of Rv0045c (PDB ID: 3P2M) have been deposited in the Protein Data Bank (www.pdb.org).

Acknowledgments

We thank Qiangjun Zhou of Institute of Biophysics, Chinese Academy of Sciences, for assistance during X-ray diffraction data collection and structure determination.

Author Contributions

Conceived and designed the experiments: HP SL. Performed the experiments: XZ JG LX HL DZ KZ FS TW. Analyzed the data: XZ JG. Contributed reagents/materials/analysis tools: HP SL. Wrote the paper: XZ JG.

References

1. Ryan KJ, Ray CG (2004) Sherris Medical Microbiology (4th Ed.). Hightstown: McGraw-Hill.
2. Cole ST, Brosch R, Parkhill J, Garnier T, Churcher C, et al. (1998) Deciphering the biology of *Mycobacterium tuberculosis* from the complete genome sequence. Nature 393: 537–544.
3. Camus JC, Pryor MJ, Médigue C, Cole ST (2002) Re-annotation of the genome sequence of *Mycobacterium tuberculosis* H37Rv. Microbiology 148: 2967–2973.
4. Sassetti CM, Rubin EJ (2003) Genetic requirements for mycobacterial survival during infection. Proc Natl Acad Sci U S A 100: 12989–12994.
5. Lun S, Bishai WR (2007) Characterization of a novel cell wall-anchored protein with carboxylesterase activity required for virulence in *Mycobacterium tuberculosis*. J Biol Chem 282: 18348–18356.
6. Ollis DL, Cheah E, Cygler M, Dijkstra B, Frolow F, et al. (1992) The alpha/beta hydrolase fold. Protein Eng 5: 197–211.
7. Heikinheimo P, Goldman A, Jeffries C, Ollis DL (1999) Of barn owls and bankers: a lush variety of alpha/beta hydrolases. Structure 7: R141–R146.
8. Nardini M, Dijkstra BW (1999) Alpha/beta hydrolase fold enzymes: the family keeps growing. Curr Opin Struct Biol 9: 732–737.
9. Hubbard TJ, Ailey B, Brenner SE, Murzin AG, Chothia C (1998) SCOP, Structural Classification of Proteins database: applications to evaluation of the effectiveness of sequence alignment methods and statistics of protein structural data. Acta Crystallogr D Biol Crystallogr 54: 1147–1154.
10. Orengo CA, Martin AM, Hutchinson G, Jones S, Jones DT, et al. (1998) Classifying a protein in the CATH database of domain structures. Acta Crystallogr D Biol Crystallogr 54: 1155–1167.
11. Cousin X, Hotelier T, Giles K, Toutant JP, Chatonnet A (1998) aCHEdb: the database system for ESTHER, the alpha/beta fold family of proteins and the Cholinesterase gene server. Nucleic Acids Res 26: 226–228.
12. Guo JB, Zheng XD, Xu LP, Liu ZY, Xu KH, et al. (2010) Characterization of a Novel Esterase Rv0045c from *Mycobacterium tuberculosis*. PLoS ONE 5: e13143.
13. Emsley P, Cowtan K (2004) Coot: model-building tools for molecular graphics. Acta Crystallogr D Biol Crystallogr 60: 2126–2132.
14. McCulloch KM, Mukherjee T, Begley TP, Ealick SE (2010) Structure determination and characterization of the vitamin B6 degradative enzyme (E)-2-(acetamidomethylene)succinate hydrolase. Biochemistry 49: 1226–1235.
15. Park SY, Lee SH, Lee J, Nishi K, Kim YS, et al. (2008) High-resolution structure of ybfF from *Escherichia coli* K12: a unique substrate-binding crevice generated by domain arrangement. J Mol Biol 376: 1426–1437.
16. Holm L, Rosenström P (2010) Dali server: conservation mapping in 3D. Nucleic Acids Res 38: W545–549.
17. Xing Y, Li Z, Chen Y, Stock JB, Jeffrey PD, et al. (2008) Structural mechanism of demethylation and inactivation of protein phosphatase 2A. Cell 133: 154–163.
18. Habe H, Morii K, Fushinobu S, Nam JW, Ayabe Y, et al. (2003) Crystal structure of a histidine-tagged serine hydrolase involved in the carbazole degradation (CarC enzyme). Biochem Biophys Res Commun 303: 631–639.
19. Nardini M, Ridder IS, Rozeboom HJ, Kalk KH, Rink R, et al. (1999) The x-ray structure of epoxide hydrolase from *Agrobacterium radiobacter* AD1. An enzyme to detoxify harmful epoxides. J Biol Chem 274: 14579–14586.
20. Murray PR, Rosenthal KS, Pfaller MA (2005) Medical Microbiology (5th Ed.). Philadelphia: Elsevier Mosby.
21. Otwinowski Z, Minor W (1997) Processing of X-ray diffraction data collected in oscillation mode. Method Enzymol 276: 307–326.
22. Pape T, Schneider TR (2004) *HKL2MAP*: a graphical user interface for macromolecular phasing with *SHELX* programs. J Appl Crystallogr 37: 843–844.
23. Terwilliger TC (2002) Automated structure solution, density modification and model building. Acta Crystallogr D Biol Crystallogr 58: 1937–1940.
24. Terwilliger T (2004) SOLVE and RESOLVE: automated structure solution, density modification and model building. J Synchrotron Radiat 11: 49–52.
25. Murshudov GN, Vagin AA, Dodson EJ (1997) Refinement of macromolecular structures by the maximum-likelihood method. Acta Crystallogr D Biol Crystallogr 53: 240–255.
26. Goodsell DS, Olson AJ (1990) Automated docking of substrates to proteins by simulated annealing. Proteins 8: 195–202.
27. Morris GM, Goodsell DS, Huey R, Olson AJ (1996) Distributed automated docking of flexible ligands to proteins: parallel applications of AutoDock 2.4. J Comput Aided Mol Des 10: 293–304.
28. Morris GM, Goodsell DS, Halliday RS, Huey R, Hart WE, et al. (1998) Automated docking using a Lamarckian genetic algorithm and an empirical binding free energy function. J Comput Chem 19: 1639–1662.

Research in Veterinary Science 90 (2011) 385–391

Contents lists available at ScienceDirect

Research in Veterinary Science

journal homepage: www.elsevier.com/locate/rvsc

Molecular characterization of *Mycobacterium tuberculosis* complex (MTBC) isolated from cattle in northeast and northwest China

Yanfen Du [a,1], Yingfang Qi [a,1], Lu Yu [b], Jingkai Lin [a], Siguo Liu [a,*], Hongbo Ni [c], Hai Pang [d], Huifang Liu [a], Wei Si [a], Hailing Zhao [a], Chunlai Wang [a]

[a] Division of Bacterial Diseases, National Key Laboratory of Veterinary Biotechnology, Harbin Veterinary Research Institute, Chinese Academy of Agricultural Sciences, Harbin 15000, PR China
[b] Institute of Zoonosis, College of Animal Science and Veterinary Medicine, Jilin University, Changchun 130052, China
[c] College of Animal Science and Technology of Hei Long Jiang August First Reclamation Land University, Daqing 163319, China
[d] School of Medicine, Tsinghua University, Hai'dian District, Beijing 100084, China

ARTICLE INFO

Article history:
Received 2 February 2010
Accepted 20 July 2010

Keywords:
Mycobacterium tuberculosis complex (MTBC)
Molecular epidemiology
Genotyping

ABSTRACT

We studied throat swabs and corresponding serum samples collected from 1067 protein purified derivative (PPD)-tuberculin skin test (TST) positive cattle from different regions of China. The 1067 throat swabs were inoculated onto modified Löwenstein–Jensen medium for the isolation and culture of Mycobacteria. Acid-fast bacilli were identified using traditional biochemical methods, polymerase chain reaction (PCR) amplification and multiplex PCR. They were distinguished as *Mycobacterium tuberculosis* complex (MTBC) and non-tuberculous mycobacteria (NTM) strains. An indirect Enzyme-Linked Immunosorbent Assay (ELISA) was applied to detect specific antibodies against bovine TB (bTB). Correlations among the ELISA, bacteriology and TST were analyzed and compared. Spoligotyping and variable number tandem repeats–mycobacterial interspersed repetitive unit (VNTR–MIRU) analysis were used to genotype the MTBC. In total, 111 strains of Mycobacteria were cultured from the 1067 throat swab samples, including 43 stains of MTBC (14 strains of *Mycobacterium bovis* and 29 of *Mycobacterium tuberculosis*) and 68 strains of NTM. Thirty-eight MTBC strains and four NTM strains were isolated from 72 throat swab samples that the ELISA determined were antibody positive; five MTBC strains and 64 NTM strains were isolated from 995 throat swab samples that were antibody negative on the ELISA. The positive isolation rates of MTBC and NTM were 38.7% (43/111) and 61.3% (68/111), respectively. The concordance rate of cultured MTBC with a positive result on the indirect ELISA for antibody was 52.8% (38/72), which was much higher than the positive rate for TST (4.0%; 43/1067). Genotyping of the 43 strains of MTBC isolated, using spoligotyping and VNTR–MIRU, showed that the 43 isolates had 26 genotypes; 16 strains had a unique genotype. Two groups of six strains and two strains, respectively, showed the same spoligotyping pattern, and belonged to the Beijing family and Beijing-like family, respectively. Combined application of spoligotyping and VNTR–MIRU typing would improve the molecular epidemiological investigation and monitoring of the etiology of bTB in China.

1. Introduction

Bovine tuberculosis (bTB) is a chronic consumptive zoonosis, which is caused by *Mycobacterium bovis* (*M. bovis*) and *Mycobacterium tuberculosis* (*M. tuberculosis*). Classical members of the *M. tuberculosis* complex (MTBC) are *M. tuberculosis, M. bovis*, *M. bovis* BCG, *M. africanum*, and three uncommon members, namely *M. microti*, *M. canettii*, and *M. pinnipedii*. These bacteria have a wide host range. The wide host range means that the bacteria can cause TB in cattle and humans, as well as in other domestic and wild animals. Tuberculosis causes serious harm to the cattle industry and to public health. *M. bovis* was a historical source of tuberculosis in humans, who became infected by inhaling aerosols or drinking unpasteurized milk from diseased farm animals (Mignard et al., 2006). In some developing countries, a high prevalence of bTB has brought great economic losses and trade restrictions on animal husbandry (The Center for Food Security & Public Health. Bovine TB. BTUB_A2007), and the disease is also a major threat to some endangered species (Lantos et al., 2003). Therefore, the prevention and control of bTB has great significance for public and animal health.

* Corresponding author. Address: Division of Bacterial Diseases, National Key Laboratory of Veterinary Biotechnology, Harbin Veterinary Research Institute, Chinese Academy of Agricultural Sciences, 427 Maduan Street, Harbin 150001, PR China. Tel.: +86 451 859 35076; fax: +86 0451 827 33132.
E-mail address: siguo_liu@yahoo.com.cn (S. Liu).
[1] Both authors contributed equally to this work.

0034-5288/$ - see front matter © 2010 Elsevier Ltd. All rights reserved.
doi:10.1016/j.rvsc.2010.07.020

With the emergence of drug-resistant strains and increasing numbers of self-employed cattle-breeding households, the incidence of bTB in China has increased yearly. Therefore, the bTB epidemic is attracting increasing attention in China. Two national surveys of cows, conducted in 1985 and 1987, showed the prevalence rates of bTB to be 5.83% and 5.43%, respectively (Xu et al., 1998). Three national epidemiological surveys of bTB, in 1979, 1985 and 1990, showed the proportion of human TB cases caused by *M. bovis* to be 3.8%, 4.2% and 6.4%, respectively (Xu et al., 1998). Since then, no national survey data have been reported. However, local epidemic surveys show that the situation is still not optimistic for control of this disease. Therefore, it is necessary to understand the spread and prevalence of bTB in China and to develop a practical plan to eliminate it.

The development of genotyping technology has given a deeper understanding of the spread of bTB, and has great significance for its effective control and the understanding of its spread in wild host reservoirs (Durret et al., 2000; Michel et al., 2008). The most widely used genotyping technologies include IS*6110* restriction fragment length polymorphism (IS*6110*–RFLP) (van Embden et al., 1993), spoligotyping (Kamerbeek et al., 1997) and variable number tandem repeats–mycobacterial interspersed repetitive unit (VNTR–MIRU) typing (Frothingham and Meeker-O'Connell, 1998; Mazars et al., 2001). In this study, we aimed at a preliminary understanding of the prevalence of bTB in China using these techniques. We intended to identify genetic differences and to establish effective genotyping methods, with the ultimate aim of the prevention and control of bTB.

2. Materials and methods

2.1. Bovine PPD, samples, reference Mycobacterial strains and recombinant protein

The bovine purified protein derivative (PPD) was produced by Harbin Pharmaceutical Group, the First Bioproduct Manufactory of Heilongjiang. The freeze-dried batch number in 2006 was 080078024; the specifications were 5 mL per bottle and 10,000 IU/mL. During 2007–2008, 1067 tuberculin skin test (TST) positive bovine throat swabs and corresponding bovine serum samples were collected from northeast (tow cow herds) and northwest (four cow herds) China. The TST for cows was performed by experienced veterinarians, as specified in the Chinese Standard for Diagnostic Techniques for Tuberculosis of Animals (GB/T 18645-2002). After clipping one third of the central lateral neck, each cow, regardless of size, was given an intradermal injection of 0.1 mL (2000 IU) of bovine PPD. The skin thickness at the injection sites was measured using vernier calipers and recorded immediately before the injection and 72 h later. A positive response was defined as an increase in skin thickness at the injection site of 4 mm, while an increase between 2 and 4 mm was inconclusive; otherwise the result was recorded as negative.

The reference strain *M. tuberculosis* H37Rv was purchased from the National Institute for the Control of Pharmaceuticals, and *M. bovis* BCG was kept in our laboratory.

Three antigen genes specific for *M. bovis*, namely *mpb70*, *mpb83*, and *esat-6*, were recombined in tandem using spliced overlap extension technology and expressed in *Escherichia coli* to obtain the recombinant protein MPB70-83-E6 (rMPB70-83-E6) (Liu et al., 2007).

2.2. Mycobacterial culture and identification

The preparation of modified Löwenstein–Jensen medium, the isolation and culture of Mycobacteria, and biochemical tests for the identification of bacterial type followed the standard techniques for diagnosing animal tuberculosis: GB/T18645-2002 (Diagnostic techniques for TB of animal. GB/T 18645-2002). Subspecies of *Mycobacterium* were identified using PCR methods (Telenti et al., 1993; Mcnabb et al., 2004). The subspecies of MTBC were differentiated further using multiplex PCR methods (Huard et al., 2003; Bakshi et al., 2005).

2.3. Serum antibody detection

Antibodies against bTB in serum were detected by the Enzyme-Linked Immunosorbent Assay (ELISA) method, according to Liu et al. (2007). The recombinant protein rMPB70-83-E6 was used to coat the wells of 96-well ELISA plates. The serum samples were diluted with 1× PBST (PBS with 0.05% Tween 20) at 1:200 before testing. Horseradish peroxidase (HRP)-conjugated rabbit anti-bovine immunoglobulins (Sigma) were used at a dilution of 1:5000. On the basis of the optical density (OD) 450 values of the samples, and of the positive and negative controls, the following formula was used to calculate the titer (S/P) of the sample serum: S/P = (difference in OD450 values between the samples and negative controls)/(difference in OD450 values between the positive and negative controls). The results were interpreted as positive when the S/P value $\geqq 0.5$; if S/P < 0.4, the reaction was negative; if $0.5 > S/P \geqq 0.4$, infection was suspected and the assay was repeated.

2.4. Preparation of chromosomal DNA

Genomic DNA was extracted as described by van Soolingen et al. (1991), with the following modifications. A loopful of cells were suspended in 400 μL TE buffer (10 mM Tris-Cl, 1 mM EDTA, pH 8.0), and inactivated at 80 °C for 30 min after centrifugation at 5000*g*. The supernatant was discarded and the pellet was resuspended in 10% sodium dodecyl sulfate (SDS) to a final concentration of 1%. After incubation with 3 μL proteinase K (20 μg/mL) at 37 °C for 2 h, the suspension was re-centrifuged and the supernatant was extracted with an equal volume of Phenol/Chloroform/Isoamyl Alcohol (25:24:1 (v/v)). The supernatant was diluted with a double volume of anhydrous ethanol for 10 min and precipitated at −20 °C after centrifugation at 12,000*g* for 20 min. The precipitate was washed twice with 70% ethanol, placed at room temperature for 20 min to evaporate the alcohol, then dissolved in 40 μL sterile deionised water and stored at −20 °C.

2.5. Spoligotyping

Spoligotyping kits and Mini-blotter MN45 were obtained from Isogen Life Science Co. (Utrecht, the Netherlands). The Streptavidin-ß-peroxidase conjugate was produced by Roche Applied Science Co. (Penzberg, Germany). The enhanced chemiluminescence (ECL) detection system was from Amersham Bioscience Inc. (Madison, WA, USA). The spoligotyping was performed with commercially available activated Biodyne C membranes with 43 synthetic oligonucleotides bound covalently to the membranes, as described by Kamerbeek et al. (1997) and the manufacturer, using a commercial kit (Isogen Bioscience BV, Maarssen, the Netherlands).

First, the direct repeat (DR) locus of each isolate was amplified by PCR and the biotin-labeled PCR amplification products were hybridized with Biodyne C membranes. The hybridization signals were detected by ECL after washing the membranes. Sterile deionised water was taken as the negative control and *M. tuberculosis* H37Rv and *M. bovis* BCG as positive controls. The data were analyzed using BioNumerics software (version 3.0, Applied Maths, Kortrijik, Belgium). The hybridization patterns were converted into binary and octal formats according to Dale et al. (2001) and compared with previously reported strains in the SpolDB4 (2006) database.

2.6. MIRU–VNTR

Based on the published literature (Roring et al., 2002; Savine et al., 2004; Yan et al., 2005) and a bacterial genome database (http://minisatellites.u-psud.fr), 13 tandem repeat loci were screened and primers were designed (Table 1) for PCR amplification. The PCR was performed using the same reagent conditions as above. The PCR amplification consisted of an initial 5 min for denaturation at 95 °C, 30 cycles of 94 °C for 1 min, annealing at 56 °C (or 58 °C) for 45 s, extension at 72 °C for 1 min and a final elongation at 72 °C for 7 min. The PCR product was detected using 2% agarose gel electrophoresis and a UV imaging detection system and compared with 100 bp DNA markers to determine the molecular weight of the PCR product. The fingerprints of the strains detected by PCR amplification were evaluated using AlphaEase® FC software (Alpha Innotech, USA), which defined the number of repeat units at each VNTR locus of every strain. This was followed by cluster analysis using the BioNumerics 3.0 database software and genotyping of the detected strains.

3. Results

3.1. Bacterial isolates and identification

A total of 111 strains of mycobacteria were isolated and cultured, include 43 MTBC strains (rate of 38.7% (43/111)) and 68 NTM strains (rate of 61.3% (68/111)), giving an isolation rate of 10.4% (111/1067). Biochemical testing and multiplex PCR showed that 29 strains of *M. tuberculosis* and 14 strains of *M. bovis* were identified from the 43 MTBC strains (Table 2).

3.2. Comparisons of detection rates using TST, ELISA and bacteriology

We performed ELISA on the collected TST positive bovine sera and bacteriological testing on the throat swabs for comparison. From 1067 positive bovine sera, based on TST, 72 bovine sera were detected to be positive and 995 bovine sera were detected as negative by ELISA. In total 111 strains of mycobacteria (43 MTBC strains and 68 NTM strains) were isolated from 1067 PPD-positive bovine throat swabs. Thirty-eight MTBC strains and four NTM strains were isolated from throat swabs from 72 cows in which the ELISA detected antibodies; five MTBC strains and 64 NTM strains were isolated from throat swabs from 995 cows that were negative for antibodies on the ELISA.

In comparison with the isolation of MTBC, the concordance rate of ELISA was 52.8% (38/72), the concordance rate of TST was 4.0% (43/1067) (Table 2).

Table 2
Comparision of detection rates among TST, ELISA, and bacteriology.

	TST positive	Culture		Total
		MTBC	NTM	
ELISA				
Positive	72	38	4	42
Negative	995	5	64	69
Total	1067	43	68	111

Note: Comparison between TST positive and bacteriological culture: the mycobacterial isolate rate was 10.4% (111/1067), MTBC isolation rate was 4.0% (43/1067), NTM isolate rate was 6.4% (68/1067). The NTM positive rates were 61.3% (68/111); the isolation rate of MTBC were 38.7% (43/111) respectively. The rate of concordance between the TST and ELISA was 6.7% (72/1067). Comparison between ELISA and bacteriological culture: the mycobacterial isolation rate was 58.3% (42/72), the MTBC isolation rate was 52.8% (38/72), the NTM isolation rate was 5.6% (4/72).

3.3. Spoligotyping

The spoligotyping result showed that the 43 MTBC isolates had 26 genotypes, 16 of which were unique. The largest genotype contained six strains (13.9%; 6/43) and showed a common "Beijing family" spoligotyping spectrum. In addition; this genotype shows two difference from the Beijng genotype, and is known as the "Beijing-like family" (Fig. 1).

Table 1
Primer sequence of 13 VNTR locus.

	Locus name	Primers	Repeat units Size (bp)	H37Rv		BCG	
				Copy number	PCR product size (bp)	Copy number	PCR product size (bp)
1	ETR-A	L: ATTTCGATCGGGATGTTGAT R: TCGGTCCCATCACCTTCTTA	75	3.4	257	8.4	632
2	ETR-C	L: GACTTCAATGCGTTGTTGGA R: GTC TTGACC TCC ACGAGT GC	58	3.6	211	4.6	269
3	Miru04	L: GCGCGA GAGCCC GAA CTGC R: GCGCAGCAGAAA CGT CAGC	77	3.3	252	4.8	366
4	Miru10	L:GTTCTTGACCAACTGCAGTCGTCC R:GCCACCTTGGTGATCAGCTACCT	53	3.0	156	2.0	103
5	Miru16	L:TCGGTGATCGGGTCCAGTCCAAGTA R:CCCGTCGTGCAGCCCTGGTAC	53	2.2	118	2.2	118
6	Miru27	L:TCGAAAGCCTCTGCGTGCCAATAA R:GCGATGTGAGCGTGCCACTCAA	53	3.5	183	3.5	183
7	Miru31	L:ACTGATTGGCTTCATACGGCTTTA R:GTGCCGACGTGGTCTTGAT	53	3.1	164	3.1	164
8	Miru40	L:AAGCGCAAGAGCACCAAG R:GTGGGCTTGTACTTGCGAAT	54	1.0	53	2.4	126
9	Mtub21	L:AGATCCCAGTTGTCGTCGTC R:CAACATCGCCTGGTTCTGTA	57	2.0	118	2.6	148
10	Mtub30	L:AGTCACCTTTCCTACCACTCGTAAC R:ATTAGTAGGGCACTAGCACCTCAAG	58	1.9	111	3.9	227
11	Mtub38	L:GCCCAAAAAGCATGGGAACGTGCCCCT R:GGTTGTCCCCGCAGTATCTC	63 (36)	2.7	168	3.8	134
12	Qub-11a	L:CCCATCCCGCTTAGCACATTCGTA R:TTCAGGGGGGATCCGGGA	69	3.0	208	10	692
13	Qub-11b	L:CGTAAGGGGGATGCGGGAAATAGG R:CGAAGTGAATGGTGGTGGCAT	69	5.2	362	4.2	293

Fig. 1. Identification of isolates from cows using spoligotyping. Identification of isolates from cows using spoligotyping. Some strains (such as 08018, 08020, 08066, 08067, 08068, 08072, 08J10 and 08J11) represent bovine *M. tuberculosis* isolates with the typical pattern of the Beijing-family genotype. *M. tuberculosis* H37Rv and *M. bovis* BCG were used as the controls. The negative control did not have target DNA.

3.4. MIRU–VNTR

All the detected strains showed different genotypes using this technique. Allele polymorphisms of loci 1, 12 and 13 were most common, whereas polymorphisms of loci 3, 4 and 11 were less frequent. The DNA fingerprinting of *M. tuberculosis* and *M. bovis* isolates showed obvious polymorphisms. The copy numbers of the repeat units in different loci were calculated based on the specific data coding of each strain (Fig. 2 and Table 3).

4. Discussion

At present, bovine tuberculosis is diagnosed primarily by TST using bovine PPD. However, owing to the continuing control of bovine tuberculosis, it is increasingly common that TST shows a positive result but cattle have no lesions of bTB. This phenomenon is mainly due to infection with non-tuberculous mycobacteria (NTM), which has resulted in an increase in false positive cases of tuberculin allergy (Peterson, 1965; Wolinsky, 1979; Wang et al., 1998; Anita, 2008).

He et al. (1994a) isolated 26 strains of mycobacteria from the lymph nodes and lesion tissues of 69 bovines that had been killed because of positive results of the TST. Five strains were MTBC, and the others were NTM, including five *M. fortuitum*, six *M. scrofulaceum*, five *M. avium-intracellulare*, two *Mycobacterium paratuberculosis*, two *Mycobacterium flavescens* and one undetermined strain from the Runyon II group. In addition, He et al. (1994b) developed a crossover test of allergy in calves, using the mycobacteria isolated above that were derived from bovids (one *M. bovis*, one *M. scrofulaceum*, one *M. fortuitum*, one type 2 *M. avium-intracellulare* complex, one type 9 *M. avium-intracellulare* complex, one *M. paratuberculosis* and one *M. flavescens*). The results suggested that all calves inoculated with each *Mycobacterium* species presented a crossover allergic reaction.

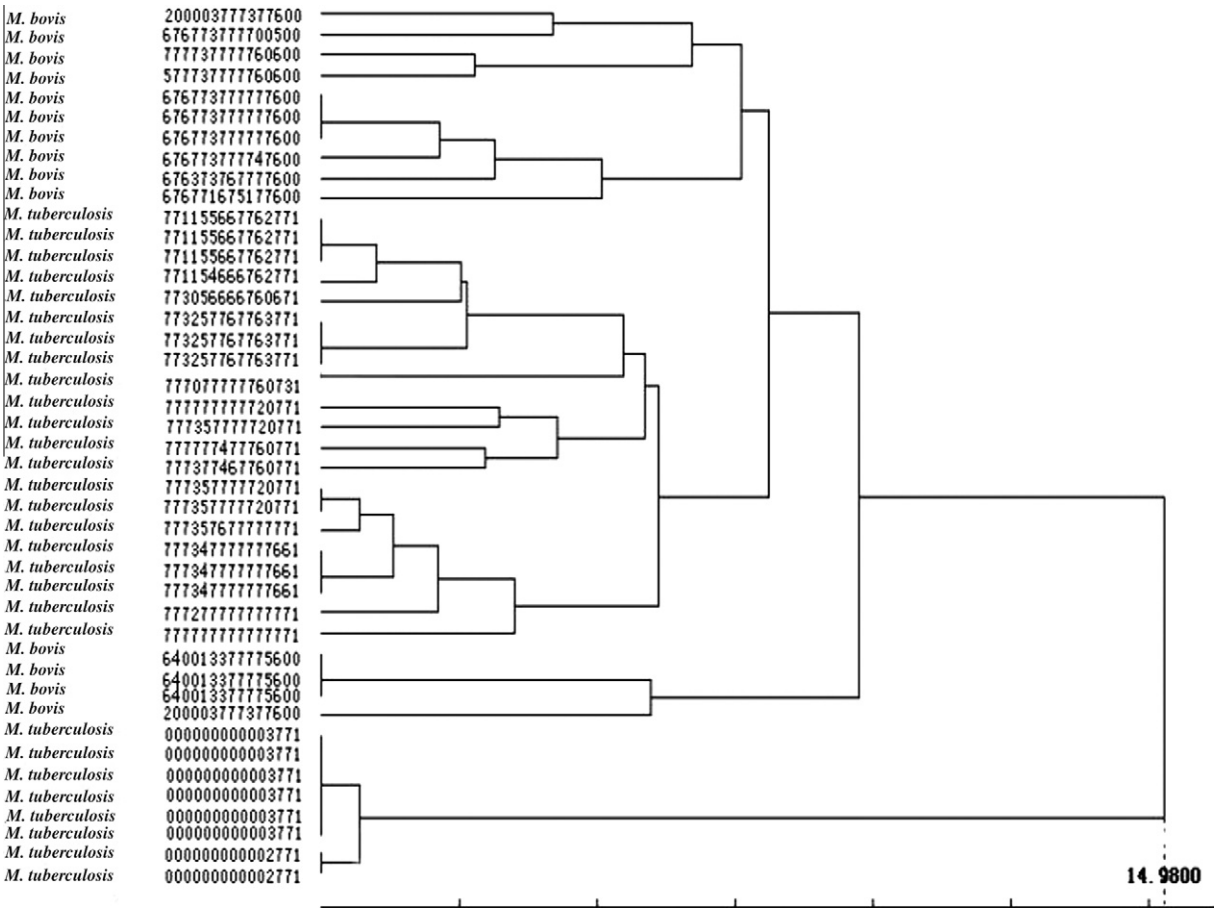

Fig. 2. Dendrogram deduced from the analysis of clustering. The order of 13 MIRU loci is ETR-A, ETR-C, Miru04, Miru10, Miru16, Miru27, Miru31, Miru40, Mtub21, Mtub30, Mtub38, Qub11a, and Qub11b.

Table 3
The VNTR-MIRU pattern of MTBC isolated strains.

No of MTBC	Copy number												
	ETR-A	ETR-C	Miru04	Miru10	Miru16	Miru27	Miru31	Miru40	Mtub21	Mtub30	Mtub38	Qub11a	Qub11b
08001	6	3	3	2	2	3	3	2	2	3	1	8	3
08002	3	6	2	2	4	2	3	2	1	3	0	3	4
08004	7	4	3	1	3	3	2	2	2	5	1	4	5
08006	7	4	3	2	1	2	2	2	2	4	1	11	4
08008	7	4	3	2	3	2	2	2	2	3	1	10	4
08010	7	4	3	2	3	4	3	2	2	3	1	4	4
08012	7	4	4	2	3	4	3	2	3	1	1	10	4
08013	5	6	3	1	3	0	2	2	4	3	1	12	2
08015	5	4	3	1	2	2	1	1	2	1	0	1	2
0015	4	3	5	2	4	3	3	2	1	1	1	5	4
08017	4	3	3	1	3	2	2	2	1	1	1	4	4
08018	3	3	2	2	2	3	4	3	4	3	0	8	5
08020	4	3	2	2	3	2	4	2	3	3	0	8	5
08061	3	4	4	4	6	6	6	5	2	1	1	5	3
08065	3	3	3	1	3	1	2	2	2	1	1	5	4
08066	4	3	3	2	3	3	6	3	4	4	1	9	6
08067	3	3	3	3	3	3	6	3	4	3	0	6	5
08068	4	3	3	3	3	4	5	3	4	3	0	8	5
08072	4	3	3	3	3	3	6	3	3	3	0	9	7
H37Rv	3	4	3	3	3	4	3	1	2	2	3	3	5
BCG	8	5	5	2	3	4	3	2	3	4	4	10	4

In the current study, 111 strains of mycobacteria were identified from 1067 bovine throat swab samples from cattle that had shown positive results of TST. The isolates included 43 MTBC and 68 NTM (described in another study); MTBC accounted for 38.7% (43/111) of the isolates, and NTM 61.3% (68/111) (Table 2). This result suggests that NTM infection is extremely common in cattle in

China, and that it interferes with the control of bovine tuberculosis. These results also indicate that the non-specific interference caused by NTM should be paid close attention in the control of bovine tuberculosis by quarantine in future.

During the infection of cattle, MTBC first induces the host to produce a cell-mediated immune response, and then probably induces humoral immunity; these two responses are antagonistic (Ritacco et al., 1991). In addition, the majority of NTM are non-pathogenic bacteria or pathogenic with low virulence; they rarely induce a humoral immune response (induction of serum antibody) after entering the body. Therefore, as a supplement to the TST, an ELISA is of vital importance for identifying negative and false positive reactions to bTB (Amadori et al., 2002), because it can exclude cattle that show positive results of non-specific allergy caused by NTM infection. In this study, the concordance between antibody against bTB detected by use of the indirect ELISA, and positive results of isolation of *M. bovis* on culture was 52.8% (38/72). The concordance between positive results for TST and MTBC was only 4.0% (43/1067), the result was coincidental with previous report which indicated that 70 Argentine cattle had a modest prevalence of *M. bovis* shedding in nasal swabs (2.9%) and milk (1.4%) (Sreevatsan et al., 2000), showing that the lack of correlation between TST and culture is most likely caused by throat swabs being a relatively insensitive method of culture for *M. bovis*. Most infected cattle are not shedding MTBC continually, thus causing the low sensitivity of culture for throat swabs (Fourie and Odendaal, 1983).

A total of 42 strains of mycobacteria were isolated from 72 throat swabs from cattle that showed antibody against bTB detected by ELISA, including 38 MTBC and four NTM; the isolation rate of MTBC was 90.5% (38/42) (Table 2). With the disease progression, the cell-mediated immune response becomes weakened and the humoral immune reaction is enhanced. The amount of *M. bovis* discharged is also increased later in the course of the infection, which increases the risk associated with *M. bovis* shed from the upper respiratory tract. This suggests that the type of immune reaction shown by the host is correlated with the course of disease in bTB and with the shedding of *M. bovis* (Welsh et al., 2005). High isolation rate of *M. tuberculosis*, possibly due to human – cattle or wild animals – cattle caused by close contact with infected individuals or animals, and the cause remains to be studied.

The range of hosts infected with *M. tuberculosis* is relatively restricted (compared to *M. bovis*); they include human beings, other primates, rodents, dogs and other animals in contact with human beings, but *M. tuberculosis* primarily causes tuberculosis in human beings (Thoen et al., 2006). *M. bovis* is considered to be one of the three major pathogenic bacteria of public health importance (OIE, 2005). Given that human beings can come into close association with cattle, the possibility that human beings can be infected with *M. bovis* is also significant (Gibson et al., 2004; Davies, 2006; Rodwell et al., 2008). The existence of wild reservoir hosts of *M. bovis* (Fitzgerald et al., 2000) makes it extremely difficult to eliminate bTB (Thoen et al., 2006). It was traditionally considered that goats, poultry and cattle are not sensitive to *M. tuberculosis* (Piercy et al., 2007), but according to recent studies this opinion should be reconsidered. In fact, *M. tuberculosis* can also infect poultry, other domestic animals, and wild animals in zoos, including bovine herds (Prasad et al., 2005; Chen et al., 2008), monkeys (Michel and Huchzermeyer, 1998), dogs (Hackendahl et al., 2004; Erwin et al., 2004; Sykes et al., 2007), Asian elephants, rocky mountain goats, rhinoceroses (Michalak et al., 1998; Oh et al., 2002), and pet birds (Steinmetz et al., 2006; Schmidt et al., 2008). Prasad et al. (2005) reported that, of 67 bovines with tuberculosis in India, 20% were infected with *M. tuberculosis* and 35% were infected with both *M. bovis* and *M. tuberculosis*. In this study, 29 strains of *M. tuberculosis* were isolated from 1067 throat swabs from cattle that presented positive results of TST, which supports previous reports that bovine herds in China are infected with various mycobacteria (Chen et al., 2008).

The spoligotyping and cluster analysis of 43 clinically isolated strains of MTBC showed that these 43 isolated strains had 26 genotypes, and that 16 strains presented a unique genotype. The largest genotype among them contained eight isolated strains, accounting for 18.6% (8/43), and was defined as from the "Beijing/Beijing-like family". It included six isolated strains with the same genotype as the "Beijing family" (Toungoussova et al., 2002; Glynn et al., 2002) and two strains of the "Beijing-like family" (Guo et al., 2005), in which there was only one fewer spacer than in the Beijing genotype, so that it hybridized with only eight spacers within 35–43 (Fig. 1). The maximal resolution of MIRU-VNTR typing was achieved using a subset of 13 loci (ETR-A, ETR-C, Miru04, Miru10, Miru16, Miru27, Miru31, Miru40, Mtub21, Mtub30, Mtub38, Qub11a, and Qub11b). The results showed that this resolution was concentrated in a core set of only five loci with comparatively high allelic diversities (ETR-A, Miru27, Miru31, Qub11a, and Qub11b). The Qub11b locus showed the highest discrimination; another eight loci (ETR-C, Miru04, Miru10, Miru16, Miru40, Mtub21, Mtub30, and Mtub38) showed lower discrimination (Fig. 2 and Table 3). Thirteen VNTR–MIRU loci with good specificity were selected for typing analysis to increase our understanding of the genotype and characteristics of MTBC isolates from cattle.

This was a preliminary investigation of the situation regarding bTB infection in China. The MIRU–VNTR technique facilitates universal access and can play an important role in the epidemiological research into bTB.

Acknowledgment

This work was supported by a Grant from the Major State Basic Research Development Program of China (973 Program) (No. 2006 CB504400).

References

Amadori, M., Lyashchenko, K.P., Gennaro, M.L., Pollock, J.M., Zerbini, I., 2002. Use of recombinant proteins in antibody tests for bovine TB. Veterinary Microbiology 85, 379–389.

Anita, L., 2008. *Mycobacterium fortuitum* infection interference with *Mycobacterium bovis* diagnostics: natural infection cases and a pilot experimental infection. Journal of Veterinary Diagnostic Investigation 20, 501–503.

Bakshi, C.S., Shah, D.H., Verma, R., Singh, R.K., Malik, M., 2005. Rapid differentiation of *Mycobacterium bovis* and MTB based on a 12.7-Kb fragment by a single tube multiplex-PCR. Veterinary Microbiology 109, 211–216.

Chen, Y.Y., Chao, Y.J., Deng, Q.T., Liu, T., Xiang, J., Chen, J., Zhou, J.H., Zhan, Z.H., Kuang, Y.J., Cai, H., Chen, H.C., Guo, A.Z., 2008. Potential challenges to the Stop TB Plan for humans in China; cattle maintain *M. bovis* and *M. tuberculosis*. Tuberculosis 7, 1–6.

Dale, J.W., Brittain, D., Cataldi, A.A., Cousins, D., Crawford, J.T., Driscoll, J., Heersma, H., Lillebaek, T., Quitugua, T., Rastogi, N., Skuce, R.A., Sola, C., Van Soolingen, D., Vincent, V., 2001. Spacer oligonucleotide typing of bacteria of the *Mycobacterium tuberculosis* complex: recommendations for standardized nomenclature. The International Journal of Tuberculosis and Lung Disease 5, 216–219.

Davies, P.D.O., 2006. Tuberculosis in humans and animals: are we a threat to each other? Journal of the Royal Society of Medicine 99, 539–540.

Diagnostic Techniques for Tuberculosis of Animals. GB/T 18645-2002.

Durret, P.A., Hewinson, R.G., Clifton-Hadley, R.S., 2000. Molecular epidemiology of bovine tuberculosis. I. *Mycobacterium bovis* genotyping. Revue scientifique et technique (International Office of Epizootics) 19, 675–688.

Erwin, P.C., Bemis, D.A., Mawby, D.I., McCombs, S.B., Sheeler, L.L., Himelright, I.M., Halford, S.K., Diem, L., Metchock, B., Jones, T.F., Schilling, M.G., Thomsen, B.V., 2004. *Mycobacterium tuberculosis* transmission from human to canine. Emerging Infectious Diseases 10 (12), 2258–2260.

Fitzgerald, S.D., Kaneene, J.B., Butler, K.L., Clarke, K.R., Fierke, J.S., Schmitt, S.M., Bruning-Fann, C.S., Mitchell, R.R., Berry, D.E., Payeur, J.B., 2000. Comparison of postmortem techniques for the detection of *Mycobacterium bovis* in white-tailed deer (Odocoileusvirginianus). Journal of Veterinary Diagnostic Investigation 12, 322–327.

Fourie, P.B., Odendaal, M.W., 1983. *Mycobacterium tuberculosis* in a closed colony of baboons (*Papio ursinus*). Laboratory Animals 17, 125–128.

Frothingham, R., Meeker-O'Connell, W.A., 1998. Genetic diversity in the MTB complex based on variable numbers of tandem DNA repeats. Microbiology 144, 1189–1196.

Gibson, A.L., Hewinson, G., Goodchild, T., Watt, B., Story, A., Inwald, J., Drobniewski, F.A., 2004. Molecular epidemiology of disease due to *Mycobacterium bovis* in humans in the United Kingdom. Journal of Clinical Microbiology 42, 431–434.

Glynn, J.R., Whiteley, J., Bifani, P.J., Kremer, K., van Soolingen, D., 2002. Worldwide occurrence of Beijing/W strains of *Mycobacterium tuberculosis*: a systematic review. Emerging Infectious Diseases 8, 843–849.

Guo, Y.L., Liu, Y., Wang, S.M., Li, C.Y., 2005. The Identification of *Mycobacterium tuberculosis* Isolates by DNA typing technique. Chinese Journal of Epidemiology 26, 361–365.

Hackendahl, N.C., Mawby, D.I., Bemis, D.A., Beazley, S.L., 2004. Putative transmission of *Mycobacterium tuberculosis* infection from a human to a dog. Journal of the American Veterinary Medical Association 225 (10), 1573–1577.

He, Z.Y., Hu, X.R., Wang, Z.G., Li, M.N., Hu, G.X., Li, Z.Q., Zhang, Y.M., Li, D.S., Gao, J., 1994a. Isolation and identification of the atypical mycobacteria from positive allergic reaction to tuberculosis. Acta Veterinaria Et Zootechnica Sinica 25 (3), 247–251.

He, Z.Y., Li, M.N., Hu, G.X., Qian, A.D., Hu, X.R., Zhang, Y.M., Gao, J., Liu, Y.M., Li, D.S., Li, Z.Q., 1994b. The calf allergic reaction experiment of the mycobacteria from cattle. Acta Veterinaria Et Zootechnica Sinica 25 (6), 545–550.

Huard, R.C., de Oliveira Lazzarini, L.C., Butler, W.R., van Soolingen, D., Ho, J.L., 2003. PCR-based method to differentiate the subspecies of the MTB complex on the basis of genomic deletions. Journal of Clinical Microbiology 41, 1637–1650.

Kamerbeek, J., Schouls, L., Kolk, A., van Agterveld, M., van Soolingen, D., Kuijper, S., Bunschoten, A., Molhuizen, H., Shaw, R., Goyal, M., van Embden, J., 1997. Simultaneous detection and strain differentiation of MTB for diagnosis and epidemiology. Journal of Clinical Microbiology 35, 907–914.

Lantos, A., Niemann, S., Mezõsi, L., Sós, E., Erdélyi, K., David, S., Parsons, L.M., Kubica, T., Rusch-Gerdes, S., Somoskovi, A., 2003. Pulmonary tuberculosis due to *Mycobacterium bovis* subsp. *caprae* in captive siberian tiger. Emerging Infectious Diseases 9, 1462–1464.

Liu, S.G., Guo, S.P., Wang, C.L., Shao, M.L., Zhang, X.H., Guo, Y., Gong, Q., 2007. A novel fusion protein-based indirect enzyme-linked immunosorbent assay for the detection of bovine tuberculosis. Tuberculosis 87, 212–217.

Mazars, E., Lesjean, S., Banuls, A.L., Gilbert, M., Vincent, V., Gicquel, B., Tibayrenc, M., Locht, C., Supply, P., 2001. High-resolution minisatellite-based typing as a portable approach to global analysis of MTB molecular epidemiology. Proceedings of the National Academy of Sciences USA 98, 1901–1906.

Mcnabb, A., Eisler, D., Adie, K., Amos, M., Rodrigues, M., Stephens, G., Black, W.A., Isaac-Renton, J., 2004. Assessment of partial sequencing of the 65-kilodalton heat shock protein gene (*hsp65*) for routine identification of *Mycobacterium* species isolated from clinical sources. Journal of Clinical Microbiology 42, 3000–3011.

Michalak, K., Austin, C., Diesel, S., Bacon, M.J., Zimmerman, P., Maslow, J.N., 1998. *Mycobacterium tuberculosis* infection as a zoonotic disease: transmission between humans and elephants. Emerging Infectious Diseases 4 (2), 283–287.

Michel, A.L., Huchzermeyer, H.F., 1998. The zoonotic importance of *Mycobacterium tuberculosis*: transmission from human to monkey. Journal of the South African Veterinary Association 69 (2), 64–65.

Michel, A.L., Hlokwe, T.M., Coetzee, M.L., Mare, L., Connoway, L., Rutten, V.P.M.G., Kremer, K., 2008. High *Mycobacterium bovis* genetic diversity in a low prevalence setting. Veterinary Microbiology 126, 151–159.

Mignard, S., Pichat, C., Carret, G., 2006. *Mycobacteriun bovis* infection, Lyon, France. Emerging Infectious Diseases 12, 1431–1433.

Oh, P., Granich, R., Scott, J., Sun, B., Joseph, M., Stringfield, C., Thisdell, S., Staley, J., Workman-Malcolm, D., Borenstein, L., Lehnkering, E., Ryan, P., Soukup, J., Nitta, A., Flood, J., 2002. Human exposure following *Mycobacterium tuberculosis* infection of multiple animal species in a metropolitan zoo. Emerging Infectious Diseases 8 (11), 1290–1293.

OIE, 2005. Bovine Tuberculosis. <http://www.cfsph.iastate.edu/Factsheets/pdfs/bovinetuberculosis.pdf> (accessed 05.04.05).

Peterson, K.J., 1965. *Mycobacterium fortuitum* as a cause of bovine mastitis: tuberculin sensitivity following experimental infection. Journal of the American Veterinary Medical Association 147, 1600–1607.

Piercy, J., Werling, D., Coffey, T.J., 2007. Differential responses of bovine macrophages to infection with bovine-specific and non-bovine specific mycobacteria. Tuberculosis 87, 415–420.

Prasad, H.K., Singhal, A., Mishra, A., Shah, N.P., Katoch, V.M., Thakralc, S.S., Singhc, D.V., Chumberd, S., Bald, S., Aggarwale, S., Padmaf, M.V., Kumarg, S., Singhh, M.K., Acharyai, S.K., 2005. Bovine TB in India: potential basis for zoonosis. Tuberculosis 85, 421–428.

Ritacco, V., López, B., De Kantor, I.N., Barrera, L., Errico, F., Nader, A., 1991. Reciprocal cellular and humoral immune responses in bovine tuberculosis. Research in Veterinary Science 50 (3), 365–367.

Rodwell, T.C., Moore, M., Moser, K.S., Brodine, S.K., Strathdee, S.A., 2008. Tuberculosis from *Mycobacterium bovis* in binational communities. Emerging Infectious Diseases 14 (6), 909–916.

Roring, S., Scott, A., Brittain, D., Walker, I., Hewinson, G., Skuce, R., 2002. Development of variable number tandem repeat typing of *Mycobacterium bovis*: comparison of results with those obtained by using existing exact tandem repeats and spoligotyping. Journal of Clinical Microbiology 40, 2126–2133.

Savine, E., Warren, R.M., Vander Spuy, G.D., Locht, C., Supply, P., 2004. Stability of variable number tandem repeats of mycobacterium interspersed repetitive units from 12 loci in serial isolates of MTB. Journal of Clinical Microbiology l40, 4561–4566.

Schmidt, V., Schneider, S., Schlmer, J., Krautwald-Junghanns, M.E., Richter, E., 2008. Transmission of tuberculosis between men and pet birds: a case report. Avian Pathology 37 (6), 589–592.

Sreevatsan, S., Bookout, J.B., Ringpis, F., Perumaalla, V.S., Ficht, T.A., Adams, L.G., Hagius, S.D., Elzer, P.H., Bricker, B.J., Kumar, G.K., Rajasekhar, M., Isloor, S., Barathur, R.R., 2000. A multiplex approach to molecular detection of *Brucella abortus* and/or *Mycobacterium bovis* infection in cattle. Journal of Clinical Microbiology 38 (7), 2602–2610.

Steinmetz, H.W., Rutz, C., Hoop, R.K., Grest, P., Bley, C.R., Hatt, J.M., 2006. Possible human–avian transmission of *Mycobacterium tuberculosis* in a green-winged macaw (*Ara chloroptera*). Avian Disease 50 (4), 641–645.

Sykes, J.E., Cannon, A.B., Norris, A.J., Byrne, B.A., Affolter, T., O'Malley, M.A., Wisner, E.R., 2007. *Mycobacterium tuberculosis* complex infection in a dog. Journal of Veterinary Internal Medicine 21, 1108–1112.

Telenti, A., Marchest, F., Balz, M., Bally, F., Bottger, E.C., Bodmer, T., 1993. Rapid identification of mycobacteria to the species level by polymerase chain reaction and restriction enzyme analysis. Journal of Clinical Microbiology 31, 175–178.

The Center for Food Security & Public Health. Bovine Tuberculosis. BTUB_A2007.

Thoen, C., LoBue, P., de Kantor, I., 2006. The importance of *Mycobacterium bovis* as a zoonosis. Veterinary Microbiology 112, 339–345.

Toungoussova, O.S., Sandven, P., Mariandyshev, A.O., Nizovtseva, N.I., Bjune, G., Caugant, D.A., 2002. Spread of drug-resistant *Mycobacterium tuberculosis* strain of the Beijing genotype in the archangel oblast, Russia. Journal of Clinical Microbiology 40, 1930–1937.

van Embden, J.D.A., Cave, M.D., Crawford, J.T., Dale, J.W., Eisenach, K.D., Gicquel, B., Hermans, P., Martin, C., McAdam, R., Shinnick, T.M., 1993. Strain identification of MTB by DNA fingerprinting: recommendations for a standardized methodology. Journal of Clinical Microbiology 31, 406–409.

van Soolingen, D., Hermans, P.W., de Haas, P.E., Soll, D.R., van Embden, J.D., 1991. and stability of insertion sequences in MTB complex strains: evaluation of an insertion sequence-dependent DNA polymorphism as a tool in the epidemiology of TB. Journal of Clinical Microbiology 29, 2578–2586.

Wang, Z.G., Luo, Y.F., Song, G.W., 1998. Isolation and identification of atypical Mycobacteria from cattle. Journal of Jilin Agricultural University 20 (2), 73–77.

Welsh, M.D., Cunningham, R.T., Corbett, D.M., Girvin, R.M., McNair, J., Skuce, R.A., Bryson, D.G., Pollock, J.M., 2005. Influence of pathological progression on the balance between cellular and humoral immune responses in bovine tuberculosis. Immunology 114, 101–111.

Wolinsky, E., 1979. Nontuberculous mycobacteria and associated diseases. The American Review of Respiratory Disease 119, 107–159.

Xu, M.Y., Liu, T.Y., Zhong, N.R., Chi, Y.P., 1998. Report of 17 cases of human pulmonary tuberculosis caused *Mycobacterium bovis*. Chinese Journal of Zoonoses 14, 76.

Yan, J.J., Jou, R., Ko, W.C., Wu, J.J., Yang, M.L., Chen, H.M., 2005. The use of variable-number tandem-repeat mycobacterial Interspersed repetitive unit typing to identify laboratory cross-contamination with MTB. Diagnostic Microbiology and Infectious Disease 52, 21–28.

第35卷 第8期
2013 年 8 月

中 国 预 防 兽 医 学 报
Chinese Journal of Preventive Veterinary Medicine

Vol. 35,No.8
Aug. 2013

doi: 10.3969/j.issn.1008-0589.2013.08.22

结核分枝杆菌 *rv3036c* 基因的原核表达及其多克隆抗体的制备

曹 俊[1*]，陈利苹[1*]，刘银冰[1,2]，鄢秋龙[1,2]，刘思国[1*]

(1. 中国农业科学院哈尔滨兽医研究所 兽医生物技术国家重点实验室 / 动物细菌病研究室，黑龙江 哈尔滨 150001；
2. 黑龙江八一农垦大学，黑龙江 大庆 163319)

摘 要：为制备结核分枝杆菌(Mtb) *rv3036c* 基因的多克隆抗体，本研究以 *Mtb* 强毒株 H37Rv 基因组 DNA 为模板，扩增 *rv3036c* 基因，克隆至表达载体 pET-28a(+)中，构建重组质粒 pET-*rv3036c*，并转化大肠杆菌 BL21 (DE3)，经 1 mmol/L IPTG 诱导表达组氨酸标签融合蛋白 Rv3036c，采用 Ni-NTA His-Bind Resin 纯化目的蛋白，经 western blot 验证纯化蛋白。将 Rv3036c 蛋白纯化产物免疫新西兰大白兔，制备多克隆抗体。SDS-PAGE 和 western blot 分析结果表明，Rv3036c 以可溶形式表达，蛋白分子量大小为 28 ku，并且具有良好的免疫原性。以上结果为进一步研究 *rv3036c* 基因在 Mtb 的致病性作用奠定了基础。

关键词：结核分枝杆菌；*rv3036c* 基因；原核表达；多克隆抗体

中图分类号：S852.61　　**文献标识码**：A　　**文章编号**：1008-0589(2013)08-0684-03

Prokaryotic expression of *rv3036c* gene from *Mycobacterium tuberculosis* and preparation of the polyclonal antibody against the bacteria

CAO Jun[1*], CHEN Li-ping[1*], LIU Yin-bing[1,2], YAN Qiu-long[1,2], LIU Si-guo[1*]

(1. Division of Bacterial Diseases, State Key Laboratory of Veterinary Biotechnology, Harbin Veterinary Research Institute, Chinese Academy of Agricultural Sciences, Harbin 150001, China; 2. Heilongjiang Bayi Agricultural University, Daqing 163319, China)

Abstract: To express the *rv3036c* gene of *Mycobacterium tuberculosis* and prepare the polyclonal antibody against the bacteria, the *rv3036c* gene was amplified by PCR from *M.tuberculosis* H37Rv genomic DNA and cloned to pET-28a(+) vector for expression in *E.coli* BL21 (DE3). The expressed product was analyzed by SDS-PAGE, then purified by Ni-NTA His-Bind Resin affinity chromatography and identified by western blot. The polyclonal antibody was prepared by immunizing New Zealand white rabbits with the purified protein. The immunizing potency of the rabbit serum was determined by ELISA. The results shown the expressed recombinant Rv3036c protein was about 28 ku, mainly existed in a soluble form and the prepared polyclonal antibody displayed good immunological activity. These results provided a basis for further studies on the role of rv3036c protein during the Mycobacterium tuberculosis pathogenesis.

Key words: *Mycobacterium tuberculosis*; *rv3036c* gene; prokaryotic expression; polyclonal antibody

*Corresponding author; Equal contributors

收稿日期：2012-05-18
基金项目：国家重点基础研究发展计划[973 计划(2012CB518801)]
共同第一作者：曹 俊(1986-)，女，辽宁灯塔人，硕士研究生，主要从事动物结核病研究；
陈利苹(1983-)，女，湖北恩施人，助理研究员，博士，主要从事动物结核病研究.
* **通信作者**： E-mail：siguo_liu@hvri.ac.cn

结核病(Tuberculosis)是由牛分枝杆菌(*Mycobacterium bovis*)和结核分枝杆菌(*Mycobacterium tuberculosis*，Mtb)所引起的一种慢性消耗性人畜共患病。尽管自 1990 年至今，结核病的病死率和新增病例有所下降，但该病仍然是人类健康的重要威胁[1-4]。

在 Mtb 强毒力标准株 H37Rv 的全基因组中，*rv3036c* 基因的功能未知，利用 *rv3036c* 基因核苷酸和氨基酸序列在数据库中比对，发现该基因在 Mtb、*M.bovis* 和非洲分枝杆菌(*Mycobacterium africanu*)中保守，而其他分枝杆菌中不存在。以上 3 种分枝杆菌为结核分枝杆菌复合群的主要成员，能够引起人和动物的结核病，提示我们 *rv3036c* 基因可能与分枝杆菌的致病性相关。目前，国内外还没有关于 Mtb *rv3036c* 基因体外表达及免疫性研究的报道。为验证该基因是否编码分泌型蛋白，本研究克隆表达并纯化了 Rv3036c 蛋白，并检测其免疫原性，为进一步研究 Rv3036c 蛋白的生物学功能奠定基础。

1　材料和方法

1.1　菌种、载体和宿主　Mtb H37Rv 菌株购自中国生物制品检定所；质粒 pET-28a(+)、宿主菌 *E.coli* DH5α 和 BL21 (DE3)感受态菌均由本实验室保存。

1.2　主要试剂　限制性内切酶 *Bam*H Ⅰ和 *Eco*R Ⅰ、*Pfu* DNA 聚合酶购自 MBI 公司；PCR 产物纯化试剂盒、质粒小提试剂盒购自 OMEGA 公司；pMD18-T 载体购自 TaKaRa 公司；抗 His 标签单克隆抗体(MAb)和 Ni-NTA His 纯化试剂盒均购自 Novagen 公司；IPTG 和 HRP 标记的山羊抗兔 IgG 均购自 Sigma 公司。

1.3　*Mtb* 基因组的提取　参照文献[5]方法提取 Mtb 基因组。

1.4　引物设计及目的基因的扩增　根据 GenBank 中 H37Rv 株 *rv3036c* 基因设计引物，由南京金思特科技有限公司合成，序列为：HYP-F：5'-TTTGGATCCCTGGGCGGCACTGTG-3'(*Eco*R Ⅰ)、HYP-R 5'-G TGGAATTCTTAGATTGCCAGCGGCGGA-3'(*Bam*H Ⅰ)。以 Mtb 基因组 DNA 为模板，采用 *Pfu* DNA 聚合酶经 PCR 扩增 *rv3036c* 基因。反应体系为 50 μL；反应程序为：95 ℃ 3 min；95 ℃ 30 s、55 ℃ 30 s、72 ℃ 1.5 min，30 个循环；72 ℃ 10 min。扩增产物以 1 %的琼脂糖凝胶电泳检测。

1.5　原核重组表达质粒的构建　将扩增的 *rv3036c* 基因连接至 pMD18-T 载体中，转化 DH5α 感受态细胞，获得重组质粒 pMD-*rv3036c*。采用 *Bam*H Ⅰ和 *Eco*R Ⅰ双酶切并胶回收 *rv3036c* 片段，克隆于 pET-28a(+)中构建重组质粒 pET-*rv3036c*。

1.6　重组质粒在 *E.coli* 中的诱导表达和重组蛋白的纯化　将 pET-*rv3036c* 转化 BL21 (DE3)感受态细胞，将重组菌于 37 ℃培养至 OD_{600nm} 值约为 0.6，以终浓度为 1 mmol/L IPTG 分别于 37 ℃、30 ℃、23 ℃和 16 ℃诱导表达目的蛋白。离心收集菌体，超声波裂解细菌，离心收集上清。按 Ni-NTA His- Bind Resin 亲和柱操作步骤纯化可溶蛋白，并进行 SDS-PAGE 分析。

1.7　重组蛋白的 western blot 分析　将纯化的重组蛋白进行 western blot 检测，以抗 His 标签 MAb (5 000×)为一抗，以 HRP 标记的山羊抗兔 IgG (5 000×)为二抗，通过 DAB 显色检测。

1.8　抗 Rv3036c 多克隆抗体的制备　将纯化的 Rv3036c 蛋白与等体积弗氏不完全佐剂乳化，使免疫新西兰大白兔的 Rv3036c 蛋白量为 400 μg/ 只。以 1 mg/kg 的剂量首免跖部，以后经背部皮下多点注射，每隔 2 周免疫 1 次，共免疫 4 次，于末次免疫 1 周后采集血液，分离血清并保存于 -20 ℃。

1.9　间接 ELISA 检测抗体效价　采用常规的间接 ELISA 法检测制备的抗体血清的效价，即以碳酸盐缓冲液稀释的 Rv3036c 蛋白(1 μg/mL)为抗原包被 ELISA 板，以 1∶800～1∶12 800 2 倍倍比稀释的兔免疫血清为一抗，以 HRP 标记的山羊抗兔 IgG 为二抗，TMB 为底物显色，检测样品 OD_{450nm} 值。

2　结果与讨论

2.1　PCR 扩增目的基因及重组质粒的鉴定　以 Mtb 强毒株 H37Rv 基因组 DNA 为模板，采用特异性引物对 *rv3036c* 基因进行 PCR 扩增。经琼脂糖凝胶电泳检测表明，该基因产物约 600 bp，与预期大小一致(图 1)。采用双酶切构建并鉴定重组质粒 pET-*rv3036c*，结果获得约 600 bp 的片段，与预期结果一致。

2.2　重组蛋白的表达、纯化及 western blot 分析　分别于 37 ℃、30 ℃、23 ℃和 16 ℃ (IPTG 终浓度 1 mmol/L)诱导表达目的蛋白，取超声波破菌离心后

的上清和沉淀进行 SDS-PAGE 分析。结果显示：诱导表达的目的蛋白约为 28 ku，与预期大小一致；在不同温度条件下大部分目的蛋白在上清中表达，23 ℃和 16 ℃时可溶性表达比例更高。采用 Ni-NTA His Bind Resin 亲和柱纯化可溶蛋白，洗脱液取样进行 SDS-PAGE 分析(图 2A)。纯化蛋白的 western blot 结果显示，经 DAB 显色后，与抗 His 标签 MAb 作用的 NC 膜在约 28 ku 处出现一明显可见条带，而阴性对照无此条带(图 2B)。

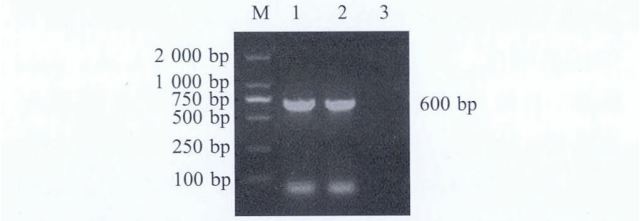

M: DNA Marker; 1-2: PCR product of *rv3036c* gene;
3: Negative control

图 1 目的基因 PCR 扩增

Fig.1 PCR amplification of *rv3036c* gene

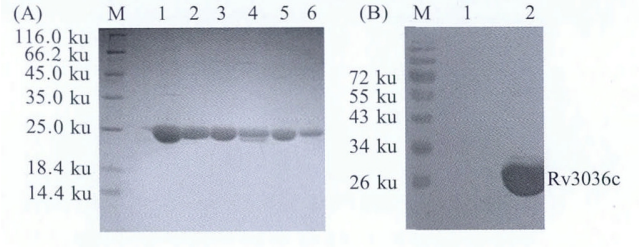

(A) M: Protein molecular weight Marker; 1-6: Purified Rv3036c protein
(B) M: Protein molecular weight Marker;
1: Negative control; 2: Product reacted with anti-His tag MAb

图 2 重组蛋白的 SDS-PAGE 分析(A)及 western blot(B)鉴定

Fig.2 The SDS-PAGE analysis(A) and western blot identification of the recombinant protein expression in *E.coli*

2.3 抗体效价的检测 实验兔经基础免疫和加强免疫后，耳缘静脉采血，收集血清，采用间接 ELISA 方法检测其血清抗体效价，结果表明，通过基础免疫和加强免疫后，获得了较高效价的抗体，目的蛋白有良好的免疫原性(表 1)。

表 1 兔血清抗体效价的间接 ELISA 测定(OD_{450nm})

Table 1 The titeration of rabbit serum by ELISA

血清 Serum	实验兔血清稀释度 Rabbit serum concentration				
	1:800	1:1600	1:3200	1:6400	1:12800
阳性血清(OD_{450nm}) Positive serum	1.749	1.635	1.454	1.131	1.037
阴性血清(OD_{450nm}) Negative serum	0.154	0.284	0.243	0.253	0.227

目前，结核病仍是对人类健康危害最严重、对社会的公共卫生安全影响最大的传染病之一。抗生素的治疗能够帮助绝大部分结核病人康复，但多重耐药 Mtb 的出现及与艾滋病的混合感染增加了治疗的难度[6-8]。本实验根据 GenBank 中 Mtb 强毒力标准株 H37Rv *rv3036c* 基因序列信息设计引物，对 *rv3036c* 进行克隆、融合表达和免疫活性检测，并制备多克隆抗体。本研究所获得的较高纯度的蛋白和针对蛋白的特异性多克隆抗体，为进一步研究 Rv3036c 蛋白的生物学功能及其在分枝杆菌致病性中的作用奠定了基础。

参考文献：

[1] 刘思国，于辉，宫强，等. 牛结核病研究进展[J]. 畜牧兽医科技信息，2003，19(10)：10-14.

[2] Tollefsen S, Vordermeier M, Olsen I, et al. DNA injection in combination with electroporation: a novel method for vaccination of farmed ruminants [J]. Scand J Immunol, 2003, 57(3): 229-238.

[3] Brock I, Weldingh K, Leyten E M, et al. Specific T-cell epitopes for immunoassay-based diagnosis of *Mycobacterium tuberculosis* infection [J]. J Clin Microbiol, 2004, 42(6): 2379-2387.

[4] Buddle B M, Parlane N A, Keen D L, et al. Differentiation between *Mycobacterium bovis* BCG-vaccinated and *M.bovis*-infected cattle by using recombinant mycobacterial antigens [J]. Clin Diagn Lab Immunol, 1999, 6(1): 1-5.

[5] 郭设平，刘思国，张秀华，等. 牛分支杆菌抗原 MPB70，MPB83，ESAT6 的融合表达及重组蛋白的初步应用[J]. 畜牧兽医学报，2006，37(7)：676-680.

[6] Alexander C, Maue W, Ray W, et al. Analysis of immune responses directed toward a recombinant early secretory antigenic target six-kilodalton protein culture filtrate protein10 fusion protein in *Mycobacterium bovis*-infected cattle [J]. Infection Immunity, 2005, 73(10): 6659-6667.

[7] Andersen P. Effective vaccination of mice against *Mycobacterium tuberculosis* infection with a soluble mixture of secreted mycobacterial proteins [J]. Infection Immunity, 1994, 62(6): 2536- 2544.

[8] Buddle B M, Terry J R, Pollock J M, et al. Use of ESAT-6 in the interferon-3 test for diagnosis of bovine tuberculosis following skin testing [J]. Vet Microbiol, 2001, 80(1): 37-46.

(本文编辑：张朝霞)

中国兽医科学 2013,43(06):594-599
Chinese Veterinary Science

中图分类号:S 852.618 **文献标志码**:A **文章编号**:1673-4696(2013)06-0594-05

结核分枝杆菌 *rv*3668*c* 基因的原核表达及多抗制备

鄢秋龙[1,2],陈利苹[2],刘银冰[1,2],曹 俊[2],倪宏波[1],刘思国[2*]

(1.黑龙江八一农垦大学 动物科技学院,黑龙江 大庆 163319;2.中国农业科学院 哈尔滨兽医研究所 兽医生物技术国家重点实验室 动物细菌病研究室,黑龙江 哈尔滨 150001)

摘要:以结核分枝杆菌强毒株 H37Rv 基因组 DNA 为模板,扩增 *rv*3668*c* 基因,将其连接于表达载体 pET-30a(+),获得重组质粒 p30a-68,并将重组质粒转化大肠杆菌 BL21(DE3),用 1 mmol/L IPTG 诱导表达组氨酸标签融合蛋白 His-Rv3668c。用 Ni-NTA His-Bind Resin 亲和层析树脂纯化目的蛋白,利用抗 6His 标签抗体验证蛋白的纯化结果;通过 Western-blot 分析纯化蛋白与牛结核病阳性血清的反应情况。用重组蛋白纯化产物免疫新西兰大白兔,制备多克隆抗体。结果显示,重组质粒的双酶切鉴定和 DNA 序列测定均完全正确;SDS-PAGE 和 Western-blot 分析结果表明,His-Rv3668c 以可溶形式表达,蛋白质分子质量为 26 ku;纯化的蛋白能与牛结核病阳性血清发生反应,表明其具有很好的免疫原性。所制备的多克隆抗体也具有良好的特异性,可运用于对 Rv3668c 蛋白的功能特性研究。

关键词:结核分枝杆菌;*rv*3668*c* 基因;原核表达;免疫原性

Prokaryotic expression of *rv*3668*c* gene from *Mycobacterium tuberculosis* and preparation of the polyclonal antibody

YAN Qiu-long[1,2],CHEN Li-ping[2],LIU Yin-bing[1,2],CAO Jun[2],NI Hong-bo[1],LIU Si-guo[2]

(1. *College of Animal Science & Veterinary Medicine, Heilongjiang Bayi Agricultural University, Daqing* 163319, *China*; 2. *State Key Laboratory of Veterinary Biotechnology/Division of Animal Bacteriosis, Harbin Veterinary Research Institute, Chinese Academy of Agricultural Sciences, Harbin* 150001, *China*)

Abstract: To construct a recombinant prokaryotic expression vector carrying the *rv*3668*c* gene from *Mycobacterium tuberculosis* and to purify the recombinant protein Rv3668c expressed in *Escherichia coli* BL21(DE3), the *rv*3668*c* gene was amplified by PCR using *M. tuberculosis* H37Rv genomic DNA and cloned into pET-30a(+) vector. The recombinant plasmid p30a-68 was transformed into *E. coli* BL21(DE3) for expression under induction with IPTG(1 mmol/L). The expressed product was analyzed by SDS-PAGE, purified by Ni-NTA His Bind Resin affinity chromatography and then identified by Western-blot. The reaction between the recombinant protein and positive serum from cattle diagnosed as tuberculosis was investigated by Western-blot. The polyclonal antibody against the recombinant protein was prepared by immunizing New Zealand white rabbits with the purified product. In result, restriction analysis proved that the recombinant plasmid p30a-68 was constructed correctly and sequencing results showed that the similarity of the cloned *rv*3668*c* gene to that reported in GenBank was 100%. The recombinant Rv3668c protein, with a molecular mass of about 26 ku, was mainly expressed in a soluble form and displayed good immunogenicity. In conclusion, the *rv*3668*c* gene can be expressed in *E. coli* in a soluble form. Polyclonal antibody against the recombinant protein, which can be used for functional study of Rv3668c, has high specificity.

Key words: *Mycobacterium tuberculosis*; *rv*3668*c* gene; prokaryotic expression; immunogenicity

收稿日期:2012-10-19;**修回日期**:2013-04-11

基金项目:国家重点基础研究发展计划(973)项目(2012CB518801)

作者简介:鄢秋龙(1988-),男,湖南娄底人,硕士生。*通信作者,Tel:18946066076,E-mail:siguo_liu@hvri.ac.cn

结核病(tuberculosis)是由结核分枝杆菌(*Mycobacterium tuberculosis*,Mtb)和牛分枝杆菌(*Mycobacterium bovis*,Mb)引起的一种慢性消耗性人畜共患病。近年来,结核病的发病率和死亡率呈下降趋势,但此病仍然是人类健康的重要威胁[1-4]。研究证明,机体主要依靠细胞免疫抵抗分枝杆菌的感染,而分枝杆菌的分泌蛋白是宿主对分枝杆菌感染早期所能识别的重要抗原,可引起 T 淋巴细胞及 B 淋巴细胞的免疫反应。人们对分枝杆菌培养液中的分泌蛋白进行了广泛的研究,发现分枝杆菌生长期分泌的蛋白对结核病的保护性免疫是很重要的,对结核病的预防和诊断具有重要意义[5]。

在 Mtb 强毒力标准株 H37Rv 的全基因组注释中,预测 *rv*3668*c* 基因具有蛋白水解酶功能[6]。利用 *rv*3668*c* 基因核苷酸和氨基酸序列在数据库中比对,发现在 Mtb、*M. bovis*、非洲分枝杆菌(*Mycobacterium africanum*),*Mycobacterium canettii*、海分枝杆菌(*Mycobacterium marinum*)和溃疡分枝杆菌(*Mycobacterium ulcerans*)中具有 *rv*3668*c* 基因,且序列保守,其他分枝杆菌中不存在。以上几种分枝杆菌能引起人或动物的结核病,提示 *rv*3668*c* 基因可能与分枝杆菌的致病性相关。目前,国内外还没有关于 Mtb *rv*3668*c* 基因体外表达及免疫原性研究的报道。本研究克隆了 *rv*3668*c* 基因,在大肠杆菌中表达并纯化了 Rv3668c 重组蛋白,为进一步研究 Rv3668c 蛋白的生物学功能奠定了基础;利用重组蛋白制备了多克隆抗体,为深入研究该蛋白在分枝杆菌致病中所扮演的角色提供了必要的工具。

1　材料与方法

1.1　菌种、载体和宿主

结核分枝杆菌 H37Rv 菌株购于中国生物制品检定所。质粒 pET-30a(+)、宿主菌 *E. coli* DH5α 和 *E. coli* BL21 (DE3)感受态细胞均由本实验室保存。

1.2　主要试剂

限制性内切酶 *Bam*HⅠ和 *Eco*RⅠ、*Pfu* DNA 聚合酶、T4 DNA 连接酶均为 MBI 公司产品。PCR 产物纯化试剂盒、DNA 胶回收试剂盒、质粒小提试剂盒均为 OMEGA 公司产品。DAB 为上海华舜生物工程有限公司产品。pMD18-T 载体为大连宝生物工程有限公司产品。抗 His 标签单抗和 Ni-NTA His Bind Purification Kit 均为 Novagen 公司产品。IPTG 和 HRP 标记的山羊抗兔酶标二抗均为 Sigma 公司产品。

1.3　结核分枝杆菌基因组的提取

参照文献[7]提取基因组的方法进行。

1.4　PCR 引物的设计及目的基因的扩增

根据 GenBank 中 H37Rv 株 *rv*3668*c* 基因序列设计扩增引物。引物Rv3668c-F(5′-TGTGGATCC-GCCGACGACAAGCTAC)和 Rv3668c-R(5′-TTT-GAATTCTCAGGCCGGTACCGGGAC)由南京金思特科技有限公司合成。在引物 Rv3668c-F 和 Rv3668c-R 的 5′端分别引入 *Bam*HⅠ和 *Eco*RⅠ酶切位点(下划线处)。以结核分枝杆菌基因组 DNA 为模板,用 *Pfu* DNA 聚合酶经 PCR 扩增 *rv*3668*c* 基因。反应体系为 50 μL:10 pmol/μL 上、下游引物各 1 μL,10 mmol/L dNTP 1 μL,1 μg/μL 模板 1 μL,PCR 缓冲液 5 μL,2.5 U/μL *Pfu* DNA 聚合酶 1 μL,加去离子水 40 μL。循环参数:95 ℃预变性 10 min;94 ℃变性 35 s,56 ℃退火 35 s,72 ℃延伸 45 s,30 个循环,最后 72 ℃延伸 10 min。PCR 产物用 10 g/L 的琼脂糖凝胶电泳进行检测,用纯化试剂盒对 PCR 产物进行纯化。

1.5　原核表达载体的构建与鉴定

将 1.4 获得的纯化 PCR 产物用 *Bam*HⅠ和 *Eco*RⅠ酶切,胶回收 *rv*3668*c* 片段,连接到用同样的酶消化的 pET-30a(+)载体,转化 DH5α 感受态细胞,获得重组质粒 p30a-68,通过酶切和序列测定鉴定克隆。

1.6　重组质粒在大肠杆菌中的诱导表达和重组蛋白的纯化

重组质粒 p30a-68 转化 BL21 (DE3)感受态细胞,涂布于含有卡那霉素(50 μg/mL)的 LB 琼脂平板上,24 h 后挑取单菌落接种于 5 mL 含有卡那霉素的 LB 液体培养基中,培养 8～12 h,以此菌液按照 1∶100 的比例接种于 200 mL 含有卡那霉素(50 μg /mL)的LB 液体培养基中,37 ℃培养至 $D_{600\ nm}$ 约为 0.6,加入 IPTG 至终浓度为 1 mmol/L,分别于 37、30 和 22 ℃诱导目的蛋白表达,诱导时间分别为 4、6 和 8 h。然后离心集菌,用 PBS(pH7.4)洗涤 1 次后,重悬于 12 mL 平衡缓冲液中,超声波裂解细菌,4 ℃ 1 000×*g* 离心 10 min,收集上清。按照 Ni-NTA His-Bind Resin 亲和柱纯化的操作步骤纯化可溶性蛋白。之后对蛋白进行 SDS-PAGE 分析。

1.7　抗 Rv3668c 多克隆抗体的制备

将纯化的 Rv3668c 蛋白与等体积的弗氏不完全佐剂混合乳化,免疫新西兰大白兔,Rv3668c 蛋白的免疫剂量为 400 μg/只。以 1 mg/kg 的剂量首免跖部,以后经背部皮下多点注射,每隔 2 周免疫 1

次，共免疫 4 次，于末次免疫后第 1 周采集血液，分离血清并保存于－20 ℃。

1.8 抗体效价的间接 ELISA 检测

采用常规间接 ELISA 法检测自制抗体血清的效价，设空白对照（免疫前血清）。以碳酸盐缓冲液稀释的 Rv3668c 蛋白（终浓度为 1 μg/mL）为抗原包被 ELISA 板，以倍比稀释的兔血清作为一抗，以辣根过氧化物酶（HRP）标记的山羊抗兔 IgG 为二抗，以 3，3′，5，5′-四甲基联苯胺（TMB）为显色底物，用酶标仪检测样品的 $D_{450\ nm}$ 值。

1.9 重组蛋白的 Western-blot 分析

将纯化的融合蛋白进行 SDS-PAGE 电泳分离，用半干转移电泳仪将蛋白从凝胶电转至硝酸纤维素膜，转膜条件为电压 15 V，时间 30 min。转上蛋白的硝酸纤维素膜以 50 g/L 脱脂奶粉封闭，1 mL/L TBST 洗膜，根据试验目的不同，加入不同种类一抗：抗 His 标签单克隆抗体（1∶5 000 稀释），或自己制备的兔血清多抗（1∶500 稀释），或牛结核病阳性血清（1∶500 稀释），或牛结核病阴性血清（1∶500 稀释）作为一抗进行结合，37 ℃、90 r/min 结合 2 h，洗膜。之后加入 HRP 标记的二抗，37 ℃、90 r/min 结合 2 h，TBST 洗膜，充分洗涤后用 DAB 显色，鉴定表达产物。

1.10 Rv3668c 蛋白免疫原性的 ELISA 检测

将纯化的 Rv3668c 蛋白用碳酸盐缓冲液稀释于 96 孔 ELISA 板中进行包被，5 μg/孔。以倍比稀释的阴性、阳性血清作为一抗（以 1∶20 为起始稀释倍数），以 HRP 标记的山羊抗牛 IgG 为二抗，每次孵育完用 0.5 mL/L 的 TBST 洗板 3 次，以 TMB 为显色底物，用酶标仪检测样品的 $D_{450\ nm}$ 值。

2 结果

2.1 目的基因 *rv*3668*c* 的 PCR 扩增

以 H37Rv 标准株为模板，对 *rv*3668*c* 基因进行 PCR 扩增，对 PCR 产物进行凝胶电泳。结果（见图 1）显示，目的片段与预期大小一致，为 600 bp 左右，且阴性对照无扩增片段。

2.2 重组质粒 p30a-68 的鉴定

对构建好的重组质粒 p30a-68 用 *Bam*HⅠ＋*Eco*RⅠ进行双酶切鉴定，对产物进行核酸凝胶电泳。结果（见图 2）显示，获得了约 600 bp 的目的片段及约 5 422 bp 的载体片段，与预期结果一致。

2.3 诱导表达的重组蛋白及其纯化

分别于 37、30 和 22 ℃（IPTG 终浓度 1 mmol/L）诱导目的蛋白表达，取超声波破菌离心后的上清和沉淀进行 SDS-PAGE 分析。结果显示，诱导产生的目的蛋白为 26 ku 左右，与预期大小一致；在 22、30 和 37 ℃条件下在上清中出现大量的目的蛋白，30 和 37 ℃时可溶性表达比例更高。用 Ni-NTA His-Bind Resin 亲和柱纯化可溶性蛋白，洗脱液取样进行 SDS-PAGE 分析。结果（见图 3）显示，获得了纯度较高的重组蛋白。

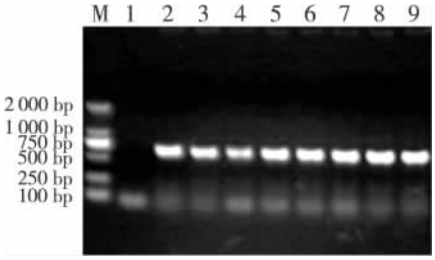

图 1 目的基因的 PCR 扩增

Fig. 1 PCR amplification for *rv*3668*c* gene

M：DNA 分子质量标准；1：空白对照；2～9：*rv*3668*c* 的 PCR 产物

M：DL2000 DNA Marker；1：Blank control；2－9：PCR-amplified *rv*3668*c* genes，respectively

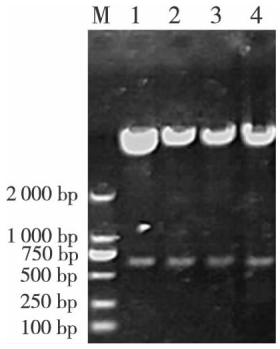

图 2 重组质粒 p30a-68 的酶切鉴定

Fig. 2 Identification of recombinant plasmid p30a-68 digested with *Bam*HⅠ and *Eco*RⅠ

M：DNA 分子质量标准；1～4：重组质粒 p30a-68 的酶切产物

M：DL2000 DNA Marker；1－4：The products from the recombinant plasmid p30a-68 digested with *Bam*HⅠ and *Eco*RⅠ，respectively

2.4 抗体效价的检测

2 只兔经过基础免疫和加强免疫后，耳缘静脉采血，分离血清，采用间接 ELISA 方法进行检测，结果（见图 4）显示，血清抗体效价达 1∶25 600 以上，表明该抗原可以诱导兔产生良好的免疫学反应。

2.5 重组蛋白的验证及免疫原性分析

经过 DAB 显色后，与抗 His 标签单克隆抗体作用的 NC 膜在约 26 ku 处出现一明显可见条带，与预期的重组蛋白大小一致，而阴性对照样品（pET-30a 空载体的全菌蛋白）没有条带出现，验证了纯化产物即为预期的重组蛋白 His-Rv3668c（见

图 5)。用牛结核病阳性血清作为一抗,可检测到目的蛋白,健康牛血清则未显示出目的蛋白的条带(见图 6)。

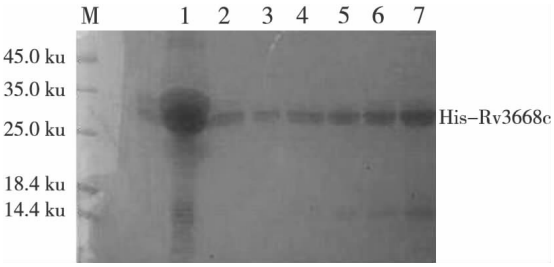

图 3　重组蛋白纯化产物的 SDS-PAGE 分析

Fig. 3　SDS-PAGE analysis of the expressed protein

M:蛋白质分子质量标准;1:10 mmol/L 咪唑洗脱的重组蛋白;2:20 mmol/L 咪唑洗脱的重组蛋白;3:40 mmol/L 咪唑洗脱的重组蛋白;4:60 mmol/L 咪唑洗脱的重组蛋白;5:80 mmol/L 咪唑洗脱的重组蛋白;6:100 mmol/L 咪唑洗脱的重组蛋白;7:500 mmol/L 咪唑洗脱的重组蛋白

M: Protein molecular weight Marker; 1: Elution buffer with 10 mmol/L imidazole; 2: Elution buffer with 20 mmol/L imidazole; 3: Elution buffer with 40 mmol/L imidazole; 4: Elution buffer with 60 mmol/L imidazole; 5: Elution buffer with 80 mmol/L imidazole; 6: Elution buffer with 100 mmol/L imidazole; 7: Elution buffer with 500 mmol/L imidazole

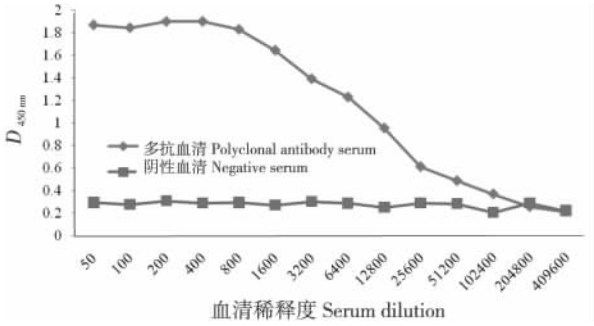

图 4　兔血清抗体效价的间接 ELISA 测定

Fig. 4　The $D_{450\ nm}$ values of rabbit sera detected by indirect ELISA

2.6　免疫原性的 ELISA 检测

采用 ELISA 方法检测阴性、阳性血清,结果(见图 7)表明,该抗原可以与阳性血清发生良好的免疫学反应。

3　讨论

目前,结核病仍是对人类健康危害最严重、对社会公共卫生安全影响最大的传染病之一。抗生素治疗能帮助绝大部分结核病人康复,但多重耐药结核分枝杆菌的出现及与艾滋病的混合感染增加了治

图 5　重组蛋白的 Western-blot 分析

Fig. 5　Western-blot analysis of the recombinant protein

M:蛋白质分子质量标准;1、3:BL21/pET-30a 空载体全菌蛋白;2、4:His-Rv3668c 纯化蛋白产物;1、2:以抗 His 标签抗体为一抗;3、4:以抗 Rv3668c 多克隆抗体为一抗

M: Protein molecular weight Marker; 1, 3: Total proteins of BL21/pET-30a vector strain, respectively; 2, 4: Purified product of His-Rv3668c, respectively; 1, 2: Reacting with anti-His tag monoclonal antibody, respectively; 3, 4: Reacting with polyclonal antibody to Rv3668c, respectively

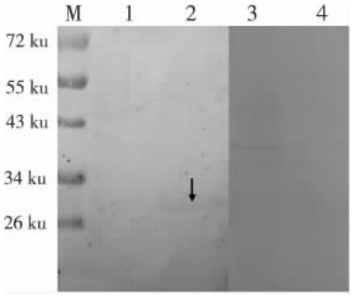

图 6　牛结核病阴性血清和阳性血清的 Western-blot 分析

Fig. 6　Western-blot analysis of the positive serum with tuberculosis and the negative serum without bovine tuberculosis

M:蛋白质分子质量标准;1、3:BL21/pET-30a 空载体全菌蛋白;2、4:His-Rv3668c 纯化蛋白产物;1、2:以 Mb 阳性血清为一抗;3、4:以 Mb 阴性血清为一抗

M: Protein molecular weight Marker; 1, 3: Total proteins of BL21/pET-30a vector strain, respectively; 2, 4: Purified product of His-Rv3668c, respectively; 1, 2: Reacting with the positive sera with bovine tuberculosis, respectively; 3, 4: Reacting with the negative sera without bovine tuberculosis, respectively

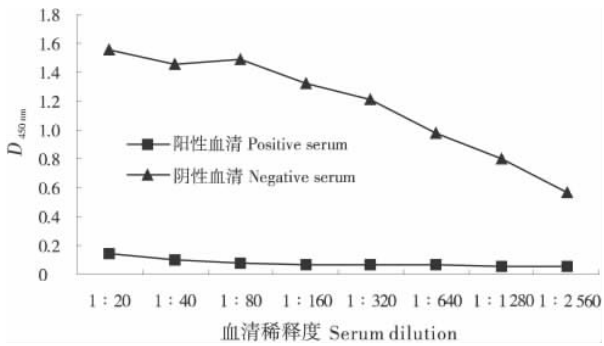

图 7　阴性牛血清和阳性牛血清免疫原性的 ELISA 测定

Fig. 7　$D_{450\ nm}$ values of the negative bovine serum and the positive bovine serum detected by ELISA

疗的难度[8-11]。近十年来，人们对分枝杆菌分泌蛋白进行了广泛的研究[12]，期望能进一步阐明其致病机制，对结核病的诊断和防治具有重要意义[13]。

本试验利用 GenBank 中结核分枝杆菌强毒力标准株 H37Rv *rv*3668*c* 基因序列信息设计引物，对 *rv*3668*c* 进行了克隆、融合表达和免疫活性检测，并制备了多克隆抗体。分别在 37、30 和 22 ℃条件下对目的蛋白进行诱导；结果发现 30 ℃，IPTG 终浓度为 1 mmol/L 为此蛋白表达的最佳条件，可获得最大量的可溶性目的蛋白。带 His 标签的融合表达蛋白，可利用 Ni^{2+} 亲和色谱进行纯化。纯化的蛋白产物用抗 His 标签抗体进行 Western-blot 分析，验证了纯化产物为重组蛋白 His-Rv3668c。利用重组蛋白对牛结核病阳性血清及阴性血清进行的 Western-blot 分析结果表明，在患有结核病的牛体内，有针对此蛋白的抗体产生，表明此蛋白具有免疫原性。同时，用纯化蛋白 His-Rv3668c 免疫新西兰大白兔，获得了较高的抗体效价。所获得的高纯度蛋白和针对此蛋白的特异性多克隆抗体，为进一步研究 Rv3668c 蛋白的生物学功能及其在分枝杆菌致病性中的作用奠定了基础。

参考文献(References)

[1] 刘思国，于辉，宫强，等. 牛结核病研究进展[J]. 畜牧兽医科技信息，2003(10)：10-14.
LIU Si-guo，YU Hui，GONG Qiang，*et al*. Recent development in bovine tuberculosis[J]. *Scientific Information of Animal Husbandry and Veterinary Medicine*，2003(10)：10-14.(in Chinese)

[2] TOLLEFSEN S，VORDEERMEIER M，ULSEN I，*et al*. DNA injection in combination with electroporation：A novel method for vaccination of farmed ruminants[J]. *Scand J Immunol*，2003，57(3)：229-238.

[3] BROCK I，WELDINGH K，LEYTEN S，*et al*. Specific T-cell epitopes for immunoassay-based diagnosis of *Mycobacterium tuberculosis* infection[J]. *J Clin Microbiol*，2004，42(6)：2379-2387.

[4] BRYCEM B，NATALIEA P，DENISEL K，*et al*. Differentiation between *Mycobacterium bovis* BCG-vaccinated and *M. bovis*-infected cattle by using recombinant mycobacterial antigens[J]. *Clin Diagn Lab Immunol*，1999，6(1)：1-5.

[5] TEIXEIRA H C，ABRAMO C，MUNK M E. Immunological diagnosis of tuberculosis：problems and strategies for success[J]. *J Bras Pneumol*，2007，33(3)：323-334.

[6] IWA M LEN H，BERVEN F S，FLADMARK K E，*et al*. Comprehensive analysis of exported proteins from *Mycobacterium tuberculosis* H37Rv[J]. *Proteomics*，2007，7(10)：1702-1718.

[7] 郭设平，刘思国，张秀华，等. 牛分支杆菌抗原 MPB70、MPB83、ESAT6 的融合表达及重组蛋白的初步应用[J]. 畜牧兽医学报，2006，37(7)：676-680.
GUO She-ping，LIU Si-guo，ZHANG Xiu-hua，*et al*. Fusion expression of MPB70，MPB83 and ESAT-6 of *Mycobacterium bovis* and its use as diagnostic reagent[J]. *Acta Veterinaria et Zootechnica Sinica*，2006，37(7)：676-680.(in Chinese)

[8] ALEXANDER C，MAUE W，RAY W，*et al*. Analysis of immune responses directed toward a recombinant early secretory antigenic target six-kilodalton protein-culture filtrate protein 10 fusion protein in *Mycobacterium bovis*-infected cattle[J]. *Infect Immun*，2005，73(10)：6659-6667.

[9] YANG H L，ZHU Y Z，QIN J H，*et al*. *In silico* and microarray-based genomic approaches to identifying potential vaccine candidates against *Leptospira interrogans*[J]. *BMC Genomics*，2006，7：293.

[10] ANDERSEN P. Effective vaccination of mice against *Mycobacterium tuberculosis* infection with a soluble mixture of secreted mycobacterial proteins[J]. *Infect Immun*，1994，62(6)：2536-2544.

[11] BUDDLE B M，RYAN T J，POLLOCK J M，*et al*. Use of EAST-6 in the interferon-γ test for diagnosis of bovine tuberculosis following skin testing[J]. *Vet Microbiol*，2001，80(1)：37-46.

[12] OTTENHOFF T H M，KAUFMANN S H E. Vaccines against tuberculosis：Where are we and where do we need to go?[J]. *PLoS Pathog*，2012，8(5)：e1002607.

[13] STEINGART K R，HENRY M，LAAL S，*et al*. Commercial serological antibody detection tests for the diagnosis of pulmonary tuberculosis：A systematic review[J]. *PLoS Med*，2007，4(6)：202.

（责任编辑 胡弘博）

第34卷 第3期
2012 年 3 月

中 国 预 防 兽 医 学 报
Chinese Journal of Preventive Veterinary Medicine

Vol. 34,No.3
Mar. 2012

doi: 10.3969/j.issn.1008-0589.2012.03.14

牛分枝杆菌与鸟型分枝杆菌2型重组蛋白Ag85b的血清学交叉反应研究

朱 婷，王华南，刘慧芳，于申业，王秀梅，陈莉苹，司 微，赵海玲，刘思国*

(中国农业科学院哈尔滨兽医研究所 兽医生物技术国家重点实验室/动物细菌病研究室， 黑龙江 哈尔滨 150001)

摘 要：牛分枝杆菌(*M. bovis*)是引起牛结核病的常见病原，而鸟分枝杆菌(*M. avium*)2型则通常交叉感染牛，但不会导致严重的病变。为鉴定 *M. bovis* 和 *M. avium* 的免疫交叉反应情况，本研究分别以 *M. bovis* 和 *M. avium* 2型的基因组为模板，扩增 ag85b 基因，分别构建了 *M. bovis* 和 *M. avium* 的原核和真核表达重组质粒进行表达。以原核表达纯化的两种重组蛋白 Ag85b (rAg85b)分别作为包被抗原，交叉检测两种真核重组质粒免疫豚鼠制备的抗血清。结果表明，原核表达的 *M. bovis* 和 *M. avium* rAg85b 与真核重组质粒免疫豚鼠制备的两种抗血清之间存在较强的免疫交叉反应。研究结果揭示 *M.bovis* 和 *M. avium* 的 Ag85b 蛋白存在很强的血清学交叉反应，这将严重干扰 *M. bovis* Ag85b 作为候选疫苗的免疫监测。

关键词：牛结核分枝杆菌；鸟型分枝杆菌；ag85b 基因；交叉反应

中图分类号：S852.61 **文献标识码：**A **文章编号：**1008-0589(2012)03-0223-04

Immune cross-reaction of recombinant proteins Ag85b between *Mycobacterium bovis* and *Mycobacterium avium* serotype 2

ZHU Ting, WANG Hua-nan, LIU Hui-fang, YU Shen-ye, WANG Xiu-mei, CHEN Li-ping, SI Wei, ZHAO Hai-ling, LIU Si-guo*

(Division of Animal Bacteriosis, State Key Laboratory of Veterinary Biotechnology, Harbin Veterinary Research Institute, Chinese Academy of Agricultural Sciences, Harbin 150001, China)

Abstract: *Mycobacterium bovis* is a common pathogen to cause bovine tuberculosis in cattle, but crossing infection of *Mycobacterium avium* is the normal cases in cattle. To identify serum crossing reactions of the 2 bacteria, the ag85b genes were amplified by PCR from genomes of *M. bovis* and *M. avium* serotype 2, respectively, and subcloned into pET28a and pcDNA3.1 (pcDNA-Ag85b). Guinea pigs were immunized with pcDNA-Ag85b of *M. bovis* and *M. avium*, respectively, and the prepared anti-Ag85bs were used to analyze the cross-reactions of the two different *Mycobacteria* by ELISA with recombinant Ag85b proteins as coating antigens expressed in *E. coli*. The results shown that *M. bovis* and *M. avium* had strong cross-reactions between the two kinds of Ag85b proteins, which provided evidence that *M. avium* infection would interfere the immunologic surveillance to the use of vaccines containing Ag85b in cattle herd.

Key words: *Mycobacterium bovis*; *Mycobacterium avium*; ag85b gene; immune cross-reaction

*Corresponding author

收稿日期：2011-09-12
基金项目：国家重点基础研究发展计划(973)项目(2012CB518801)；国家科技基础性工作专项(2008FY210200)
作者简介：朱 婷(1987-)，女，山东临沂人，硕士研究生，主要从事动物细菌病研究.
* **通信作者：**E-mail：Siguo_liu@hvri.ac.cn

牛分枝杆菌(*Mycobacterium bovis*)属于结核分枝杆菌复合群，主要引起牛结核病，是一种人畜共患的慢性消耗性传染病[1]，严重威胁着我国奶牛养殖业的健康发展和公共卫生的安全。此外，自然界中还存在多种致病性的非结核分枝杆菌复合群，引起的疾病也表现结核样症状，结核病的诊断造成一定的影响[2]。杜艳芬等报道，从1 067份PPD阳性样品中，结核分枝杆菌复合物分离率为38.7 %，非结核分枝杆菌分离率为61.3 %，表明我国非结核分枝杆菌的感染率是非常高的，这给牛结核病的诊断和预防带来了较大的困难[3]。

鸟分枝杆菌复合体(*Mycobacterium avium* complex，MAC)是一类重要的非结核分枝杆菌，它包括鸟分枝杆菌(*M. avium*)和胞内分枝杆菌(*M. intracellulare*)，MAC可以引起非典型肺炎，并且对抗结核药物耐药，因此越来越受到人们的重视。除对人畜造成危害，MAC感染还干扰结核病的诊断，造成假阳性，影响牛结核病的防控[4-6]。

Ag85是分枝杆菌的一种分泌蛋白，在分枝杆菌粘附细胞的过程中起重要作用[7-8]，*M. bovis*和*M. avium*培养滤液中均存在大量Ag85b蛋白[9]，Ag85b的核苷酸序列表明两者之间具有较高的一致性。因此，本研究构建*M. bovis*和*M. avium* 2型的ag85b基因的原核及真核表达重组质粒，用构建的真核重组质粒免疫豚鼠，制备抗血清，以纯化的原核表达的重组Ag85b (rAg85b)蛋白为包被抗原，间接ELISA方法检测两种rAg85b蛋白与抗血清间的交叉反应，评价*M. avium*对*M. bovis* Ag85b蛋白作为牛结核病新型候选疫苗的免疫检测造成的影响。

1 材料和方法

1.1 菌株、载体、实验动物 *M. bovis* Vallee株购自中国药品生物制品鉴定所*M. avium* 2型、pET-28a、pcDNA3.1、鼠抗*M. avium*和*M. bovis*的Ag85b抗血清、宿主菌*E. coli* DH5α和*E. coli* BL21 (DE3)感受态细胞均由本实验室保存；2月龄豚鼠购自本研究所实验动物中心。

1.2 主要试剂 限制性内切酶、*Taq* DNA聚合酶和T4 DNA连接酶均购自MBI公司；DNA胶回收试剂盒、除内毒素质粒提取试剂盒和DAB购自上海华舜生物工程有限公司；ECL发光显色液购自天根生化科技有限公司；抗His标签单克隆抗体(MAb)购自Novagen公司；兔抗豚鼠酶标二抗(HRP-IgG)和山羊抗小鼠酶标二抗(FITC-IgG)均购自Sigma公司。

1.3 PCR引物的设计与合成 根据GenBank中*M. bovis*的基因组序列(AF2122/97)和*M. avium*基因组序列(CP000479.1)分别设计两对Ag85b引物，引物由南京金思特科技有限公司合成，*M. bovis* Ag85b的一对引物为U-*Eco*RⅠ：ATTGAATTCATGACAGACGTGAGC，L-*Sal*Ⅰ：TATGTCGACGCCTAACGAACTCT；*M. avium* Ag85b的一对引物为U-*Eco*RⅠ：GTGGAATTCATGACAGATCTGAGCGAGAAG，L-*Xho*Ⅰ：ATCTCGAGTTAGGTGCCCTGCAGGTC。扩增片段分别为978 bp和993 bp。

1.4 原核及真核表达载体的构建 将扩增到的*M. bovis*目的基因双酶切后与经*Eco*RⅠ和*Sal*Ⅰ双酶切的pET28a、pcDNA3.1连接；*M. avium*目的基因双酶切后与经*Eco*RⅠ和*Xho*Ⅰ双酶切的pET28a、pcDNA3.1连接。产物转化大肠杆菌DH5α感受态细胞，提取重组质粒进行双酶切及测序鉴定，将获得的原核表达重组质粒转化BL21 (DE3)感受态细胞进行表达。

1.5 原核表达重组蛋白的诱导及纯化 分别培养含有*M. bovis*和*M. avium* pET-Ag85b重组质粒的重组菌，并以IPTG (1 mmol/L)进行诱导表达，离心收集沉淀，PBS洗涤菌体沉淀后用Bind Buffer (20 mmol/L咪唑、20 mmol/L NaH_2PO_4、0.5 mol/L NaCl、4 mol/L尿素pH7.4)重悬，超声破碎后4 ℃离心收集上清，采用AKTA Explorer蛋白纯化系统操作规程进行纯化，洗脱液为500 mmol/L咪唑、20 mmol/L NaH_2PO_4、0.5 mol/L NaCl、4 mol/L尿素pH7.4。

1.6 表达产物的组氨酸标签western blot鉴定 将纯化的重组蛋白进行SDS-PAGE，用半干式转膜仪电转硝酸纤维素膜，50 g/L BSA封闭过夜，以鼠抗His MAb (1∶5 000)为一抗，以山羊抗鼠HRP-IgG (1∶5 000)为二抗，采用ECL显色鉴定表达产物。

1.7 真核表达重组质粒的转染及间接免疫荧光(IFA)鉴定 分别提取*M. bovis*和*M. avium*的pcDNA-Ag85b重组质粒。根据Lipofectamine 2000转染试剂说明书方法将其分别转染293T细胞。转染72 h后，70 %的冷乙醇固定细胞，以抗rAg85b蛋白的

小鼠的血清(1∶200)为一抗，以山羊抗小鼠 FITC-IgG (1∶500)为二抗，在荧光显微镜下检测。

1.8　真核表达重组质粒的提取及免疫　分别培养含有 *M. bovis* 和 *M. avium* pcDNA-Ag85b 重组质粒的重组菌，离心收集沉淀并以碱裂解法大量提取质粒和 PEG 法纯化质粒。将纯化的重组质粒以 200 μg/ 只肌肉注射免疫豚鼠，设置 pcDNA3.1 空质粒免疫组作为对照，每隔两周免一次，三免后加强免疫，两周后前肢静脉采血检测效价。

1.9　ELISA 测定交叉反应　间接 ELISA 法测定两种 rAg85b 与抗血清之间的免疫交叉反应，将纯化的原核表达的 rAg85b 均以 10 μg/mL 包被酶标反应板，5 %的鱼皮胶 37 ℃封闭 1 h，分别以倍比稀释的两种抗豚鼠血清作为一抗，兔抗豚鼠 HRP-IgG 为二抗 (1∶5 000)，TMB 避光显色 10 min～15 min，2 mol/L H_2SO_4 终止反应。

2　结　果

2.1　目的基因的扩增　分别以 *M. bovis* 和 *M. avium* DNA 为模板，PCR 扩增结果显示，扩增片段约 1 kb (图 1A)。测序结果与预期结果相符，分别为 978 bp 和 993 bp。

2.2　重组蛋白的诱导表达和纯化　经 IPTG 诱导的重组菌进行 SDS-PAGE 分析，表达的 *M. bovis* 和 *M. avium* rAg85b 重组蛋白分别与预期结果相符，重组蛋白主要以包涵体的形式存在，采用 AKTA Explorer 蛋白纯化系统进行纯化，SDS-PAGE 电泳分析纯化的结果(图 1B)。

2.3　重组蛋白的 western blot 分析　将表达纯化的重组蛋白与抗 His MAb 进行 western blot 分析，结果出现的特异目的条带与预期大小相符(图 1C)。

2.4　转染细胞的 IFA 鉴定　将 *M. bovis* 和 *M. avium* 重组真核表达质粒分别转染 293T 细胞，转染的细胞培养 72 h 后，IFA 检测结果显示，构建的真核重组质粒在真核细胞中均获得表达(图 2)。

2.5　rAg85b 交叉反应的 ELISA 检测　纯化的两种原核表达的 rAg85b 均以 0.5 μg/ 孔包被酶标板，将真核重组质粒分别免疫豚鼠制备的两种抗血清倍比稀释后，采用间接 ELISA 法检测两种 rAg85b 与抗血清之间的交叉反应情况。结果显示原核表达的 *M. bovis* 和 *M. avium* rAg85b 与 *M. bovis* 和 *M. avium* Ag85b 基因核酸免疫制备的豚鼠抗血清均存在交叉应，S/P 均大于 0.5，并且免疫 *M. avium* pcDNA-Ag85b 重组质粒的豚鼠分离的抗血清与原核表达的 *M. bovis* rAg85b 反应更为强烈(图 3)。

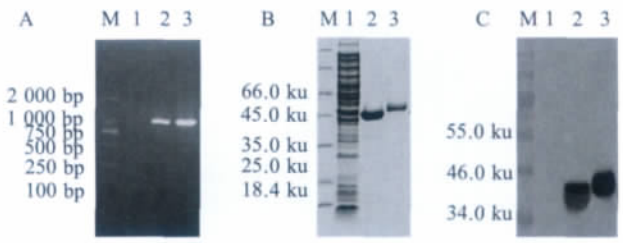

A. M: DNA Marker DL2000; 1-3: Negative control, product of *M. bovis* gene and product of *M. avium* gene.
B. M: Protein Marker; 1-3: Lysate of pET28a/BL21, purified *M. avium* rAg85b and purified *M. bovis* rAg85b.
C. M: Protein Marker; 1-3: Negative control, purified *M. avium* rAg85b and *M. bovis* rAg85b reacted with anti-His MAb

图 1　基因的 PCR 扩增(A)、融合蛋白的表达纯化(B)及 western blot 检测分析(C)

Fig.1　PCR amplification of *ag85b* gene (A) and analysis of expressed recombinant Ag85b by SDS-PAGE (B) and western blot (C)

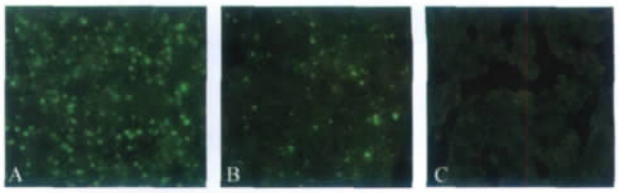

A: 293T cells transfected with *M. bovis* pcDNA-Ag85b;
B: 293T cells transfected with *M. avium* pcDNA-Ag85b;
C: 293T cells transfected with pcDNA3.1

图 2　IFA 鉴定结果

Fig.2　The identification of rAg85b in transfected 293T cells by IFA

3　讨　论

M. bovis 分泌的蛋白对结核病的保护性免疫至关重要[10]，Ag85b 是 *M. bovis* 一种分泌蛋白[11]，它可以诱导机体产生 Th1 型细胞免疫应答，分泌高水平的 IFN-γ ，产生 CTL，它抵抗结核杆菌再感染的能力优于 BCG[12]。Silver 等发现 Ag85b 可以刺激 PPD 实验阳性的健康人群外周血单核细胞明显增殖并产生 IFN-γ [13]。

Ag85b 主要存在于人型或者 *M. bovis* 中，在其它非结核分枝杆菌中也有存在，但 *M. bovis* 与非结核分枝杆菌 Ag85b 的血清学交叉反应情况尚未见报道，本实验分别构建了 Ag85b 的原核和真核重组表

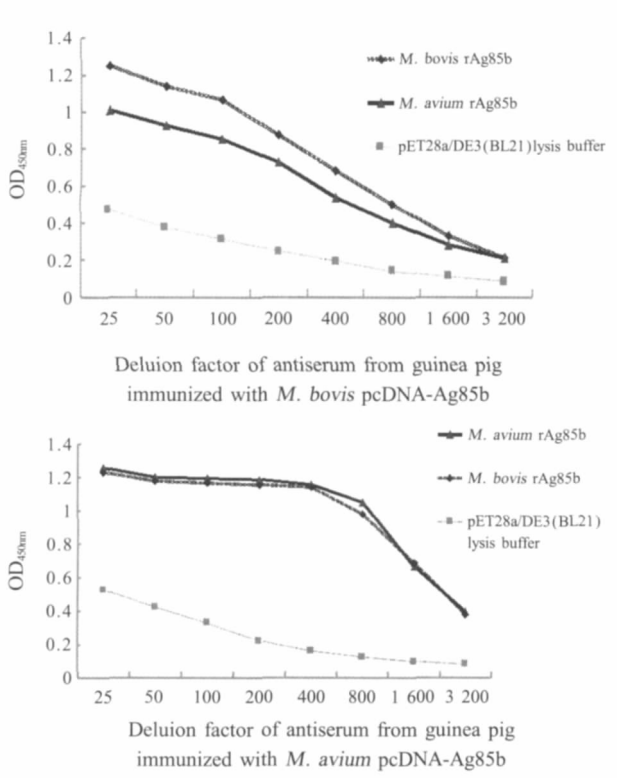

图 3 抗血清检测两种 rAg85b 蛋白的交叉反应情况

Fig.3 The cross-reaction between two rAg85b proteins with antiserum by ELISA

达质粒，以原核表达纯化的两种菌的 rAg85b **作为包被抗原，真核重组质粒免疫豚鼠获得的抗血清作为一抗，采用间接** ELISA **法检测两种菌的** rAg85b **之间的血清学交叉反应情况。为消除豚鼠抗血清中** *E. coli* **抗体的干扰，对免疫后获得的抗血清采用** *E. coli* **裂解物进行吸收。实验结果表明原核表达的** *M. bovis* **与** *M. avium* 2 **型** rAg85b **与真核重组质粒免疫豚鼠获得的抗血清之间存在着很强的交叉反应，并且免疫** *M. avium* pcDNA-Ag85b **的豚鼠的抗血清与** *M. bovis* rAg85b **的交叉反应更为强烈，这也提示它们之间存在交叉保护作用，为寻找** *M. bovis* Ag85b **与非结核分枝杆菌** ag85b **的共同抗原决定簇提供了实验依据，同时也为牛结核病病原及其抗体快速、敏感的检测奠定了基础。该实验结果还表明，** *M. avium* **对** *M. bovis* Ag85b **蛋白作为牛结核病新型候选疫苗特别是以** ag85b **基因的核酸疫苗及** Ag85b **亚单位疫苗的免疫检测造成的影响。因此，新型疫苗的研制应采用可以鉴别疫苗免疫与自然感染的分子标记物，对于牛群的净化具有重要的意义。**

参考文献：

[1] **刘思国，王春来，张秀华，等. 牛结核病病原生态学和流行病学研究**[J]. **中国畜牧兽医，**2005，32(3)：60-62.

[2] **刘建东，刘思国，王春来，等. 基因免疫制备牛分枝杆菌** MPB64 **抗原单克隆抗体**[J]. **中国预防兽医学报，**2007，29(11)：870-873.

[3] **杜艳芬. 牛结核病病原学调查及分子流行病学研究**[D]. **中国农业科学院**. 2009.

[4] Matlova L, Dvorska L, Ayele W Y, et al. Distribution of *Mycobacteriu avium* complex isolates in tissue samples of pigs fed naturally contaminated with mycobacteria as a supplement [J]. J Clin Microbiol, 2005, 43(3): 1261-1268.

[5] Soini H, Musser J M. Molecular diagnosis of mycobacte-ria [J]. Clin Chem, 2001, 47(5): 809-814.

[6] **王洪生，吴勤学. 非结核分枝杆菌感染与艾滋病**[J]. **国外医学：皮肤性病学分册，**2005，31(3)：166-168.

[7] Belisle J T, Vissa V D, Sievert T, et al. Role of the major antigen of *Mycobacterium tuberculosis* in cell wall biogenesis [J]. Science, 1997, 276(5317): 1420-1422.

[8] Ohara N, Ohara-Wada N, Kitarua H, et al. Analysis of the genes encoding the antigen 85 complex and MPT51 from *Mycobacterium avium* [J]. Infect Immun, 1997, 65(9): 3680-3685.

[9] Horwitz M Z, Lee B W, Dillon B J, et al. Protective immunity against tuberculosis induced by vaccination with major extracellular proteins of *Mycobacterium tuberculosis* [J]. Proc Natl Acad Sci USA, 1995, 92(5): 1530-1534.

[10] Wiker H G, Harboe M. The antigen 85 complex: a major secretion product of *Mycobacterium tuberculosis* [J]. Microbiol Rev, 1992, 56(4): 648-661.

[11] Sinha R K, Verma I, Khuller G K, et al. Immunobiological properties of a 30 kDa secretory protein of *Mycobacterium tuberculosis* H37Ra [J]. Vaccine, 1997; 15(6/7): 689-699.

[12] Sinha R F, Wallis R S, Ellner J J. Mapping of T cell epitopes of the 30KDa alpha antigen of *Mycobacterium Bovis* strain Bacillus Calmette-Guerin in purified protein derivative (PPD) -positive individuals [J]. Immumology, 1995, 154 (9): 4665-4674.

[13] Silver R F, Wallis R S, Ellner J J. Mapping of T cell epitopes of the 30 KDa alpha antigen of *Mycobacterium bovis* strain Bacillus Calmette-Guerin in purified protein derivative (PPD) -positive individuals [J]. Immunology, 1995, 154(9): 4665-4874.

(本文编辑：赵晓岩)

Research in Veterinary Science 94 (2013) 406–412

Contents lists available at SciVerse ScienceDirect

Research in Veterinary Science

journal homepage: www.elsevier.com/locate/rvsc

A novel B cell epitope in cold-shock DEAD-box protein A from *Mycobacterium tuberculosis*

Huanan Wang [a,b], Ting Zhu [a], Shenye Yu [a], Huifang Liu [a], Xiumei Wang [a], Liping Chen [a], Wei Si [a], Hai Pang [b,*], Siguo Liu [a,*]

[a] Division of Bacterial Diseases, State Key Laboratory of Veterinary Biotechnology, Harbin Veterinary Research Institute, Chinese Academy of Agricultural Sciences, Harbin 15000, PR China
[b] School of Medicine, Tsinghua University, Beijing, PR China

ARTICLE INFO

Article history:
Received 26 May 2012
Accepted 22 November 2012

Keywords:
Mycobacterium tuberculosis
Cold-shock DEAD-box protein A
Phage random peptide library
mAb
Epitope

ABSTRACT

In this study, a hybridoma-based technique and phage display technology were used to obtain mouse monoclonal antibodies (mAb) against cold-shock DEAD-box protein A (CsdA) from *Mycobacterium tuberculosis* and to determine the location of the relevant epitope. One highly specific mAb, named A3G5, was developed against the recombinant CsdA protein (rCsdA) and could detect rCsdA protein in enzyme-linked immunosorbent assays (ELISA) and Western blot assays. By screening a phage displayed library of random 12-mers (Ph.D.-12), 10 positive phage clones were randomly selected after three rounds of bio-panning and identified by ELISA. Eight of these clones were sequenced, and their amino acid sequences were deduced. One B-cell epitope (-APDPPLSRR-) in the rCsdA protein was identified with mAb A3G5. A synthetic peptide (-MAPDPPLSRR-) (Cpep) matched well with the CsdA sequence at 443–451 aa and was confirmed by affinity ELISA, competitive inhibition assays and the development of an immune response in mice. These results may be of great potential value in the further analysis of the function and structure of the CsdA protein from *M. tuberculosis*.

1. Introduction

Tuberculosis (TB) is an infectious disease caused by *Mycobacterium tuberculosis* (*M. tuberculosis*) and *Mycobacterium bovis* (*M. bovis*) around the world. That causes serious harm to the cattle industry and to public health (Lesslie and Birn, 1970; Schliesser, 1976; Thoen et al., 1981; Smith, 1984; Pavlik et al., 2003; Gibson et al., 2004; Jou et al., 2008; Du et al., 2011; Jorda and Vieira, 2011). Currently, TB is one of the major causes of illness and death around the world, since approximately one-third of the world's population is infected and an estimated 1.7 million people die annually from the disease (WHO, 2009, 2010a; Jorda and Vieira, 2011). The prevention and control of TB has great significance for public health.

There are no effective TB vaccines, and the Bacille Calmette–Guerin (BCG) vaccine does not prevent TB infection. Clinical BCG vaccine trials have demonstrated a wide range of efficacy, and meta-analyses estimate an approximately 50% overall level of prevention of the disease (Rodrigues et al., 1993; Colditz et al., 1994, 1995). Because of the lack of an effective vaccine, choosing the proper drug treatment is very important in preventing and treating TB. However, the number of drug-resistant TB cases has risen in recent years, and resistant cases have been identified across the world (WHO, 2010b). Thus, new anti-TB drugs are required to control and treat TB. Identifying new targets, especially proteins (primarily enzymes) that have significant physiological functions, is an important part of developing new drugs (Zhang et al., 2006). RNA helicases play important roles in various cellular processes that require the modulation of RNA structure; these processes include RNA splicing, ribosome biogenesis, translational initiation, mRNA degradation and cell division (Schmid and Linder, 1992; Luking et al., 1998; de la Cruz et al., 1999; Bizebard et al., 2004). According to the predicted three-dimensional structure from the SWISS-MODEL website, cold-shock DEAD-box protein A (CsdA) from *M. tuberculosis* may function as an RNA helicase. Considering the important functions of RNA helicases, CsdA may have potential as a target of new drugs against *M. tuberculosis*.

In the present study, the *csdA* gene from *M. tuberculosis* was cloned and expressed in *Escherichia coli* (*E. coli*), and the purified recombinant protein (rCsdA) was used to immunize mice. After cell fusion and screening, a stable hybridoma cell line was obtained. The cell line produced a high level of secreted monoclonal antibody (A3G5). Phage display is described as an *in vitro* selection technique in which a peptide is genetically fused to a coat protein

* Corresponding authors.
E-mail addresses: pangh@xtal.tsinghua.edu.cn (H. Pang), siguo_liu@yahoo.com.cn (S. Liu).

0034-5288/$ - see front matter Crown Copyright © 2012 Published by Elsevier Ltd. All rights reserved.
http://dx.doi.org/10.1016/j.rvsc.2012.11.013

of the bacteriophage (Devlin et al., 1990). We used phage display technique to screen and localize the epitope on the rCsdA protein. The results provide an experimental platform for the study of the structure and function of CsdA.

2. Materials and methods

2.1. Purification of the recombinant protein

The *csdA* DNA fragments from *M. tuberculosis* were inserted into the pET28a vector (from stock from the authors' laboratory). The *csdA* gene was expressed in *E. coli* BL21 (DE3) cells, and the recombinant protein (rCsdA) was purified with an Ni–NTA column. Briefly, the expression of rCsdA was induced with 0.1 mM isopropyl β-D-1-thiogalactopyranoside (IPTG) overnight at 16 °C. The cells were suspended in suspension buffer (20 mM, 150 mM NaCl pH 8.0) and lysed by sonication for 15 min on ice. The rCsdA protein expressed in form of inclusion bodies, which were collected by centrifugation and then disrupted in buffer (20 mM Tris, 150 mM NaCl, 2 M urea, 0.5% NP_{40}, pH 8.0). The resulting solution was centrifuged at 10,000*g* for 20 min. The supernatant was collected and applied to a Ni–NTA affinity column, and the protein was eluted in elution buffer (20 mM Tris, 150 mM NaCl, 3 M urea, 0.5% NP_{40}, 500 mM imidazole pH 8.0).

2.2. Western blot analysis

The purified rCsdA-His protein was analyzed by sodium dodecyl sulfate polyacrylamide gel electropheresis (SDS–PAGE) and Western blot analysis as previously described (Sambrook and Russell, 2001). Briefly, the protein was transferred onto a nitrocellulose (NC) membrane followed by blocking with 5% skimmed milk in PBS (137 mM NaCl, 2.7 mM KCl, 10 mM Na_2HPO_4, 2 mM KH_2PO_4) overnight at 4 °C. The membrane was exposed to mouse antiserum against rCsdA and incubated for 1 h at 37 °C and then washed three times for 10 min each. The strips were washed again and allowed to react with horseradish peroxidase (HRP)-conjugated sheep anti-mouse IgG for 1 h at 37 °C. After the last washing, the strips were developed with water containing 3,3-diaminobenzidine tetrahydrochloride (DAB) substrate until bands appeared. The reaction was stopped by rinsing the strips with distilled water. Serum from unimmunized mice was used as a negative control.

2.3. Identification and preparation of a mAb

BALB/c female mice ($N = 5$) approximately 4–6 weeks old were purchased from the Animal Center of Harbin Veterinary Research Institute. All animal experiments were performed in accordance with the guidelines of the Chinese Council on Animal Care. The five mice were immunized intraperitoneally with 100 μg of purified rCsdA protein emulsified with an equal volume of Freund's complete adjuvant, followed by two other injections using incomplete adjuvant at ten-day intervals. Three days after the last injection, the mice were injected with 100 μg of purified rCsdA protein without adjuvant. The spleen cells of the mice were harvested and hybridized with SP2/0 mouse myeloma cells. The hybridized cells were cultivated for 10 days in hypoxanthine–aminopterin–thymidine (HAT) medium.

To produce mAbs, briefly, the rCsdA protein was used both as the immunogen and the screening antigen. Hybridomas were screened by indirect ELISA. Once established, hybridoma cells were passaged several times *in vitro*, and cell culture medium collected to measure the antibody titres. The isotypes of the mAbs were determined using the Mouse MonoAb ID Kit (Southern Biotechnology Associates, Inc., Birmingham, AL, USA) according to the manufacturer's instructions. The positive hybridoma cells identified in the screen were expanded and injected into the abdominal cavity of mice to produce ascites. Finally, immunoglobulin G (IgG) was purified from the ascites by protein A-agarose affinity chromatography (Horenstein et al., 2003). Western blot analysis was used to assess the reactivity of specificity of the mAb, purified empty plasmid pET32a his tag protein as a control.

2.4. Phage peptide library screening using the mAb

The Ph.D.-12 library was purchased from New England Biolabs, Inc. The library displays 12-mer peptides at the N-terminus of pIII of the M13 phage and consisted of 2.7×10^9 electroporated sequences (approximately 1.5×10^{13} pfu/ml). Phage M13 was amplified in *E. coli* 2738 grown in LB broth at 37 °C. Three rounds of biopanning were carried out according to the manufacturer's instructions with minor modifications. Briefly, purified mAb A3G5 was coated onto the ELISA plates [150 μl/well, 100 μg/ml in coating solution (0.1 M $NaHCO_3$, pH 9.6)] and incubated overnight at 4 °C. The well was washed six times with TBST (50 mM Tris, 150 mM NaCl, pH 7.5, and 0.1% Tween-20), followed by blocking with blocking buffer (0.1 M $NaHCO_3$, pH 8.6, 5 mg/ml BSA and 0.02% NaN_3) and incubated for 2 h at 4 °C. In the first round of biopanning, 1.5×10^{11} pfu (4×10^{10} phages, 10 μl from the initial library) in 100 μl of TBST was added to each well, and the plates incubated for 1 h at room temperature with gentle shaking. After repeat washes with TBST, the unbound phages were removed. The bound phages were then eluted in 100 μl elution buffer (0.2 M glycine–HCl, pH 2.2) containing 1 mg/ml BSA. The eluate was neutralized with 15 μl of 1 M Tris–HCl, pH 9.1, and 1 μl of eluate collected for dilution with LB medium and subsequent determination of the titre of the phages. The remaining eluate was then amplified in early-log *E. coli* ER2738 cells. The culture was incubated for 4.5 h at 37 °C with vigorous shaking. Phage supernatants were obtained and concentrated using PEG/NaCl precipitation. The percent recovery of the screened phages was calculated by the following formula: percent recovery = (eluted phage/input phage) × 100%. In the second and third rounds of biopanning, the procedures were similar to that of the first round except that the Tween-20 concentration in the TBST was raised to 0.5% for the second and third rounds of biopanning.

2.5. Indirect ELISA

After three rounds of panning, ten individual phage clones were selected and assayed for target binding by ELISA according to the instructions of the manufacturer. The wells of 96-well plates were coated overnight with mAb [150 μl/well, 100 μg/ml in coating solution (0.1 M $NaHCO_3$ pH 9.6)] and bovine serum albumin (BSA) as a cross-reactivity control by incubation at 4 °C. The wells were blocked with 200 μl of blocking buffer [5% BSA in TBST (0.5% Tween-20)] for 2 h at 37 °C. After the wells were washed three times with TBST, phage clones were added to the wells (2×10^{11} pfu in 100 μl/well), and the plates were incubated with agitation for 1 h at 37 °C. Phage clones from the original library were used as the negative phage control. Again, after the third washing with TBST, bound phages were reacted with 100 μl of HRP-conjugated anti-M13 antibody at 1:10,000 in TBST for 1 h at 37 °C. Following another three washes with TBST, 50 μl of TMB was added to each well, and the plates were incubated for 10 min. Finally, 50 μl of 2 M sulphuric acid was added to each well to stop the reaction. The absorbance values of the wells were read at 450 nm using an ELISA plate reader.

2.6. Sequence analysis of single-stranded phage DNA

The positive phages selected from the ELISA were cloned and sequenced with the 96 gIII sequencing primer 5′-TGAGCGGATA-ACAATTTCAC-3′ according to the manufacturer's instructions. The amino acid sequences of the peptides were deduced from the displayed sequences of the phages and compared with the native CsdA protein sequence, which was obtained from GenBank (NC_000962) using Lasergene software. The peptide was synthesized by GenScript.

2.7. Synthetic peptides

The affinity of the mAb for the synthesized peptide (-APDPPLSRR-) (named Cpep) was determined by ELISA. Briefly, the Cpep was coated onto the ELISA plates overnight at 4 °C [100 μl/well, 10 μg/ml in coating solution (0.1 M $NaHCO_3$ pH 9.6)]. The plate was then blocked with blocking buffer [5% BSA in TBST (0.5% Tween-20)]. After incubation at 37 °C for 2 h, the wells were washed with PBST and incubated with the different concentrations of mAb for 1 h at 37 °C. Then, the wells were again washed with PBST, and the plate incubated at 37 °C for 1 h in the presence of goat anti-mouse IgG–HRP (1:10,000 diluted with PBST). After the last wash with PBST, the wells were developed with the substrate tetra-methyl benzidine (TMB), and the absorbance values of the wells read at 450 nm using an ELISA plate reader.

2.8. Competitive inhibition

2.8.1. Competitive inhibition assay using increasing rCsdA concentrations

The mAb (0.2 μg/ml) was coated onto ELISA plates with coating solution [(0.1 M $NaHCO_3$, pH 9.6)], and then the wells blocked with buffer [5% BSA in TBST (0.5% Tween-20)]. The rCsdA protein was diluted to 10, 1 and 0.1 μg/ml and mixed with eight positive clones (each 5×10^{11} pfu). The rCsdA protein/phage solutions were added to each well, and the rCsdA protein alone (without phage) was used as a positive control. After incubation at 37 °C for 2 h, the wells were washed with 0.1% TBST, and the plate incubated at 37 °C for 1 h in the presence of anti-M13 HRP–IgG (1:5000 diluted with 0.1% TBST). The wells were developed with TMB and read at 450 nm. The inhibition ratio was calculated as follows: [OD_{450} (without phage) − OD_{450} (with phage)]/OD_{450} (without phage) × 100%.

2.8.2. Competitive inhibition assay using increasing phage concentrations

The rCsdA protein, 10 μg/ml, was coated onto the ELISA plates with coating solution [(0.1 M $NaHCO_2$ and pH 9.6)], after which the wells were blocked with buffer [5% BSA in TBST (0.5% Tween-20)]. Then, 0.2 μg/ml of mAb and eight positive clones (each at 10^{12}, 10^{10}, 10^8, and 10^6) were mixed, and these solutions added to each well. The mAb alone (without phage) was used as a positive control. After incubation at 37 °C for 2 h, the wells were washed with 0.1% TBST, and the plates incubated at 37 °C for 1 h in the presence of anti-M13 IgG–HRP (1:5000 diluted with 0.1% TBST). The wells were developed with TMB and read at 450 nm. The inhibition ratio was calculated using the following formula: [OD_{450} (without phage) − OD_{450} (with phage)]/OD_{450} (without phage) × 100%.

2.8.3. Competitive inhibition assay using increasing concentrations of the rCpep peptide

Both the mAb and purified rCsdA were used in the competitive inhibition ELISA to test the specificity of the synthesized peptide. Briefly, 96-well plates were first coated with the CsdA protein (10 μg/ml) and then incubated with 0.2 μg/ml of mAb plus increasing concentrations (5, 10, 15, 25, 50, 75, 100 μg/ml) of the synthesized peptide. An unrelated synthetic peptide ($-_{74aa}$YSIALGNTDSDGINYW$_{88aa}$-) (from SapA protein of *Campylobacter fetus*) was used as a negative control. The subsequent procedures were performed as described above for the ELISA method.

2.9. Immunization of mice with the purified phages

The purified phages (clones 1–8) were used to immunize BALB/c mice through intraperitoneal injection. For each immunization, approximately 10^{12} pfu of phage was used, and TBS was used as the negative control. Three groups of mice were immunized with each sample, and preimmune sera (negative control) were obtained. The mice were immunized every two weeks. The immunized mice were bled after the third immunization. Then, the Cpep was coated onto the ELISA plates at 4 °C [100 μl/well, 10 μg/ml in coating solution (0.1 M $NaHCO_3$, pH 9.6)]. Each serum sample was tested by ELISA. The serum of mice immunized with the rCsdA protein was used as a positive control.

3. Results

3.1. Reactivity of specificity and purification of the rCsdA protein

The SDS–PAGE results show that, after cell sonication and the fourth wash using the wash buffer, the size of the recombinant protein was consistent with the expected size of 64 kD (Fig. 1A). Western blot analysis showed that the recombinant protein had a very good reactivity of specificity (Fig. 1B).

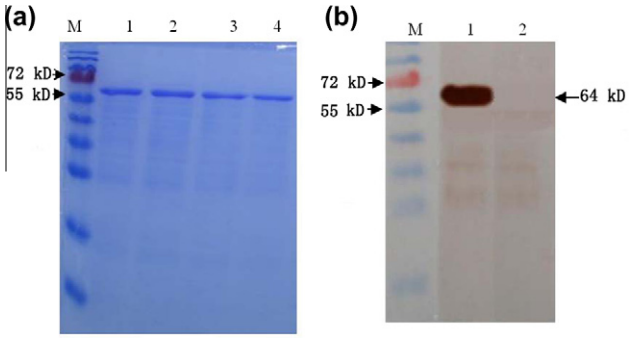

Fig. 1. Purification of the recombinant CsdA protein (A) and Western blot analysis (B). M: protein marker; A1–4: purified csdA protein; B1: purified fusion protein reacted with mouse anti-serum against CsdA; B2: negative control.

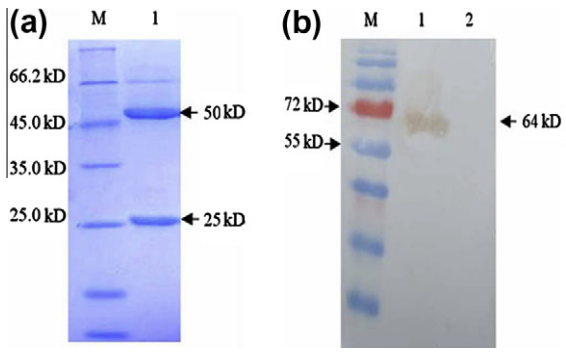

Fig. 2. Analysis of the purified IgG from mouse ascites by SDS–PAGE (A) and Western blot (B). M: protein marker; A1: purified mAb A3G5; B1: rCsdA protein; B2: control.

Table 1
The yield of peptide library biopanning.

Panning no.	Input (pfu)	Output (pfu)	Recovery
First round	1.5×10^{11}	4.5×10^{6}	3.0×10^{-5}
Second round	1.5×10^{11}	9.5×10^{7}	6.4×10^{-3}
Third round	1.5×10^{11}	3.0×10^{9}	2.0×10^{-2}

3.2. Characterization of the mAb

One hybridoma clone, which produced the mAb named A3G5, was obtained. The mAb was purified using a protein A-Sepharose 4FF (Pharmacia) column. The results showed that a higher purity mAb was obtained (Fig. 2A). The characterization of the mAb was performed using an antibody subclass identification kit. The results revealed that the subtype of A3G5 was IgG1 and that the light chain was the κ chain. The relative titre of the mAb was measured by ELISA using serial dilutions and was found to be 200,000. Western blot analysis showed that A3G5 only reacted with the CsdA protein and not with the His tag, suggesting that the mAb is specific to the CsdA protein (Fig. 2B).

3.3. Yield of phage panning

Because the phage yield for A3G5 after the third round of screening was low due to the low titre, we stopped panning at this step. It was found that the recovery of each round (the quantity of output phage divided by the quantity of input phage) increased from 4.5×10^{6} to 3.0×10^{9} (Table 1). The increasing yield of phage after each round of selection indicated that phages with affinity for A3G5 accumulated; thus, the phage enrichment was successful.

3.4. Detection of phage clones by ELISA

After three rounds of selection, random phages were amplified, and their reactivities with the mAb were assessed by indirect ELISA analysis. The results showed that these 10 single phages expressed peptides that interacted with mAb A3G5 ($OD_{450\,nm} > 0.3$). These interactions were specific because no interaction was detected in the BSA control wells ($OD_{450\,nm} < 0.08$) (Fig. 3).

3.5. Sequencing of positive phage clones and homology comparison

The DNA sequences of ten positive clones were determined, and the deduced amino acid sequences of the corresponding peptides are shown in Fig. 4. Comparison of the protein sequence of CsdA and the deduced sequence revealed that the amino acid sequence -APDPPLSRR-, named Cpep, was conserved in CsdA (residues 443 aa-451 aa) (Fig. 4). This result suggested that APDPPLSRR is the core amino acid sequence of CsdA that forms the epitope recognized by A3G5. In addition, comparison of the CsdA protein amino acid sequences from 27 mycobacterial strains showed that all CsdA protein of the members of the *M. tuberculosis* complex were the same. In nontuberculous mycobacteria (NTM), the amino acid residues -PP- were the same, and the conservation of amino acids residues -RR- in all NTM was very high; the amino acid residues -APD- also showed a high level of conservation (Fig. 5).

Fig. 4. Sequences of the 12 peptides displayed by the eight phage clones. Note: red letters indicate that the sequences are identical; black letters indicate differences in the sequences. (For interpretation of the references to color in this figure legend, the reader is referred to the web version of this article.)

3.6. Competitive inhibition assay using increasing rCsdA concentrations

Pre-incubation with the rCsdA protein inhibited binding between the mAb A3G5 and the eight clones. This result showed that the inhibition rate of the rCsdA protein against mAb A3G5 and seven of the clones decreased with decreasing rCsdA protein concentration. These results also demonstrated that the epitope recognized by A3G5 and the epitope displayed by seven screened phage clones were identical or similar. The inhibition ratio of the remaining clone, phage clone 12, was very low (Fig. 6).

3.7. Competitive inhibition assay using increasing phage concentrations

The competitive inhibition analysis of eight clones showed that the concentration of positive phage was significantly related to its inhibitory effect on the binding of mAb A3G5 and rCsdA. These results showed that the blocking effect of all clones except clone No. PH12 gradually decreased, further indicating that the epitope

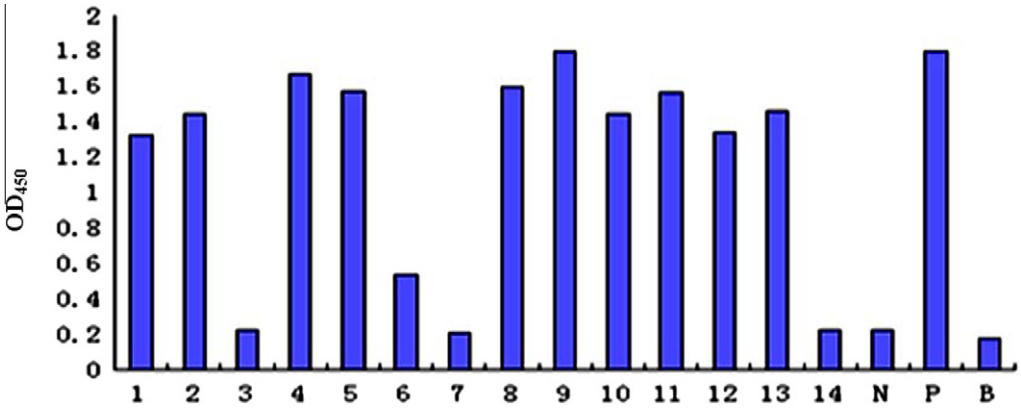

Fig. 3. Detection of the binding activities of the phage clones by ELISA. N: negative control; P: positive control; B: BSA; 1–14: phage clones from the third round of biopanning.

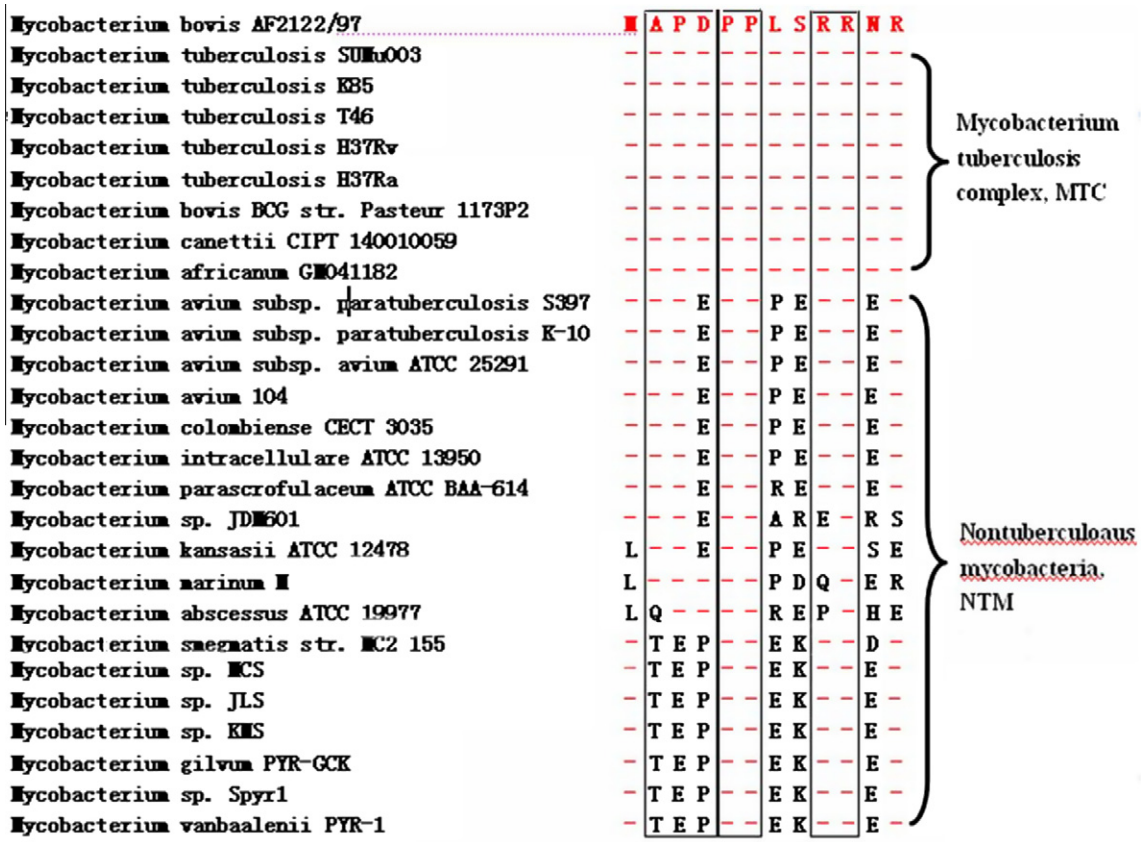

Fig. 5. Competitive binding assays using 12-amino-acid peptides from the CsdA proteins of twenty-seven mycobacterial strains.

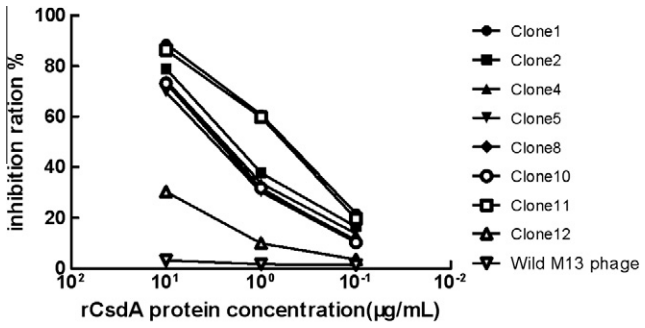

Fig. 6. Competitive inhibition assay using increasing rCsdA concentrations.

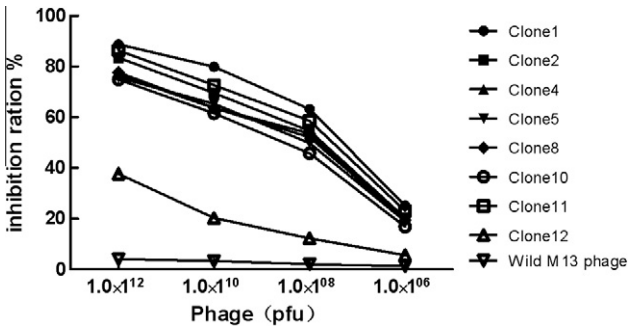

Fig. 7. Competitive inhibition assay using increasing phage concentrations.

recognized by A3G5 and the epitope displayed by the seven screened phage clones were identical or similar (Fig. 7).

3.8. Identification of the synthetic peptide epitope

The analysis of the affinity of the synthetic peptide Cpep for A3G5 showed that with increasing concentrations of mAb, the OD values became larger, and the affinity was very strong (Fig. 8). The results of the competitive inhibition experiments using increasing concentrations of peptide Cpep are presented in Fig. 9. When the concentration of A3G5 was 0.2 μg/ml and the rCsdA protein was coated at 10 μg/ml, the binding of A3G5 to the rCsdA protein was significantly inhibited by the synthetic peptide Cpep (Fig. 9). The strength of the inhibition was dependent on the concentration, and with the increasing concentration of the synthetic peptide, the strength of the inhibition was enhanced. We conclude

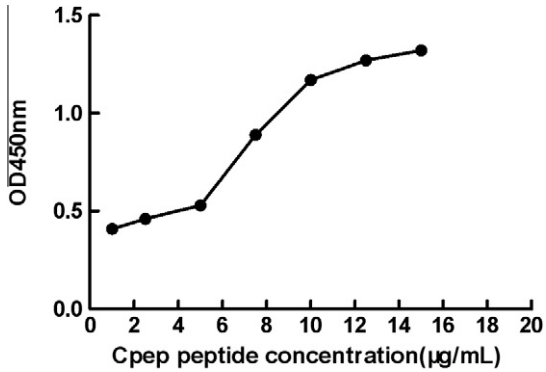

Fig. 8. Affinity peptide Cpep for mAb A3G5.

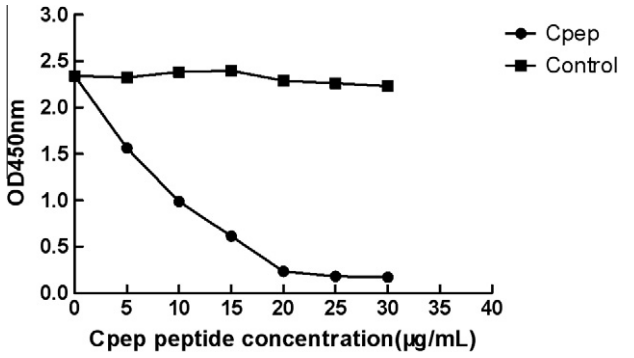

Fig. 9. Competitive inhibition assay using increasing concentrations of the rCpep peptide C–P: APDPPLSRR; control: YSIALGNTDSDGINYW.

that the synthesized peptide was the epitope of the rCsdA protein, which was recognized by the mAb A3G5.

3.9. Immune response induced by positive phage clones

The titres of the serum of mice immunized by the eight positive phage clones were measured by ELISA. Seven of the clones induced specific immune responses; these clones were No. PH1, No. PH8, No. PH5, No. PH2, No. PH10, No. PH4, and No. PH5 (Fig. 10). It was also observed that mice injected with PH12 did not exhibit an immune response. The results further indicated that the selected phages were specific to the mAb A3G5.

4. Discussion

RNA helicases are enzymes that unwind double-stranded RNA in an energy-dependent manner. They hydrolyze a nucleotide triphosphate and release the energy to dissociate duplexes or displace bound proteins. Based upon the several conserved motifs, RNA helicases are classified into three superfamilies and two families named SF1 to SF5 (Gorbalenya and Koonin, 1993). Superfamily 2 (SF2) has eight conserved motifs and includes the DEAD, DEAH, DExH, and DExd families (Tanner and Linder, 2001; Chamot et al., 1999). The DEAD-box family is the largest family, and these proteins include the Q motif and the Asp-Glu-Ala-Asp (DEAD) motif (Linder et al., 1989). CsdA is one of five DEAD-box proteins (SrmB, CsdA (also called DeaD), DbpA, RhlB, and RhlE) (Iost and Dreyfus, 2006), which all possess ATPase and helicase activities (Diges and Uhlenbeck, 2001; Chandran et al., 2007). In vivo, these proteins participate in at least two fundamental cellular processes (mRNA degradation (Iost and Dreyfus, 1994; Py et al., 1996; Prud'homme-Généreux et al., 2004; Khemici et al., 2005; Awano et al., 2007) and ribosome assembly (Charollais et al., 2003, 2004; Elles and Uhlenbeck, 2008; Jain, 2008; Peil et al., 2008; Sharpe Elles et al., 2009)) that require that RNA adopt a particular conformation (single-stranded structure for mRNA degradation and native rRNA structure for ribosome assembly) that may be favored by DEAD-box proteins (Cartier et al., 2010). Cold-shock DEAD-box proteins from some bacteria, such as *E. coli* (Jones et al., 1996), *Anabaena* spp. (cyanobacteria) (Chamot et al., 1999), and *Bacillus subtilis* (Aubourg et al., 1999; Charollais et al., 2004; Hunger et al., 2006) have been studied; however, it is unclear what role this protein plays in *M. tuberculosis*.

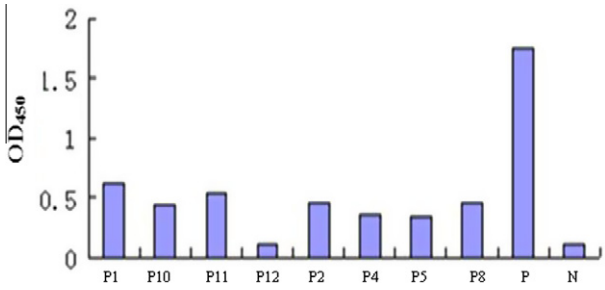

Fig. 10. Reaction of peptide Cpep and the positive clone. N: negative control; P: positive control.

In the present study, we cloned the CsdA gene and expressed the rCsdA protein in *E. coli*. Using the hybridoma technique, the mAb A3G5 was prepared. To determine the important amino acid sequences in CsdA, the distinct epitope recognized by the antibody A3G5 was determined using phage display technology. The identified epitope provides some important information about the structure of the protein. The selected sets of peptides may also lead to the future design of useful drugs for therapeutic and/or diagnostic purposes. The antibody A3G5 is specific to the CsdA protein. To obtain the specific phages, multiple rounds of selection were carried out in the present study. The specific phages that bound to anti-rCsdA A3G5 were enriched after three rounds of biopanning and were finally obtained from the phage peptide library. Competitive inhibition assays and immunization of mice with eight positive phage clones showed that among eight phage clones, seven phage clones (No. PH1, No. PH2, No. PH4, No. PH5, No. PH8, and No. PH11) had good inhibitory effects and were able to induce the production of high-titre antibodies in the immunized mice. This was because the amino acid sequences of the seven positive phage clones and peptide sequence, APDPPLSRR, of the CsdA protein from the reference strain *M. tuberculosis* H37RV, were in good agreement. The level of similarity between the sequence of No. PH12, the phage clone that did not show good inhibitory effects or result in high-titre antibody production by mice, and the peptide sequence (-APDPPLSRR-) was lower. Furthermore, the sequence (APDPPLSRR) was confirmed by competitive inhibition ELISA and the immune response in mice. These results suggest that the core sequence of the amino acid epitope of the antibody produced in mice and induced during immune responses plays an important role (Figs. 4–5 and 10). Based on these results, we concluded that the peptide -APDPPLSRR- may include the key amino acids that forming a motif in CsdA.

The results of the sequence analysis of the epitope amino acids of 27 CsdA proteins from the members of *Mycobacterium* are presented in Fig. 5. The peptide sequence of the epitope recognized by the monoclonal antibody A3G5, -APDPPLSRR-, is entirely conserved in the *M. tuberculosis* complex. Among NTM strains, this sequence is relatively conserved, especially the amino acids -APDPP-RR-. In addition, the identified epitope peptide sequence showed good agreement, suggesting that the epitope identified in this work may be conserved among mycobacteria. The identified epitope is very important for the further study of the function of the CsdA protein from mycobacteria. Our results may lay the ground work for the further study of the mechanism of *M. tuberculosis* survival at low temperatures because the CsdA protein is essential in low-temperature environments (Jones et al., 1996; Cartier et al., 2010).

Acknowledgments

This work was supported by grants from the National "973" program (No. 2012CB518800) and from the National "863" program (No. 2011AA10A210).

References

Aubourg, S., Kreis, M., Lecharny, A., 1999. The DEAD box RNA helicase family in Arabidopsis thaliana. Nucleic Acids Research 27, 628–636.

Awano, N., Xu, C., Ke, H., Inoue, K., Inouye, M., Phadtare, S., 2007. Complementation analysis of the cold-sensitive phenotype of the *Escherichia coli* csdA deletion strain. Journal of Bacteriology 189, 5808–5815.

Bizebard, T., Ferlenghi, I., Iost, I., Dreyfus, M., 2004. Studies on three *E. coli* DEAD-box helicases point to an unwinding mechanism different from that of model DNA helicases. Biochemistry 43, 7857–7866.

Cartier, G., Lorieux, F., Allemand, F., Dreyfus, M., Bizebard, T., 2010. Cold adaptation in DEAD-Box Proteins. Biochemistry 49, 2636–2646.

Chamot, D., Magee, W.C., Yu, E., Owttrim, G.W., 1999. A cold Shock-induced cyanobacterial RNA helicase. Journal of Bacteriology 181, 1728–1732.

Chandran, V., Poljak, L., Vanzo, N.F., Leroy, A., Miguel, R.N., Fernandez-Recio, J., Parkinson, J., Burns, C., Carpousis, A.J., Luisi, B.F., 2007. Recognition and cooperation between the ATP-dependent RNA helicase RhlB and ribonuclease RNase E. Jounal of Molecular Biology 367, 113–132.

Charollais, J., Dreyfus, M., Iost, I., 2004. CsdA, a cold-shock RNA helicase from *Escherichia coli*, is involved in the biogenesis of 50S ribosomal subunit. Nucleic Acids Research 32, 2751–2759.

Charollais, J., Pflieger, D., Vinh, J., Dreyfus, M., Iost, I., 2003. The DEAD-box RNA helicase SrmB is involved in the assembly of 50S ribosomal subunits in *Escherichia coli*. Molecular Microbiology 48, 1253–1265.

Colditz, G.A., Berkey, C.S., Mosteller, F., Brewer, T.F., Wilson, M.E., Burdick, E., Fineberg, H.V., 1995. The efficacy of bacillus Calmette–Guerin vaccination of newborns and infants in the prevention of tuberculosis: meta-analyses of the published literature. Pediatrics 96, 29–35.

Colditz, G.A., Brewer, T.F., Berkey, C.S., Wilson, M.E., Burdick, E., Fineberg, H.V., Mosteller, F., 1994. Efficacy of BCG vaccine in the prevention of tuberculosis. Meta-analysis of the published literature. Journal of the American Medical Association 271, 698–702.

de la Cruz, J., Kressler, D., Linder, P., 1999. Unwinding RNA in *Saccharomyces cerevisiae*: DEAD-box proteins and related families. Trends in Biochemical Sciences 24, 192–198.

Devlin, J.J., Panganiban, L.C., Delvin, P.E., 1990. Random peptide libraries: a source of specific protein binding molecules. Science 249, 404–406.

Diges, C.M., Uhlenbeck, O.C., 2001. *Escherichia coli* DbpA is an RNA helicase that requires hairpin 92 of 23S rRNA. The EMBO Journal 20, 5503–5512.

Du, Y.F., Qi, Y.F., Yu, L., Lin, J.K., Liu, S.G., Ni, H.B., Pang, H., Liu, H.F., Si, W., Zhao, H.L., Wang, C.L., 2011. Molecular characterization of *Mycobacterium tuberculosis* complex (MTBC) isolated from cattle in northeast and northwest China. Research in Veterinary Science 90, 385–391.

Elles, L.M., Uhlenbeck, O.C., 2008. Mutation of the arginine finger in the active site of *Escherichia coli* DbpA abolishes ATPase and helicase activity and confers a dominant slow growth phenotype. Nucleic Acids Research 36, 41–50.

Gibson, A.L., Hewinson, G., Goodchild, T., Watt, B., Story, A., Inwald, J., Drobniewski, F.A., 2004. Molecular epidemiology of disease due to *Mycobacterium bovis* in humans in the United Kingdom. Journal of Clinical Microbiology 42, 431–434.

Gorbalenya, A.E., Koonin, E.V., 1993. Helicases: amino acid sequence comparisons and structure-function relationships. Current Opinion in Structural Biology 3, 419–429.

Hunger, K., Beckering, C.L., Wiegeshoff, F., Graumann, P.L., Marahiel, M.A., 2006. Cold induced putative DEAD box RNA helicases CshA and CshB are essential for cold adaptation and interact with cold shock protein B in *Bacillus subtilis*. Journal of Bacteriology 188, 240–248.

Horenstein, A.L., Crivellin, F., Funaro, A., Said, M., Malavasi, F., 2003. Design and scaleup of downstream processing of monoclonal antibodies for cancer therapy: from research to clinical proof of principle. Journal of Immunological Methods 275, 99–112.

Iost, I., Dreyfus, M., 1994. MRNAs can be stabilized by DEAD-box proteins. Nature 372, 193–196.

Iost, I., Dreyfus, M., 2006. DEAD-box RNA helicases in *Escherichia coli*. Nucleic Acids Research 34, 4189–4197.

Jain, C., 2008. The *E. coli* RhlE RNA helicase regulates the function of related RNA helicases during ribosome assembly. RNA 14, 381–389.

Jones, P.G., Mitta, M., Kim, Y., Jiang, W., Inouye, M., 1996. Cold shock induces a major ribosomal-associated protein that unwinds double-stranded RNA in *Escherichia coli*. Proceedings of the National Academy of Sciences of the United States of America 93, 76–80.

Jorda, L., Vieira, V., 2011. Tuberculosis: new aspects of an old disease. International Journal of Biochemistry & Cell Biology 40, 3623–3636.

Jou, R.W., Huang, W.L., Chiang, C.Y., 2008. Human tuberculosis caused by *Mycobacterium bovis*. Taiwan Emerging Infectious Diseases 14, 515–517.

Khemici, V., Poljak, L., Toesca, I., Carpousis, A.J., 2005. Evidence in vivo that the DEAD-box RNA helicase RhlB facilitates the degradation of ribosome-free mRNA by RNase E. Proceedings of the National Academy of Sciences of the United States of America 102, 6913–6918.

Lesslie, I.W., Birn, K.J., 1970. *Mycobacterium avium* infections in cattle and pigs in Great Britain. Tubercle 51, 446–451.

Linder, P., Lasko, P.F., Ashburner, M., Leroy, P., Nielsen, P.J., Nishi, K., Schnier, J., Slonimski, P.P., 1989. Birth of the D-E-A-D box. Nature 337, 121–122.

Luking, A., Stahl, U., Schmidt, U., 1998. The protein family of RNA helicases. Critical Reviews in Biochemistry and Molecular Biology 33, 259–296.

Pavlik, I., Yayo, A, W., Parmova, I., Mwlicharek, I., Hanzlikova, M., Svejnochova, M., Körmendy, B., Nagy, G., Cvetnic, Z., Katalinic, J.V., Ocepek, M., Zolnir, D.M., Lipiec, M., Havelkova, M., 2003. *Mycobacterium tuberculosis* in animal and human populations in six Central European countries during 1990–1999. Veterinarni Medicina 48, 83–89.

Peil, L., Virumae, K., Remme, J., 2008. Ribosome assembly in *Escherichia coli* strains lacking the RNA helicase DeaD/CsdA or DbpA. FEBS Journal 275, 3772–3782.

Prud'homme-Généreux, A., Beran, R.K., Iost, I., Ramey, C.S., Mackie, G.A., Simons, R.W., 2004. Physical and functional interactions among RNase E, polynucleotide phosphorylase and the cold-shock protein, CsdA: Evidence for a 'cold shock degradosome'. Molecular Microbiology 54, 1409–1421.

Py, B., Higgins, C.F., Krisch, H.M., Carpousis, A.J., 1996. A DEAD-box RNA helicase in the *Escherichia coli* RNA degradosome. Nature 381, 169–172.

Rodrigues, L.C., Diwan, V.K., Wheeler, J.G., 1993. Protective effect of BCG against tuberculous meningitis and military tuberculosis: a metaanalysis. International Journal of Epidemiology 22, 1154–1158.

Sambrook, J., Russell, D., 2001. Molecular Cloning: A Laboratory Manual, third ed. Cold Spring Harbor Laboratory Press, Cold Spring Harbor, NY.

Schliesser, T., 1976. Presence and significance of mycobacteria in animals (proceedings). Zentralbl Bakteriol Orig A 235, 184–194.

Schmid, S.R., Linder, P., 1992. D-E-A-D protein family of putative RNA helicases. Molecular Microbiology 6, 283–292.

Sharpe Elles, L.M., Sykes, M.T., Williamson, J.R., Uhlenbeck, O.C., 2009. A dominant negative mutant of the *E. coli* RNA helicase DbpA blocks assembly of the 50S ribosomal subunit. Nucleic Acids Research 37, 6503–6514.

Smith, I.G.N., 1984. A herd breakdown due to *Mycobacterium tuberculosis*. State Veterinary Journal 38, 40–44.

Tanner, N.K., Linder, P., 2001. DExD/H box RNA helicases: from generic motors. Molecular Cell 8, 251–262.

Thoen, C.O., Karlson, A.G., Himes, E.M., 1981. Mycobacterial infections in animals. Reviews of Infectious Diseases 3, 960–972.

WHO, 2009. Tuberculosis Facts – 2009 Update.

WHO, 2010. Tuberculosis, Fact Sheet No. 104.

WHO, 2010. Multidrug and Extensively Drug-Resistant TB (M/XDR-TB): 2010 Globle Report on Surveillance and Response.

Zhang, L., Wang, Q.Z., Xu, Y., Chen, J.Z., Lu, F.P., Wang, H.H., 2006. Expression, purification and enzyme activity determination of pantothenate kinase from *Mycobacterium tuberculosis*. Journal of the Fourth Military Medical University 27, 2135–2318 (in Chinese).

人畜间结核病流行病学的调查与研究

经济社会效益分析报告

乌鲁木齐市动物疾病控制与诊断中心

新疆畜牧科学院兽医研究所

中国农业科学院哈尔滨兽医研究所

二〇一五年七月

人畜间结核病流行病学的调查与研究
经济社会效益分析报告

结核病（Tuberculosis）是由结核分枝杆菌引起的一种慢性的消耗性人畜共患传染病，是人类已知的最古老的严重危害人类健康的慢性呼吸道传染病。牛结核病目前被 OIE 列为多种动物疫病，我国列为二类动物疫病。本项目在实施的 8 年当中，取得了可观的经济效益和巨大的社会效益，现总结报告如下：

一、经济效益

项目实施 8 年中，采用国标 PPD 皮试变态反应开展检疫，对检出的阳性牛进行扑杀和无害化处理，牛结核病的阳性率从 8 年平均阳性率 0.4%，下降到 2014 年的 0.1%，下降了 0.3%，按照乌鲁木齐市 3.6 万头奶牛存栏计，每年净减少结核病阳性奶牛 108 头，每头牛按 1.5 万元的市场价格计算，8 年共挽回了直接经济损失 1296 万元。

为了减少非特异反应，提高牛结核病的检疫准确性，以达到净化牛场之目，对 PPD 牛结核病阳性牛进一步用发达国家通用的比较变态反应（进口禽型和进口牛型结核菌素）试验和 γ-干扰素实验进行检测，并对 PPD 阳性牛进行剖检，观察病理变化，采集病变肺脏和肺门淋巴结、下颌淋巴等进行分类、培养分离结核分枝杆菌和菌型鉴定。较之 PPD 检疫方法提高了特异性 21%，按照乌鲁木齐市 3.6 万头奶牛存栏计，每年净减少误杀假阳性奶牛 30 头，每头牛按 1.5 万元的市场价格计算，8 年共减少直接经济损失 363 万元。

2011 年新疆有活动性肺结核病 29.4 万人；菌阳肺结核病人 6.7 万；每年新发肺结核病人约 4.2 万；每年死于肺结核的人数达 6800 人。而通过本项目证实新疆结核病人中，有牛型结核分枝杆菌的占 1.9%，按照国家规定每个结核病人国家承担 9000 元的治疗费用，每年给国家节约结核病人的治疗费用 718.2 万元。8 年共计节约 5744 万元。

通过项目的实施，8 年共减少直接经济损失 7403 万元。同时还将加快乌鲁木齐市和全疆消灭净化结核病的进程，减少结核病扩散蔓延和对环境的污染，将减少间接经济损失达到上亿元。

二、社会效益

牛结核病还对人类健康构成巨大威胁。由于人口的增长、流动人口的增加、艾滋病毒感染的传播、耐药菌株的产生等原因，致使结核病疫情加重，全球 22 个结核病高负担国家中，中国居世界第二，仅次于印度，新疆是全国结核病高发地区；新疆和乌鲁木齐市的人感染结核病的数量也在不断增加。人结核病的致死率已排列在各种死因的第 9 位，相当于我国各种其他传染病和寄生虫病死亡总和的 2 倍。对此牛结核病对人的危害非常大。在那些还流行牛结核病的国家中，人类始终受到该病的威胁，除非消灭牛结核病，否则人类结核病控制是不会成功的。

奶牛患有结核病，人类可通过饮用患畜的牛奶或接触患畜等而得结核病，而且患病牛和人的粪便等排泄物污染环境，造成环境中的土壤、水源和用具等的二次污染。如果净化和消灭了牛结核病，使人们可饮用无结核病病原污染的健康安全牛奶，这样不仅有利于人类健康，而且可给人、畜间提供一个无病原污染和传播的良好社会环境。

动物疫病防控水平反映了一个地区现代化养殖业发展的水平。有效防控结核病，必将促进畜牧业尤其是奶牛业和肉牛业大发展，为社会有效提供更多的廉价、优质的肉和奶，丰富人民的物质生活，提高人民生活质量，稳定动物性食品物价。有效防治牛结核病将减少人结核病的发生，使各族人民的健康得到保障，同时维护好新疆的和谐、稳定。保障人的身体健康和社会公共卫生安全，促进构建和谐社会和社会稳定。乌鲁木齐市作为新疆牛奶和乳制品最大的消费城市，控制结核病的发生社会意义更大。随着学生奶项目的实施，我市有 28 万学生饮用奶制品，奶制品的质量安全关系到下一代的身体健康，同时也关系到全市 338 万市民的身体健康和社会稳定，控制和消灭结核病对促进社会公共卫生安全和和谐首府的建

立具有重大意义。